Karlsruher Institut für Technologie

Vorlesung Batterie- und Brennstoffzellensysteme

(Langzeit-) Stabilität von SOFC-Komponenten

André Weber

Institut für Angewandte Materialien – Elektrochemische Technologien (IAM-ET)
Adenauerring 20b, Geb. 50.40 (FZU), Raum 314
phone: 0721/608-7572, fax: 0721/608-7492
andre.weber@kit.edu
www.iam.kit.edu/et

Basic Concepts in Reliability Engineering
Definition of Failure Event and Time-To-Failure

soft failure

gradual performance loss until (pre-defined) critical level is reached.

example

- voltage/ power degradation in fuel cells

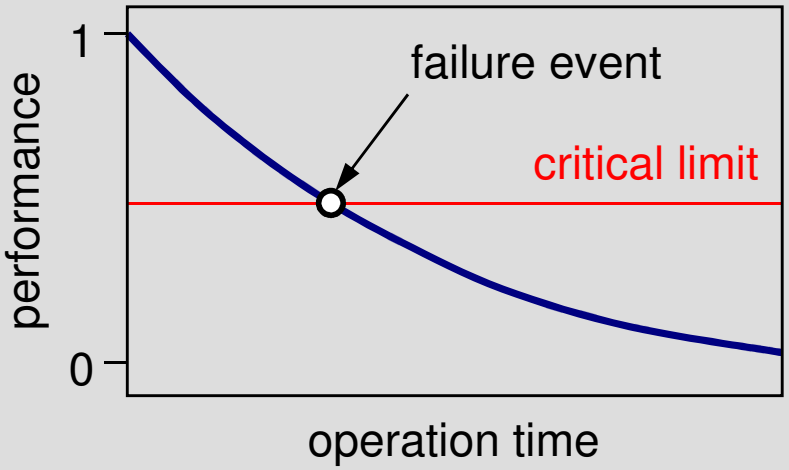

(Meeker et al., Technometrics, 40, 1998)

hard failure

sudden loss of functionality – the device stops working.

example

- light bulb burns out

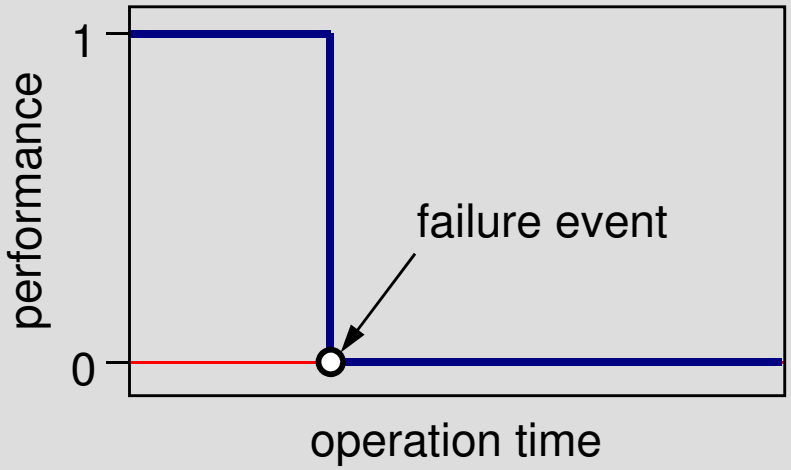

Lifetime and Degradation Assessment
Overview of Life Testing Methods

"conventional" life testing

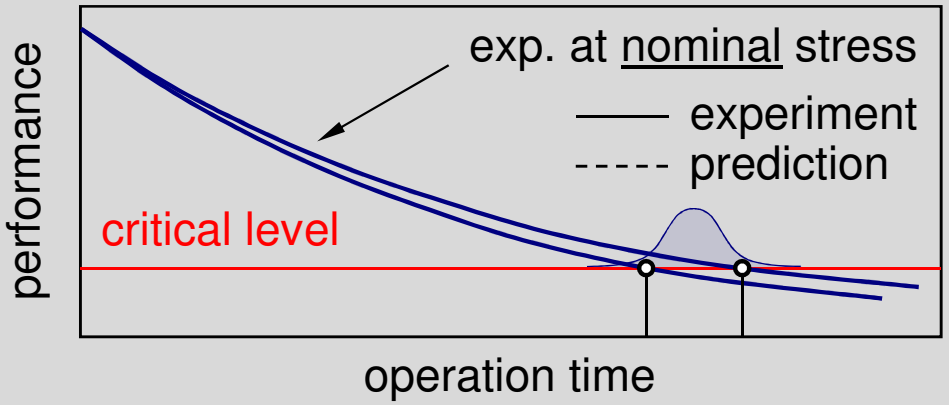

degradation testing

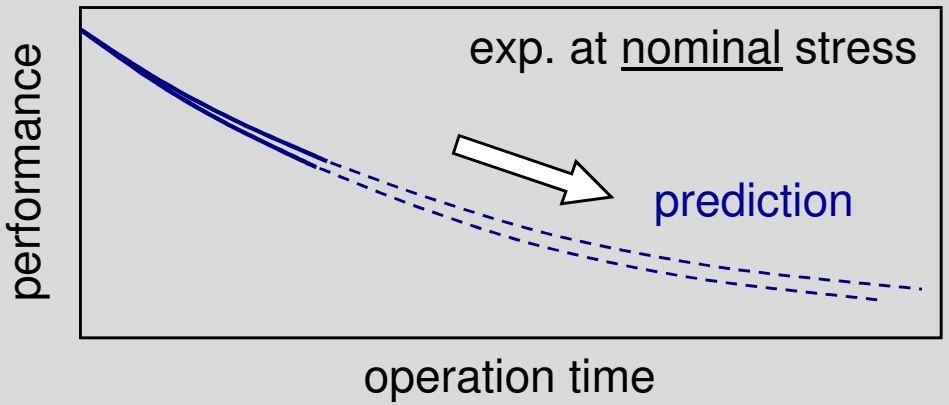

Durability Testing of Solid Oxide Cells
Research Center Jülich ASC-Stacks (2007 ff)

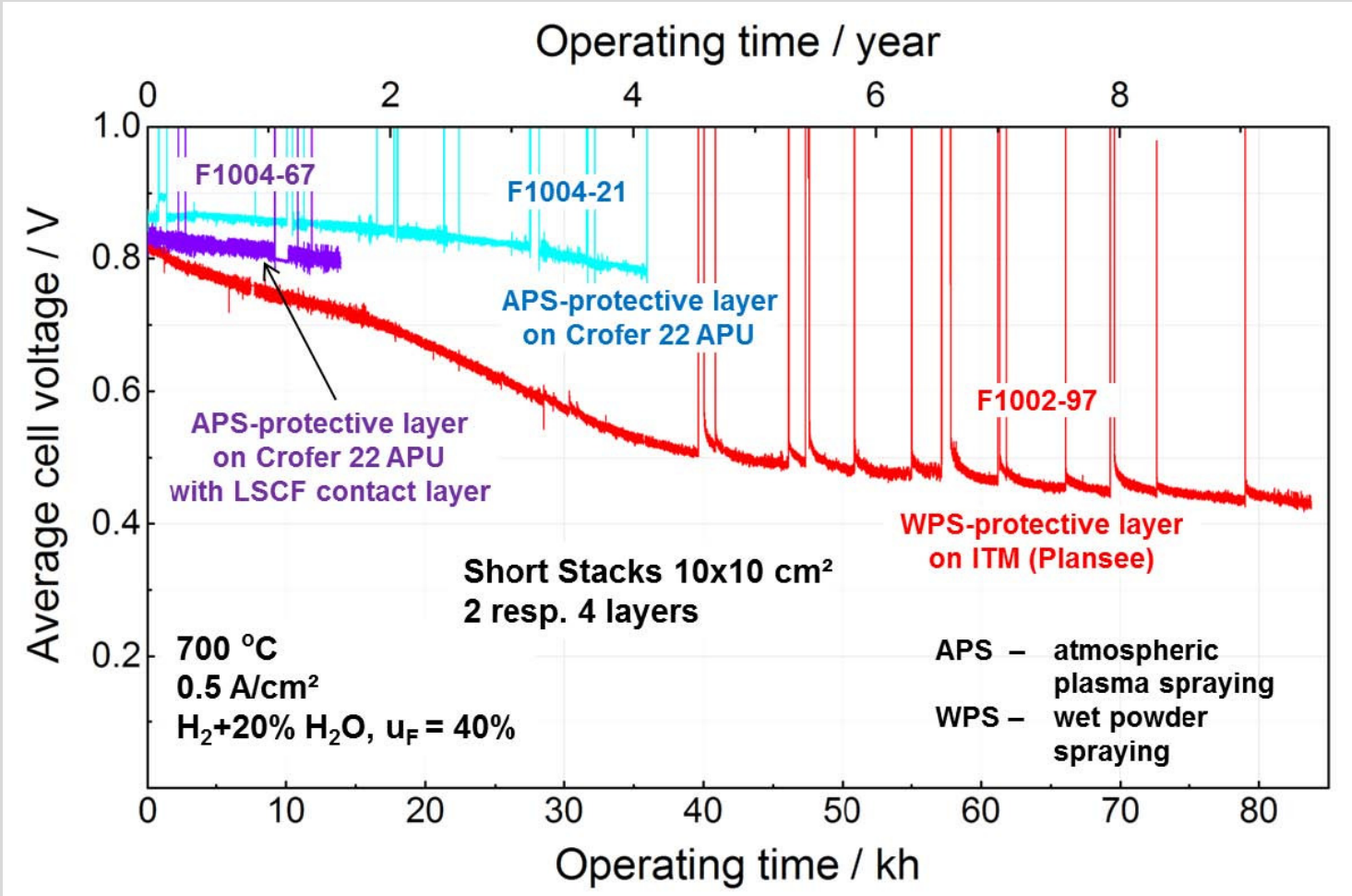

L. Blum et al., *ECS Trans.*, **78** (1), p. 1791 (2017)

Degradation Processes in Solid Oxide Fuel Cells

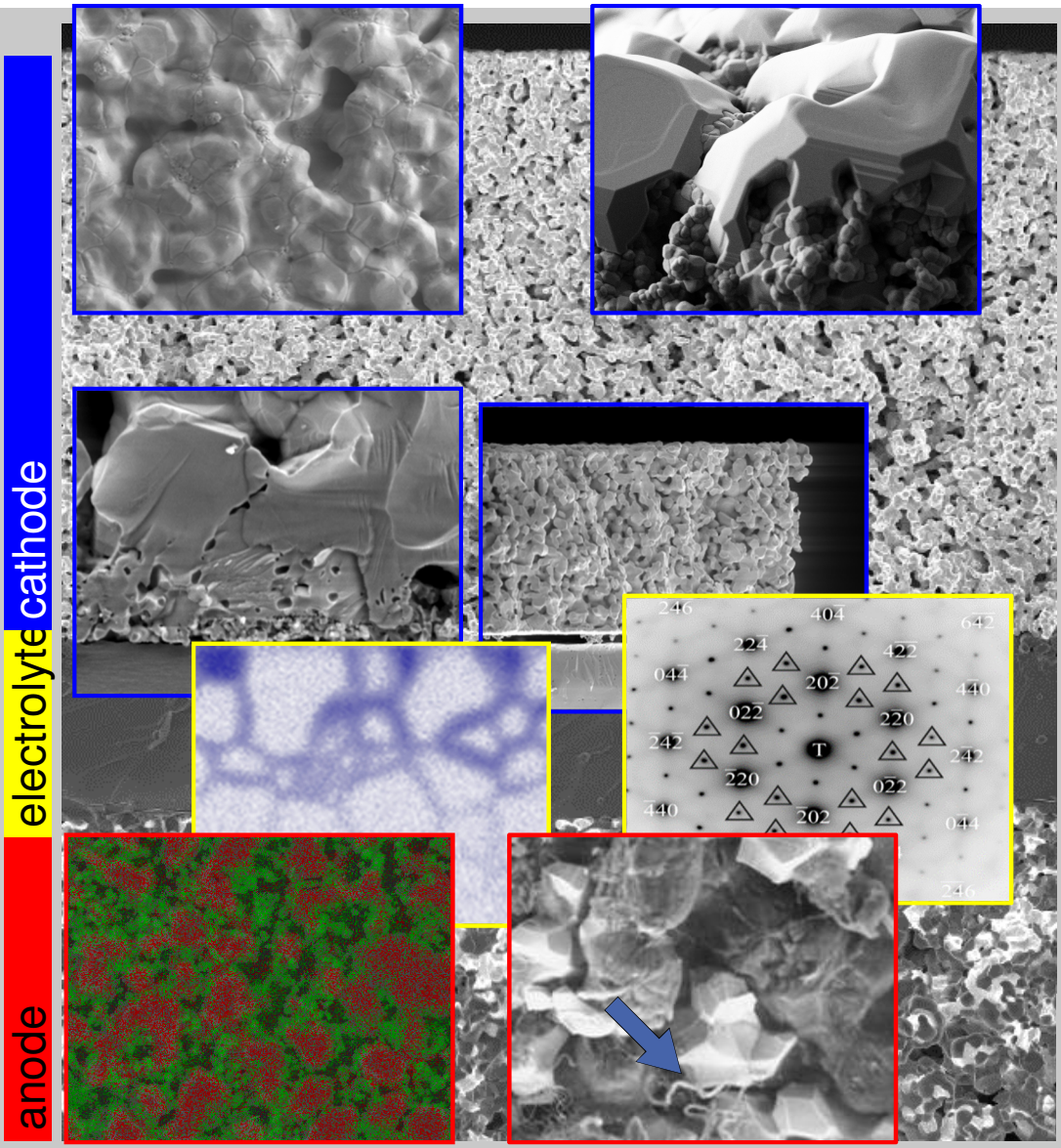

in SOFC many potentially competing degradation mechanisms are known:

- densification of electrodes
- formation of micropores
  A. Weber et. al., *Denki Kagaku* **64**, pp. 582-589 (1996).
- formation of chromium compounds on the cathode
- delamination of the cathode
  M. J. Heneka et. al., Proc. 9th Int. Symp. on SOFC, pp. 534-543 (2005).
- Mn-interdiffusion
  A. Weber, in J. Garche (Ed.), Encyclopedia of Electrochemical Power Sources, Amsterdam: Elsevier, pp. 120-134 (2009).
- intrinsic electrolyte degradation
  B. Butz et. al., *Solid State Ionics* **177**, pp. 3275-3284 (2006).
- Ni-agglomeration
  A. C. Müller et. al., *Proc. 3rd European SOFC Forum*, pp. 353-362 (1998).
- carbon deposition
  E. Ivers-Tiffée et. al., *Handbook of Fuel Cells – Fundamentals, Technology and Applications*, pp. 933-956 (2009).

⇨ in addition, activation processes that improve the performance take place
A. Weber et. al., *Denki Kagaku* **64**, pp. 582-589 (1996).

Degradation Processes in Solid Oxide Fuel Cells
Electrolyte

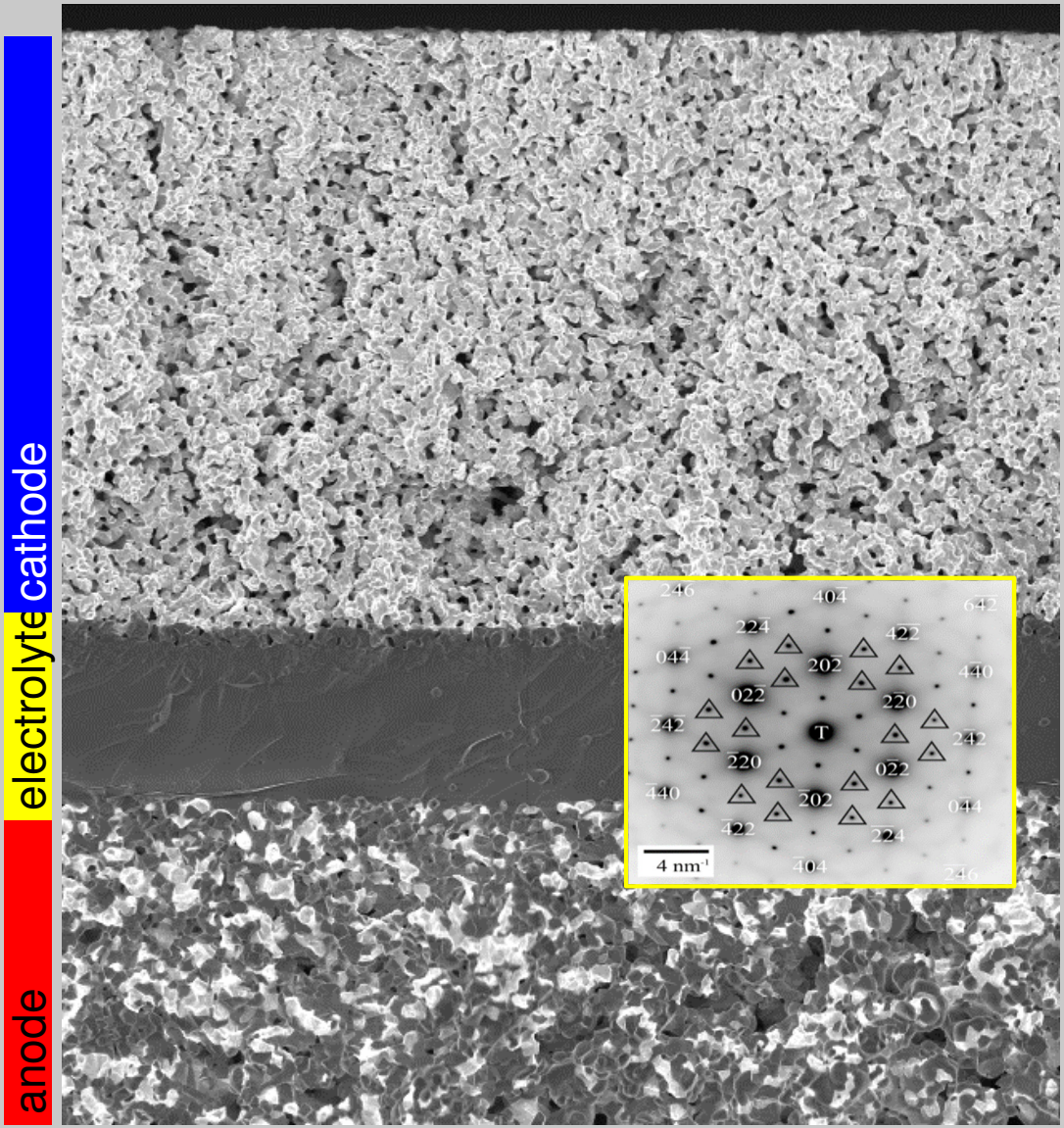

- intrinsic electrolyte degradation
  B. Butz et. al., *Solid State Ionics* **177**, pp. 3275-3284 (2006).

Long term stability of of ZrO2 – Me2O3 Oxide Ion Conductors
FSZ: 8YSZ

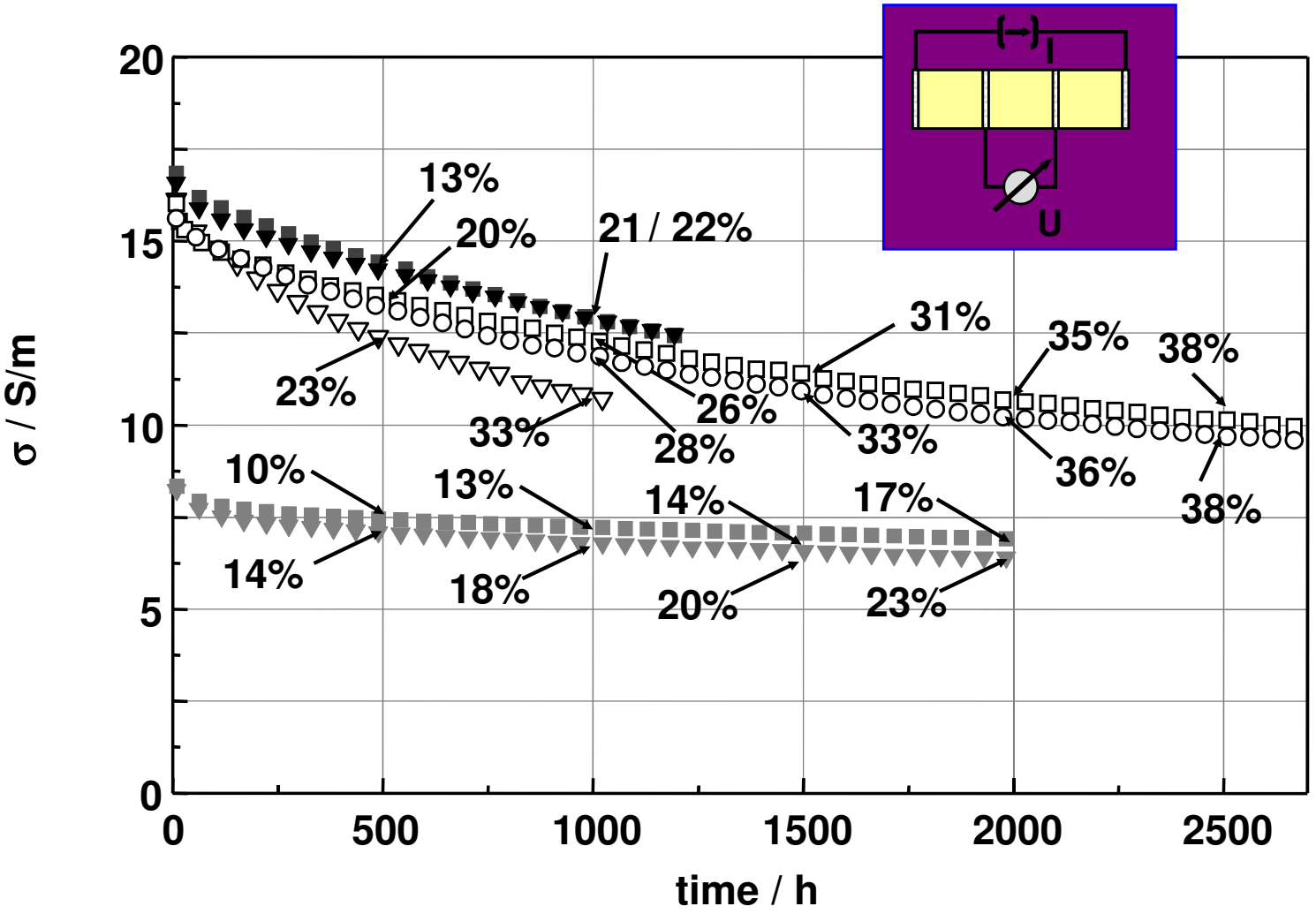

T_{op}=956°C, 170mA/cm²

○ 8YSZ, T_{sint}=1550°C

□ 8YSZ, RCS @ 1500°C

▽ 8YSZ, RCS @ 1350°C

T_{op}=956°C, 600mA/cm²

■ 8YSZ, RCS @ 1500°C

▼ 8YSZ, RCS @ 1350°C

T_{op}=861°C, 120mA/cm²

■ 8YSZ, RCS @ 1500°C

▼ 8YSZ, RCS @ 1350°C

RCS:
rate controlled sintering
constant shrinkage

Electrical Conductivity of Fluorites ZrO2 – Me2O3
Impact of various dopants on the conductivity of ZrO2

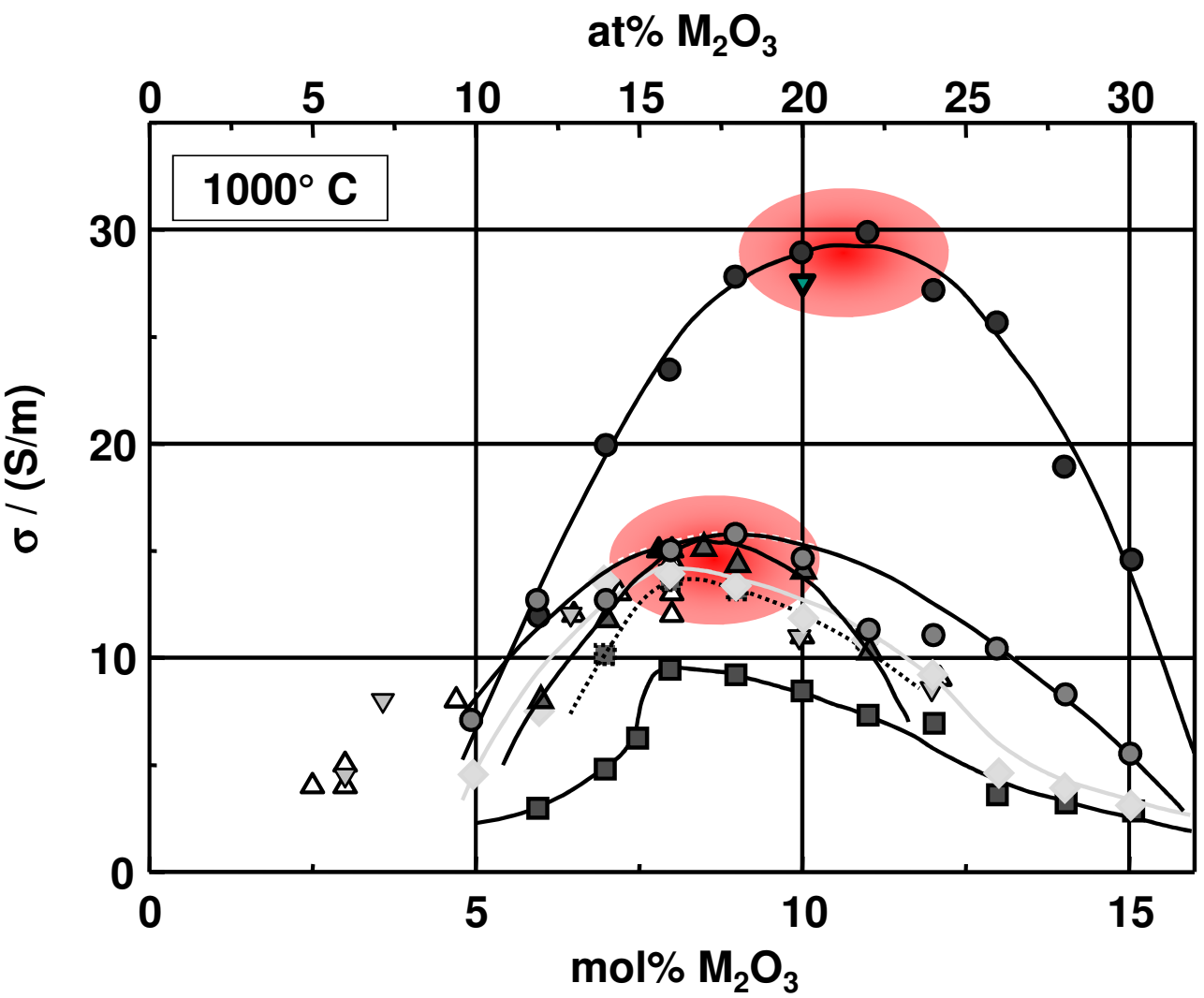

- Y [1]
- Y [2]
- Y [3]
- Gd [1]
- Yb [1]
- Er [1]
- Dy [1]
- Sc [1]
- Sc [4]

[1] O. Yamamoto, Electrochimica Acta 45, p. 2423 (2000)

[2] R. Männer, Electroceramics and Ceramics for Special Applications, Vol. 3, DKG (1992)

[3] Siemens, unpublished data

[4] D. Herbstritt, The Electrochemical Society, PV 2001-16, p. 349, (2001)

Long term stability of of ZrO2 – Me2O3 Oxide Ion Conductors FSZ: 10YSZ and 10ScSZ

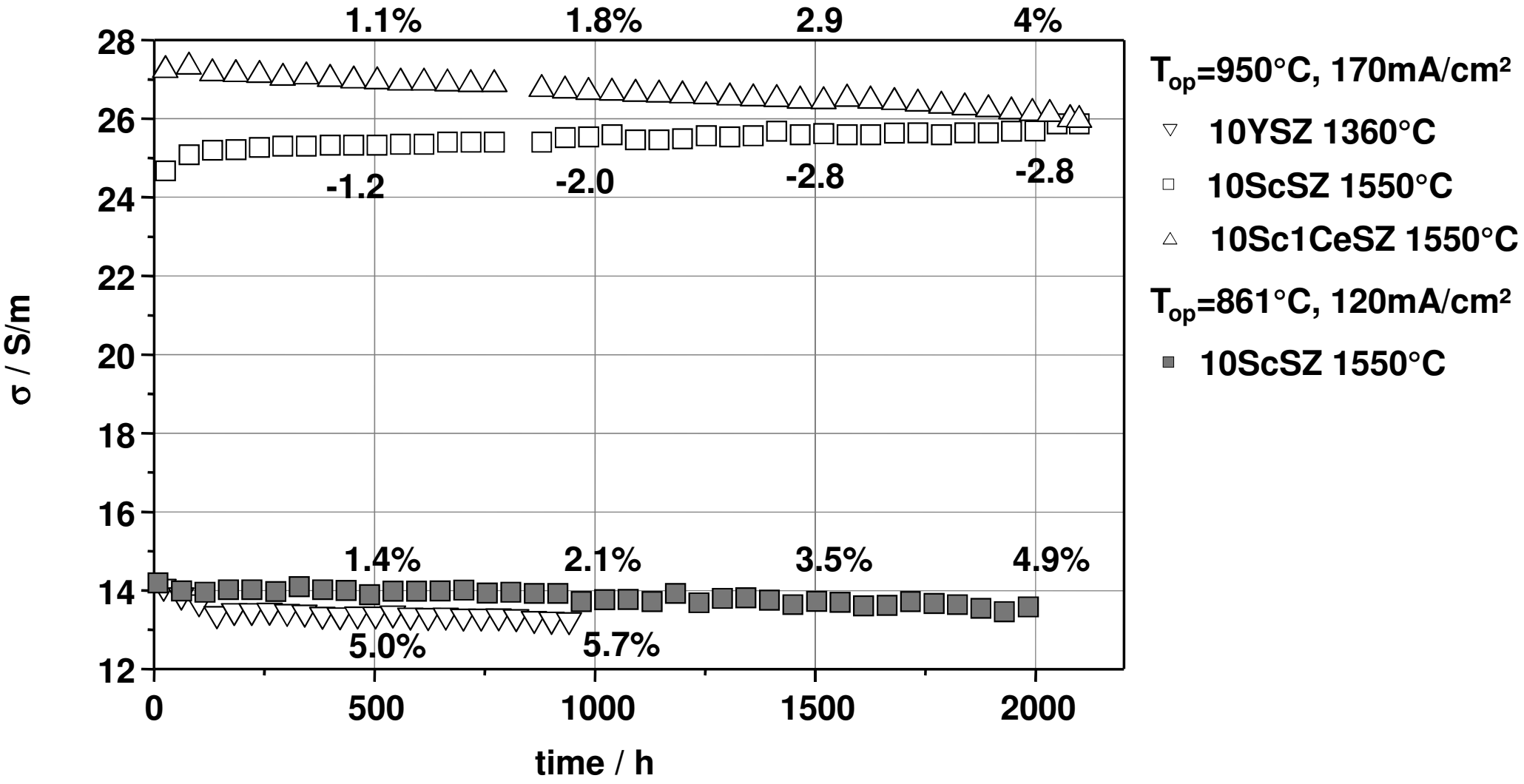

Electron diffraction: Tetragonal Phase

[110], [111], [112], [013], [123]

- Three variants of tetragonal phase:
  c-axis along all cubic <100>-axes
- Double diffraction in thicker sample regions

→ Clear identification of tetragonal phase
(no superstructures!)

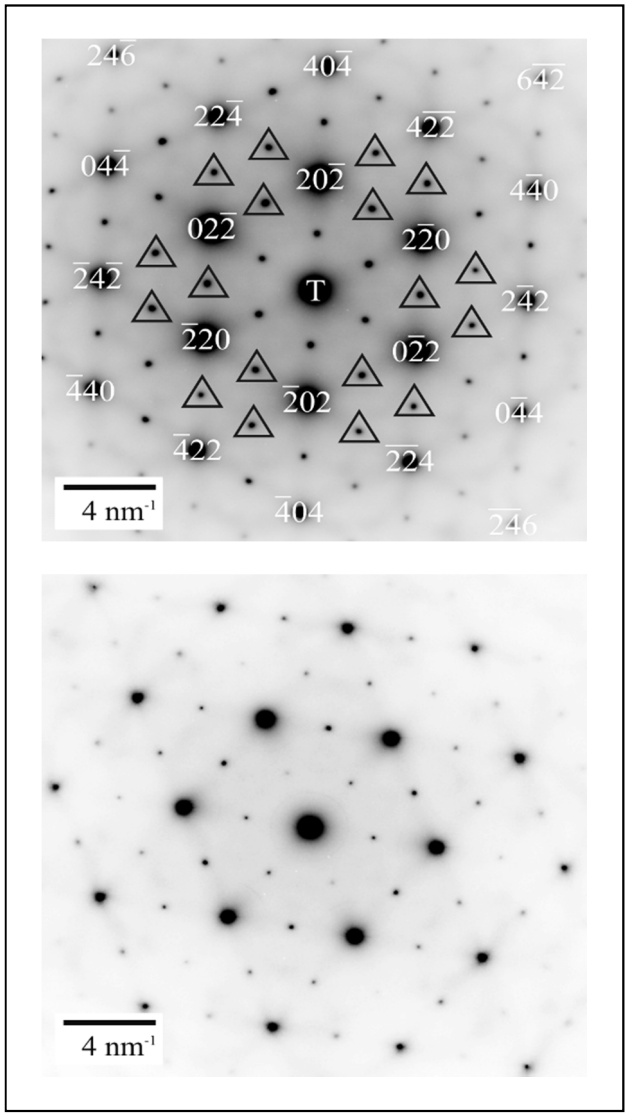

[111] 8YSZ

Electron diffraction

- Exists in 8YSZ and 10YSZ, not in 16YSZ
- Decreasing volume fraction with increasing doping concentration

→ Dark field images with tetragonal intensity

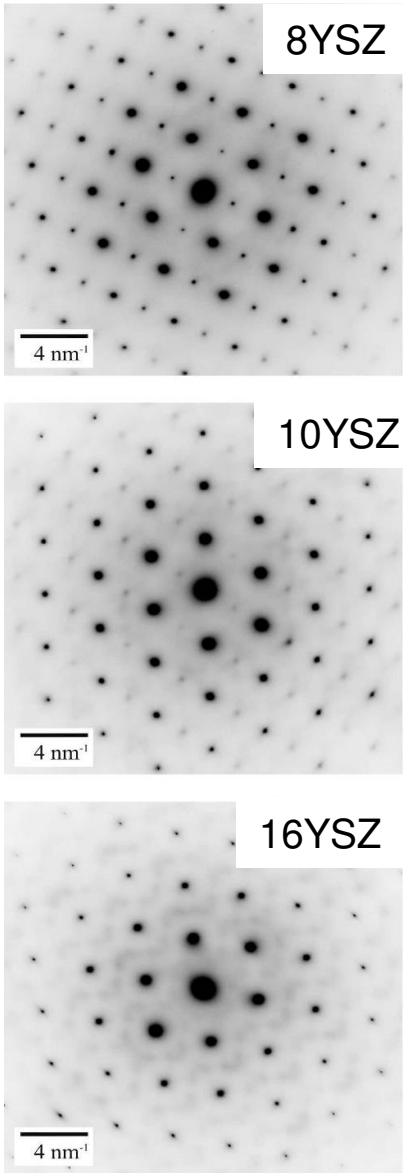

Degradation Processes in Solid Oxide Fuel Cells
Cathode & Cathode/Electrolyte-Interface

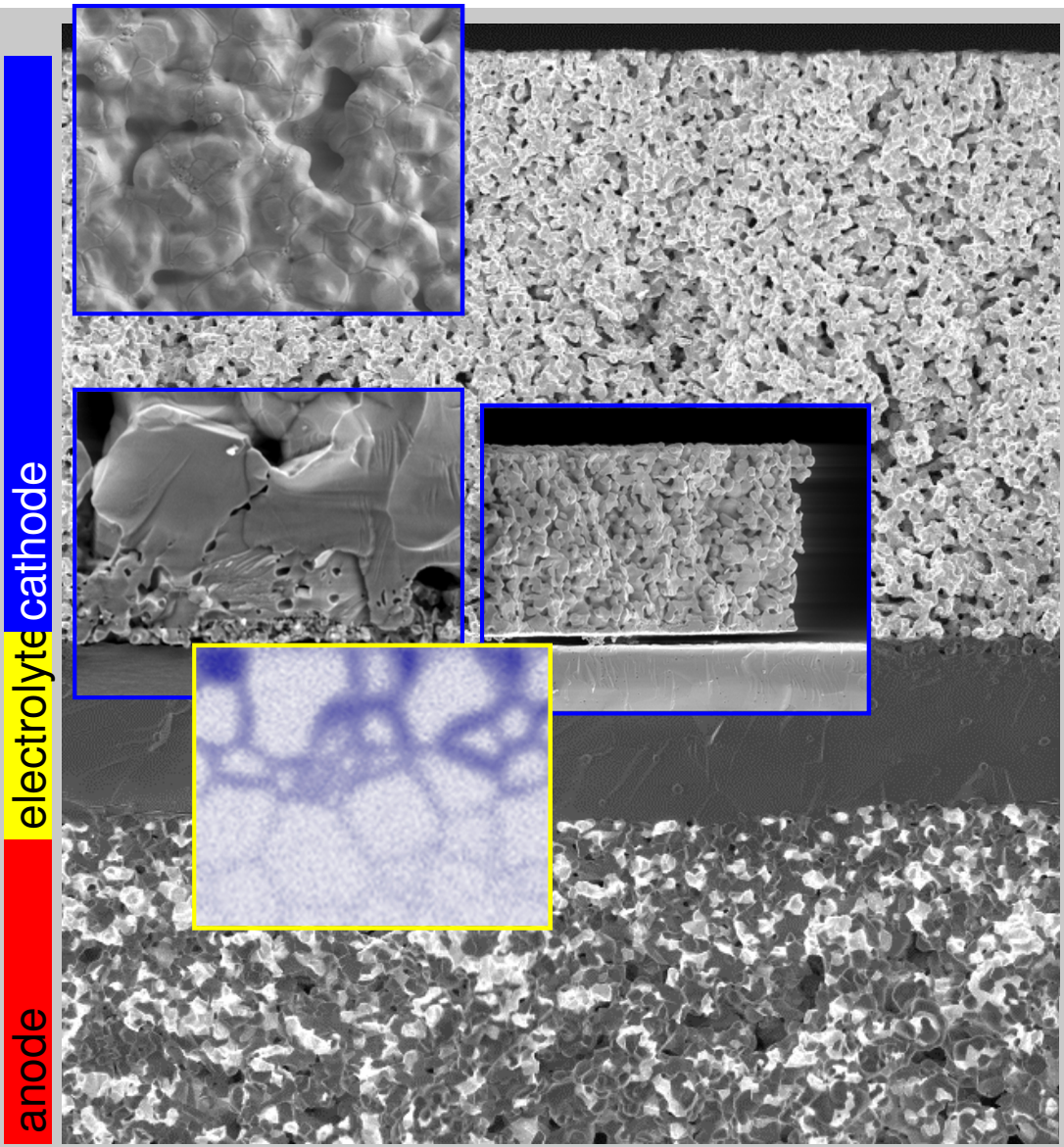

- densification of electrodes
- formation of micropores

  A. Weber et. al., *Denki Kagaku* **64**, pp. 582-589 (1996).

- delamination of the cathode

  M. J. Heneka et. al., Proc. 9th Int. Symp. on SOFC, pp. 534-543 (2005).

- Mn-interdiffusion

  A. Weber, in J. Garche (Ed.), Encyclopedia of Electrochemical Power Sources, Amsterdam: Elsevier, pp. 120-134 (2009).

⇨ in addition, activation processes that improve the performance take place

A. Weber et. al., *Denki Kagaku* **64**, pp. 582-589 (1996).

Stability of Interfaces

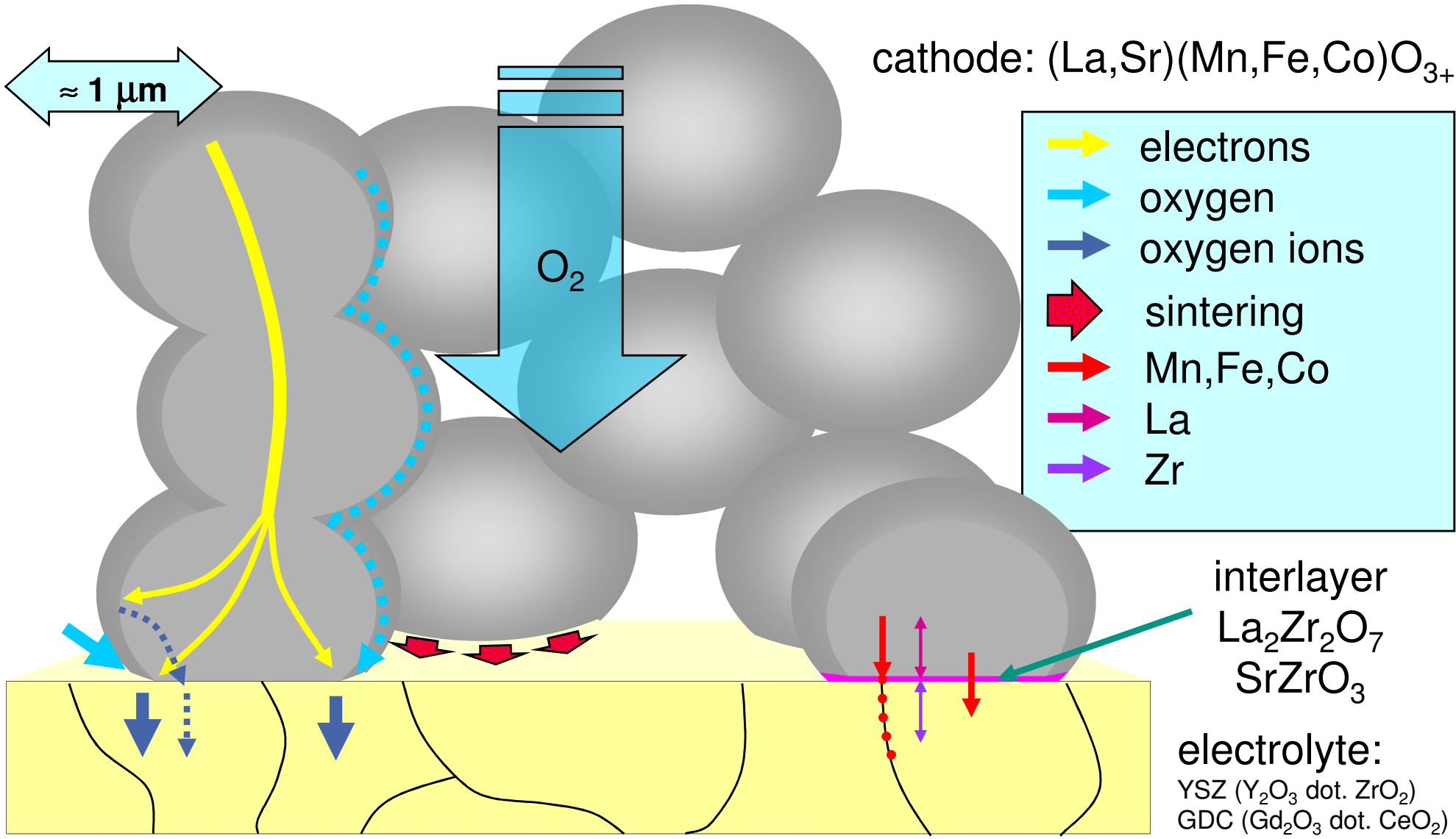

Startup Behavior of SOFC Single Cells and Stacks
Formation and Degradation

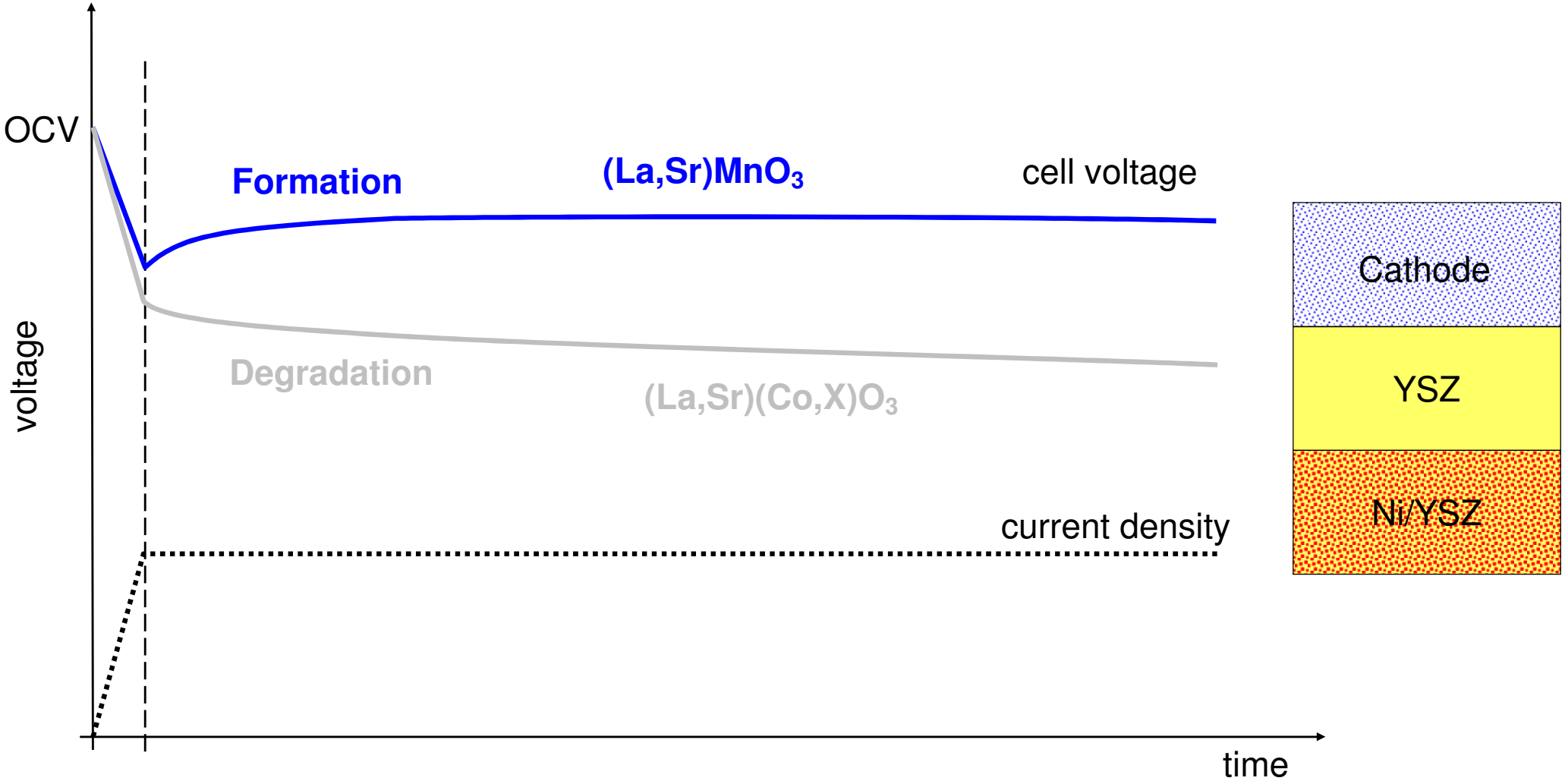

SOFC: Formation and Long Term Test of a tubular Cell Siemens-Westinghouse SWPC (1997)

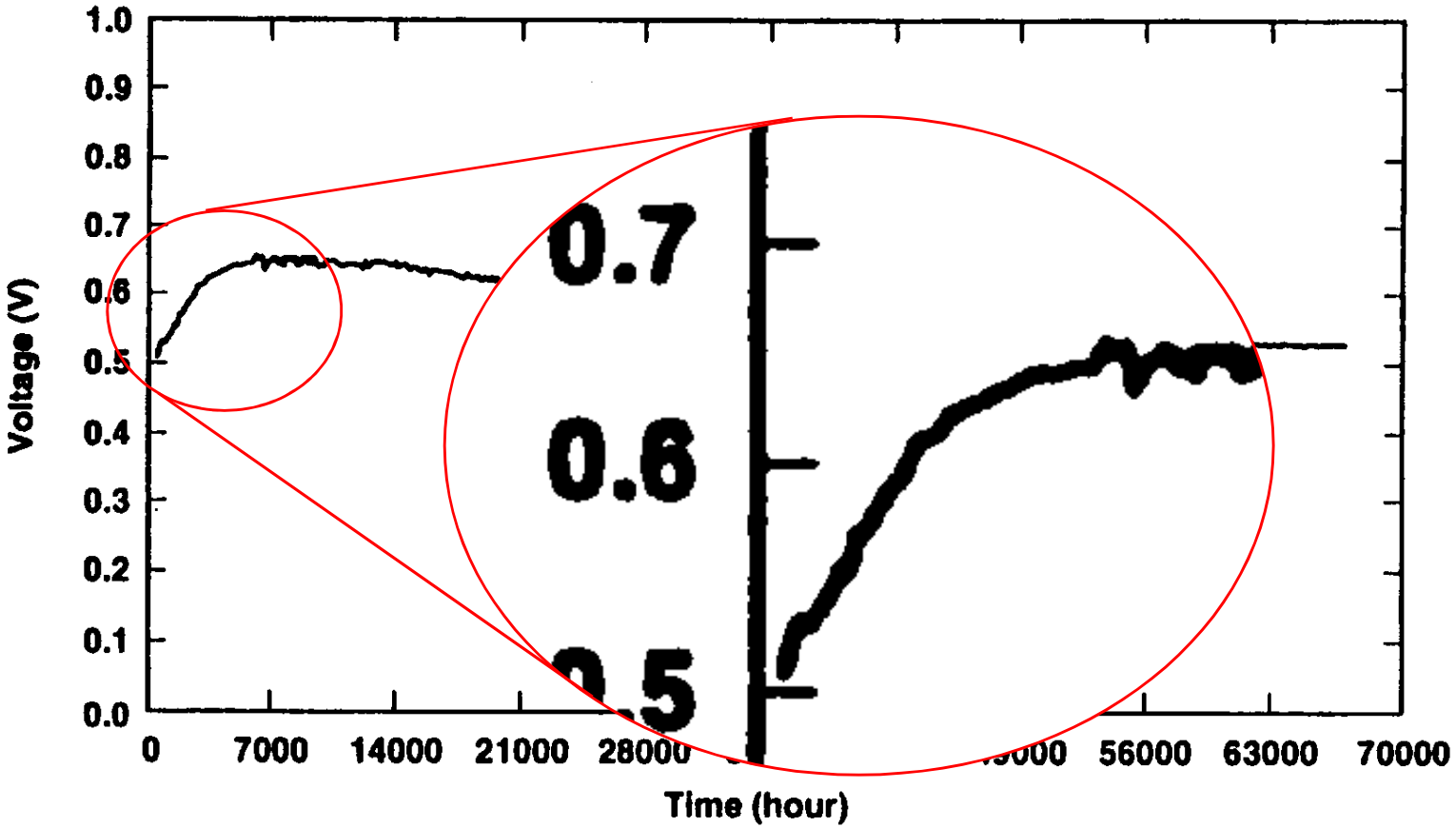

Fig. 1. Long term test of an early-technology PST cell.

V_{start} : 0.50 V

V_{max} : 0.65 V

► V_{max}: Point of max. performance

►time to V_{max} :

≈ 5.000 hours

S. C. Singhal, Recent Progress in Tubular Solid Oxide Fuel Cell Technology, Proc. 5th Int. Symposium on SOFC, Ed. U. Stimming, S. C. Singhal, H. Tagawa, W. Lehnert, The Electrochemical Society, PV 97-40, 37-50, (1997)

SOFC: Formation and Long Term Test of a 5-cell Stack Sulzer Hexis (1999)

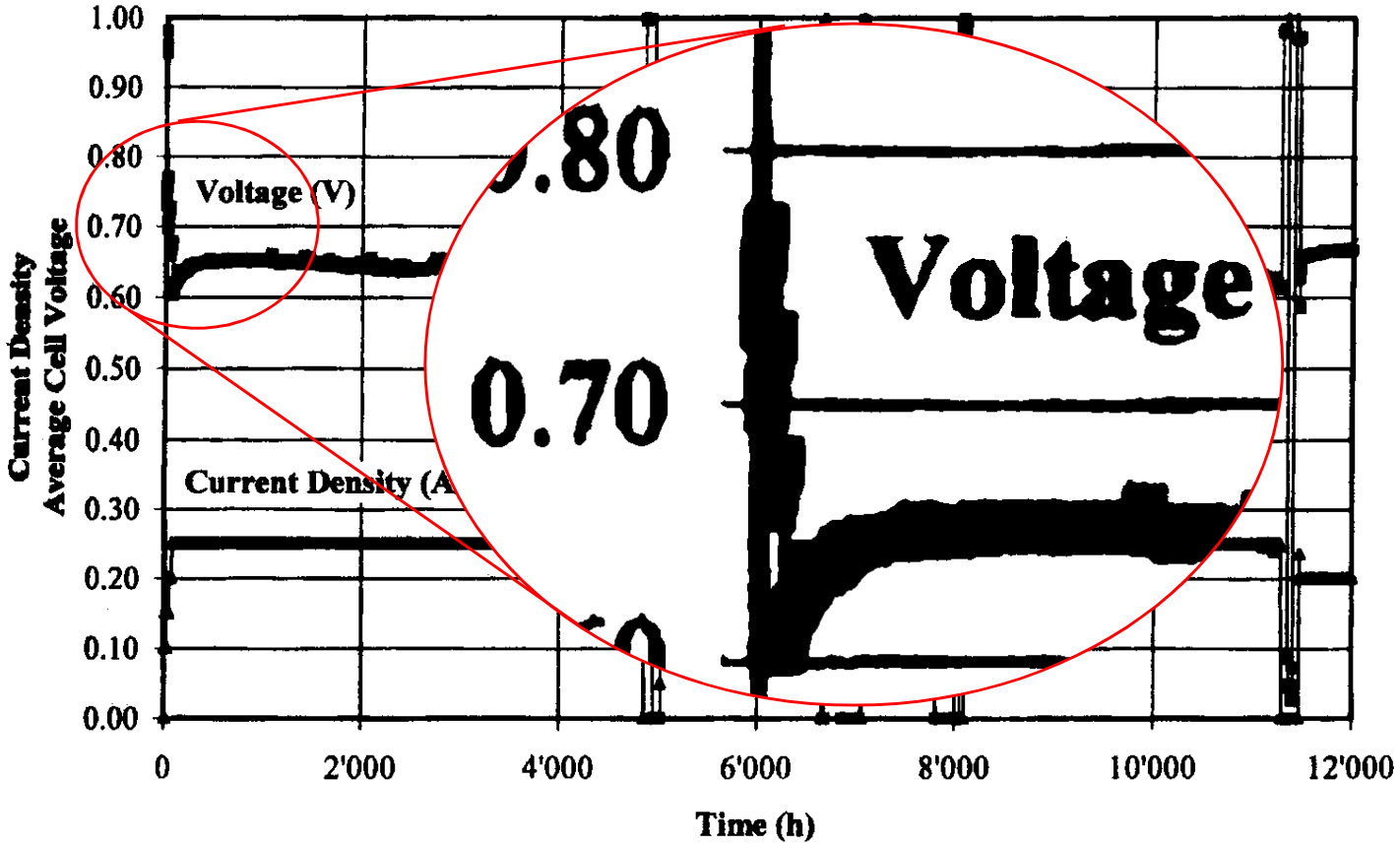

Figure 2: Negligible degradation of a five cell stack

V_{start} : 0.60 V

V_{max} : 0.65 V

► V_{max}: Point of max. performance

► time to V_{max} :

≈ 200 hours

R. Diethelm, M. Schmidt, Status of the Sulzer Hexis Product Development, Proc. 6th Int. Symp. on SOFC, Ed. S. Singhal und M. Dokiya, The Electrochemical Society, PV 99-19, 60-67, (1999)

SOFC: Formation and Long Term Test of a planar Cell Ceramic Fuel Cells Ld. CFCL (1999)

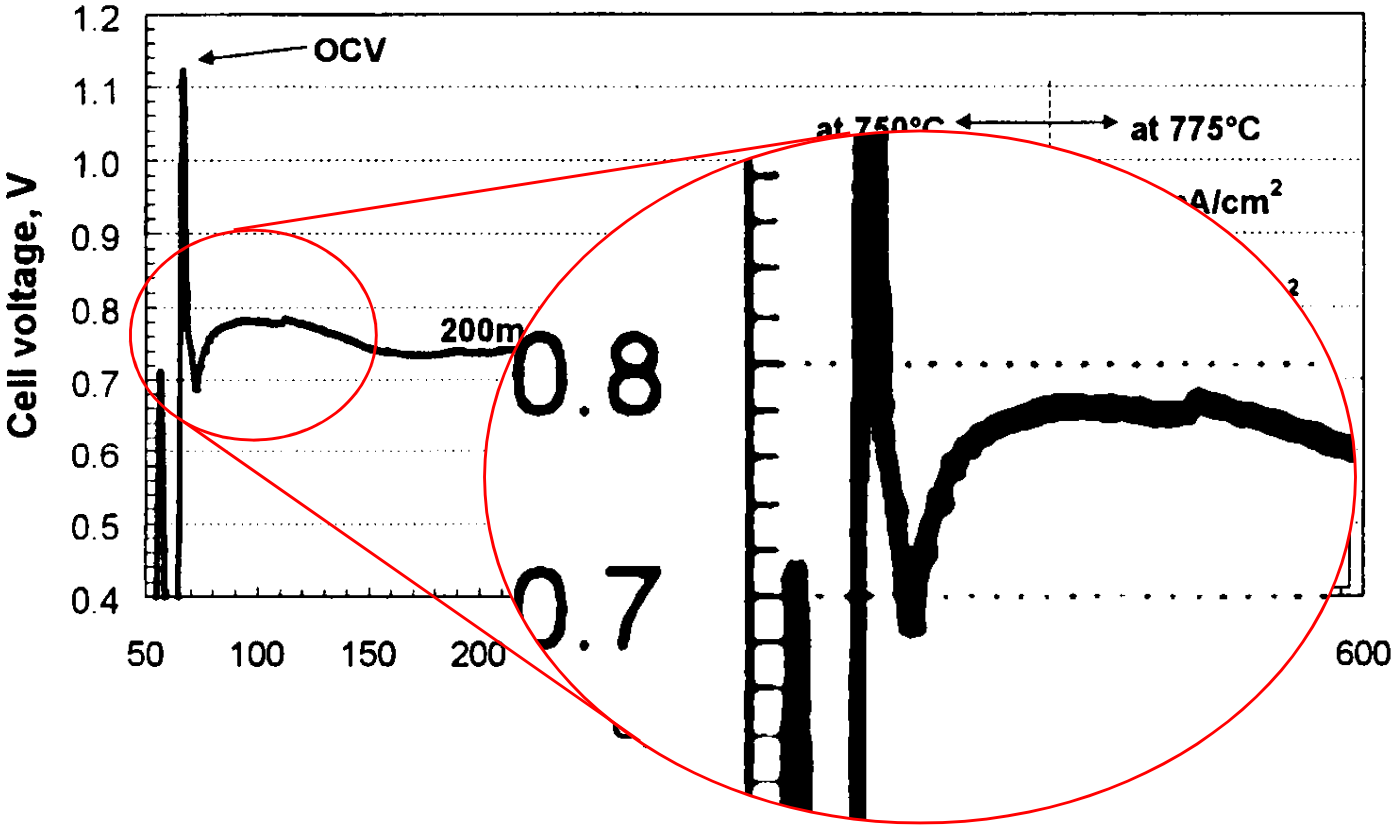

Figure 2. Cell performance at 750 and 775°C tested in alumina assembly

V_{start} : 0.68 V

V_{max} : 0.78 V

► V_{max}: Point of max. performance

► time to V_{max} : ≈ 50 hours

K. Föger et al., Demonstration of Anode Supported Cell Technology in kW Class Stack, Proc. 6th Int. Symp. on SOFC, Ed. S. Singhal und M. Dokiya, The Electrochemical Society, 95-100, PV 99-19, (1999)

SOFC: Formation and Long Term Test of a 1 kW Stack Mitsubishi Heavy Industries MHI (1999)

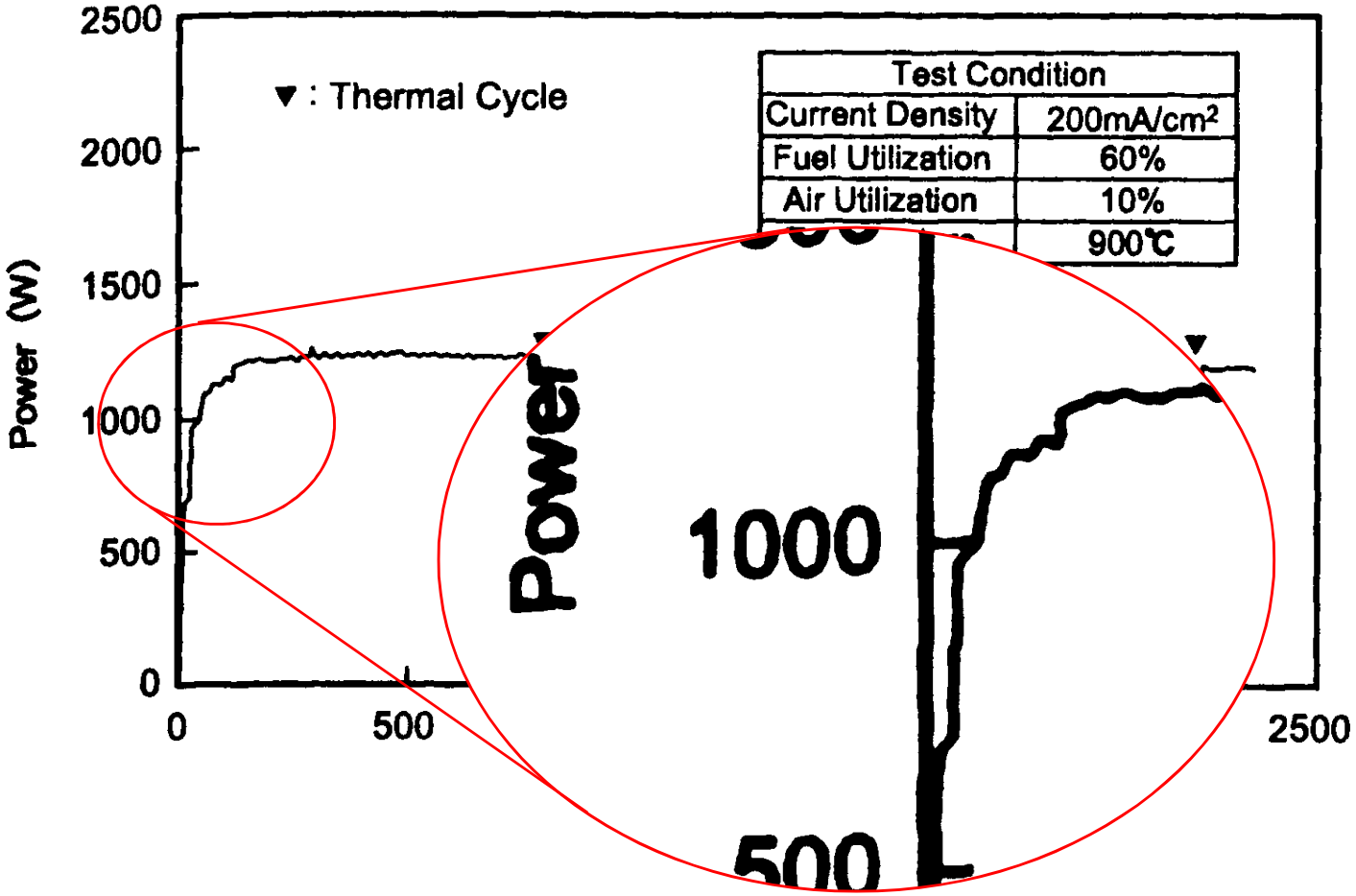

Fig. 12 Endurance Test of 1kW Module with Co-Sintered Cell Stack

P_{start} : 700 W

P_{max} : 1250 W

► P_{max}: Point of max. performance

► time to P_{max} :

≈ 300 hours

H. Mori et al., Pressurized 10 kW Class Module of SOFC, Proc. 6th Int. Symp. on SOFC, Ed. S. Singhal und M. Dokiya, - The Electrochemical Society, PV 99-19, 52-59, (1999)

Grenzfläche Kathode-Elektrolyt vor und nach Aktivierung Mikrostruktur

unbelastete MEA

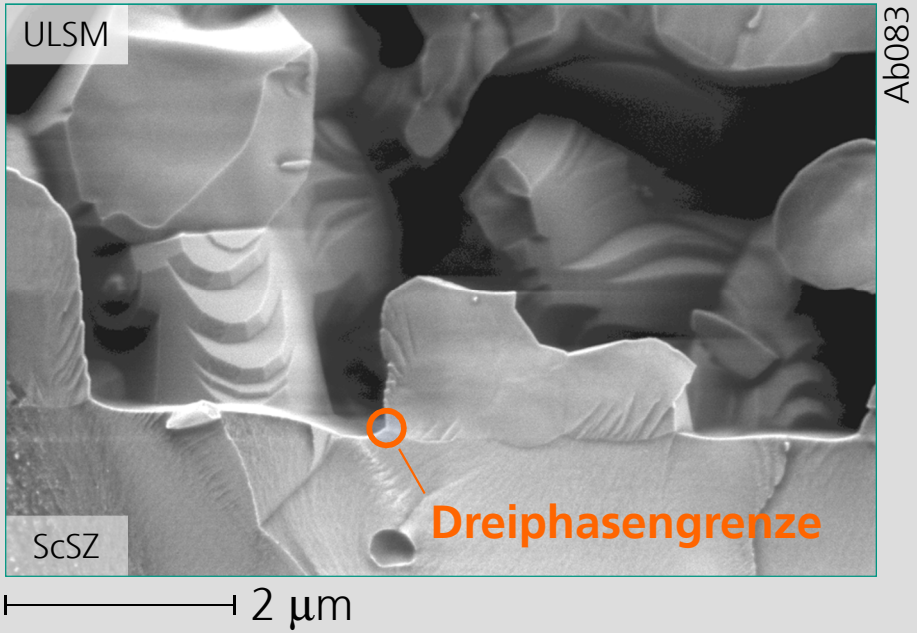

nach Aktivierung

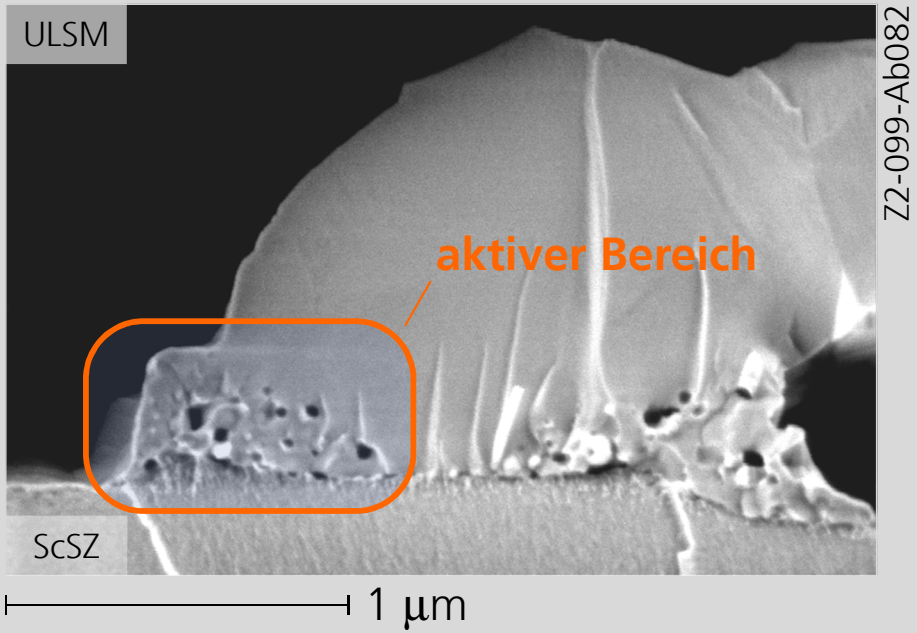

- Bildung eines porösen Bereichs im ULSM-Korn nahe der Grenzfläche unter Belastung
- Reaktionsraum vergrößert ⇨ höhere elektrochemische Leistungsfähigkeit der Kathode

Grenzfläche Kathode-Elektrolyt vor und nach Aktivierung
Chemische Zusammensetzung

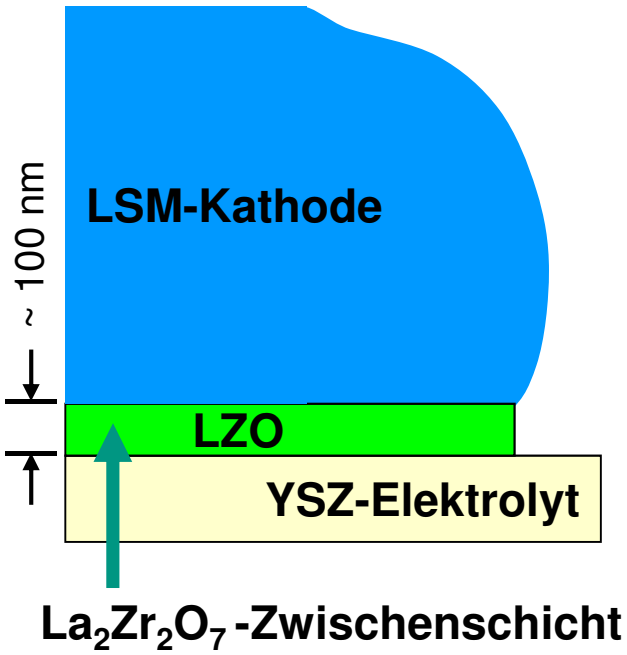

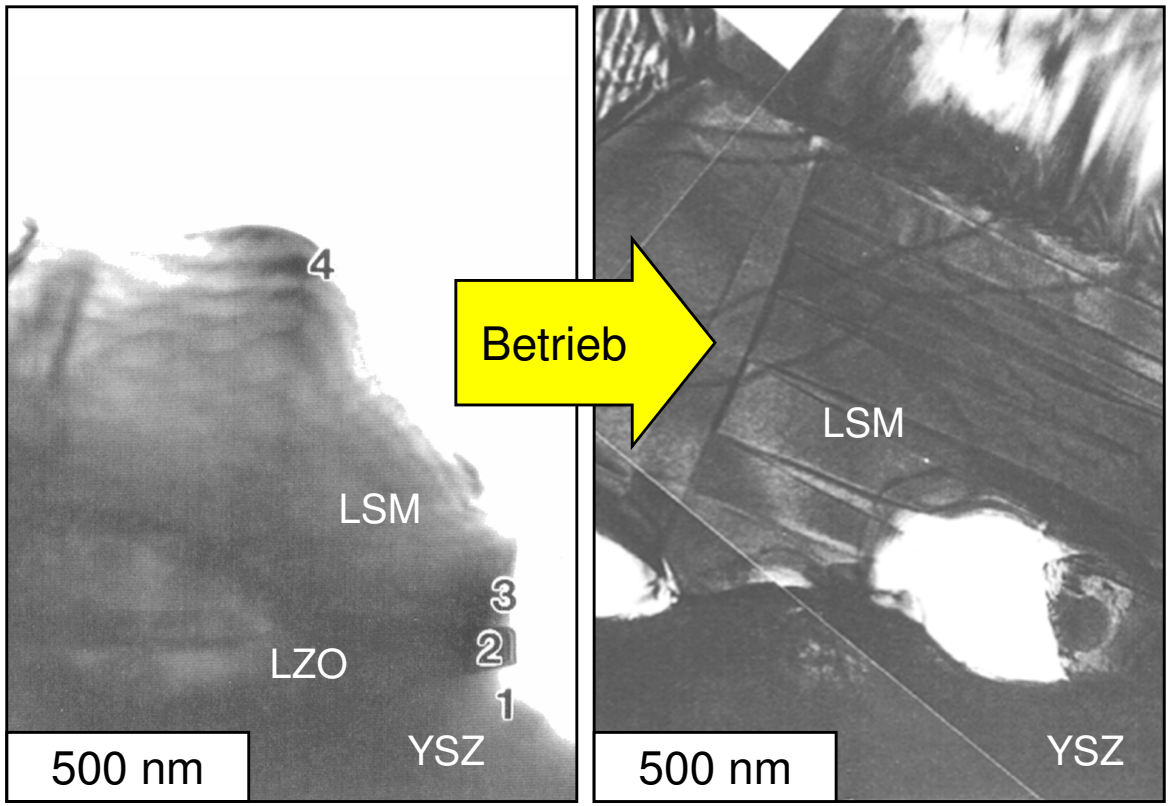

- **Abbau der $La_2Zr_2O_7$-Zwischenschicht**

Startup Behavior of SOFC Single Cells and Stacks
Formation and Degradation

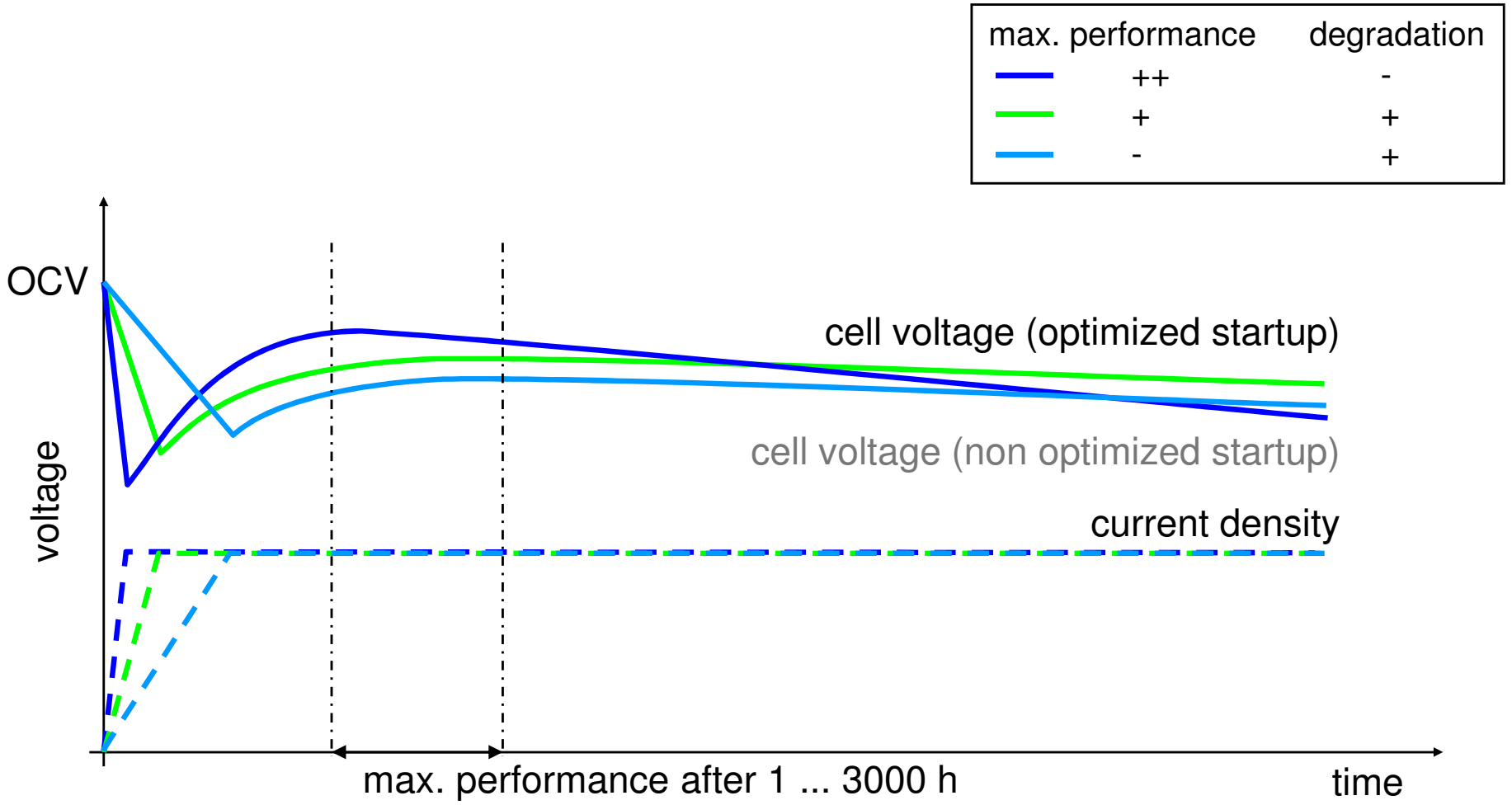

Modeling of Degradation Phenomena
Chemical Potential Diagrams and Thermodynamic Equilibrium Calculations

MALT (MAterials oriented Little Thermodynamic database*)

$\Delta_f G°$, $\Delta_f H°$, $S°$, $C_p°$ at 298.15 K

temperature coefficients of heat capacities, transition temperatures, transition enthalpies

Calculation of Chemical Potential Diagrams
(CHD)

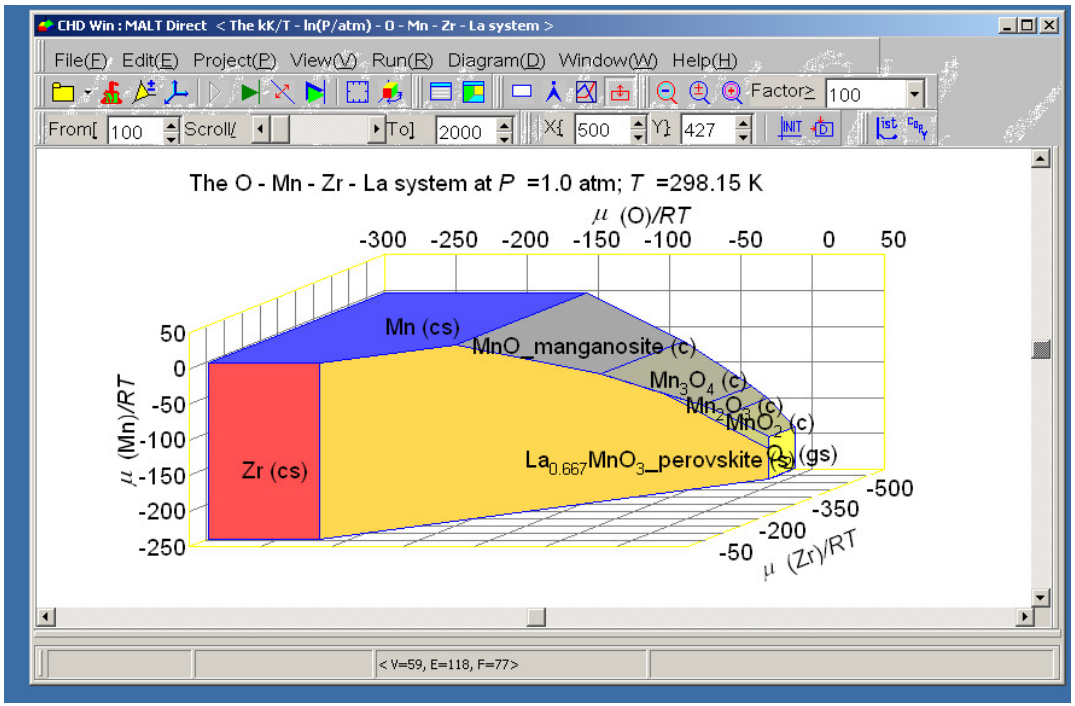

Thermodynamic Equilibrium Calculations
(GEM: Gibbs Energy Minimizer)

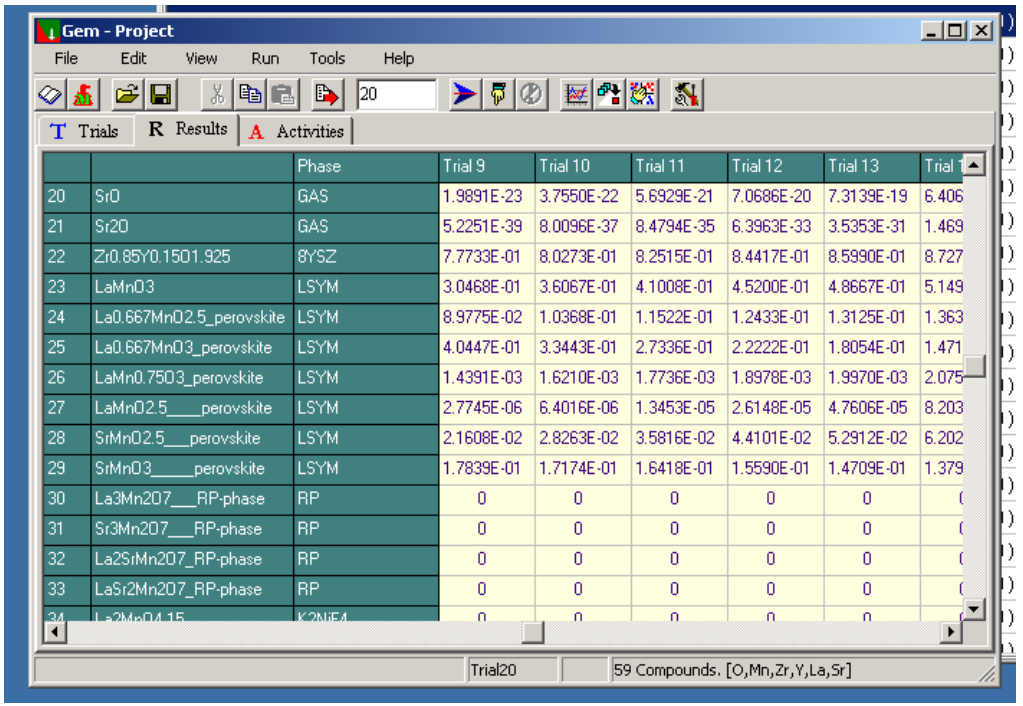

		Phase	Trial 9	Trial 10	Trial 11	Trial 12	Trial 13
20	SrO	GAS	1.9891E-23	3.7550E-22	5.6929E-21	7.0686E-20	7.3139E-19
21	Sr2O	GAS	5.2251E-39	8.0096E-37	8.4794E-35	6.3963E-33	3.5353E-31
22	Zr0.85Y0.1501.925	8YSZ	7.7733E-01	8.0273E-01	8.2515E-01	8.4417E-01	8.5990E-01
23	LaMnO3	LSYM	3.0468E-01	3.6067E-01	4.1008E-01	4.5200E-01	4.8667E-01
24	La0.667MnO2.5_perovskite	LSYM	8.9775E-02	1.0368E-01	1.1522E-01	1.2433E-01	1.3125E-01
25	La0.667MnO3_perovskite	LSYM	4.0447E-01	3.3443E-01	2.7336E-01	2.2222E-01	1.8054E-01
26	LaMn0.7503_perovskite	LSYM	1.4391E-03	1.6210E-03	1.7736E-03	1.8978E-03	1.9970E-03
27	LaMnO2.5___perovskite	LSYM	2.7745E-06	6.4016E-06	1.3453E-05	2.6148E-05	4.7606E-05
28	SrMnO2.5___perovskite	LSYM	2.1608E-02	2.8263E-02	3.5816E-02	4.4101E-02	5.2912E-02
29	SrMnO3_____perovskite	LSYM	1.7839E-01	1.7174E-01	1.6418E-01	1.5590E-01	1.4709E-01
30	La3Mn2O7___RP-phase	RP	0	0	0	0	0
31	Sr3Mn2O7___RP-phase	RP	0	0	0	0	0
32	La2SrMn2O7_RP-phase	RP	0	0	0	0	0
33	LaSr2Mn2O7_RP-phase	RP	0	0	0	0	0

*** H. Yokokawa et al.,Thermochimica Acta 245, 45-55 (1994)**
MALT for Windows, see http://www.kagaku.com/malt/index.html

Modeling of Degradation Phenomena
Chemical Potential Diagram for the polarized LSM / 8YSZ - Interface

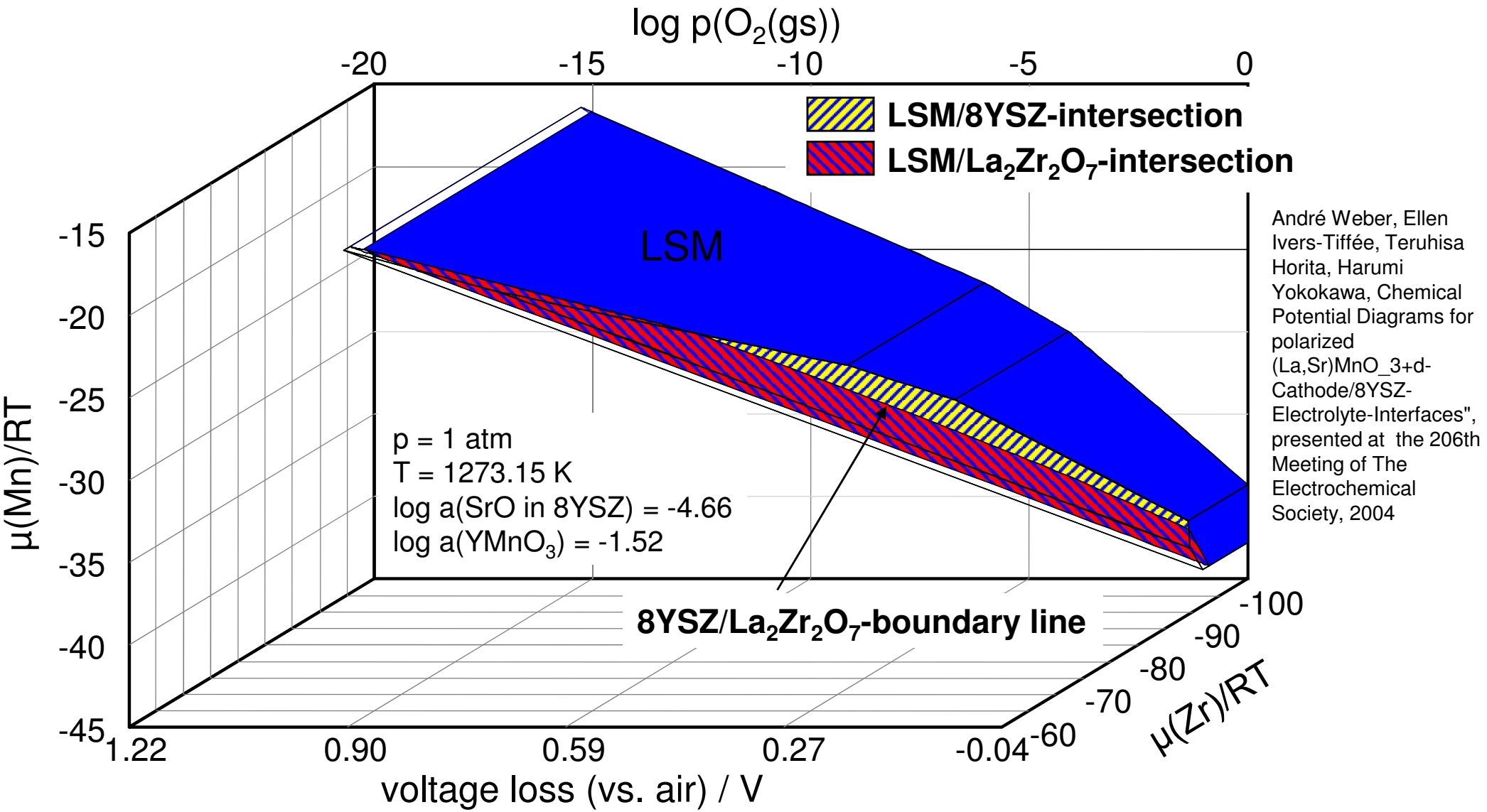

André Weber, Ellen Ivers-Tiffée, Teruhisa Horita, Harumi Yokokawa, Chemical Potential Diagrams for polarized (La,Sr)MnO_3+d-Cathode/8YSZ-Electrolyte-Interfaces", presented at the 206th Meeting of The Electrochemical Society, 2004

Modeling of Degradation Phenomena
Formation of insulating LZO-layers at the LSM/8YSZ Interface

calculated amount of LZO

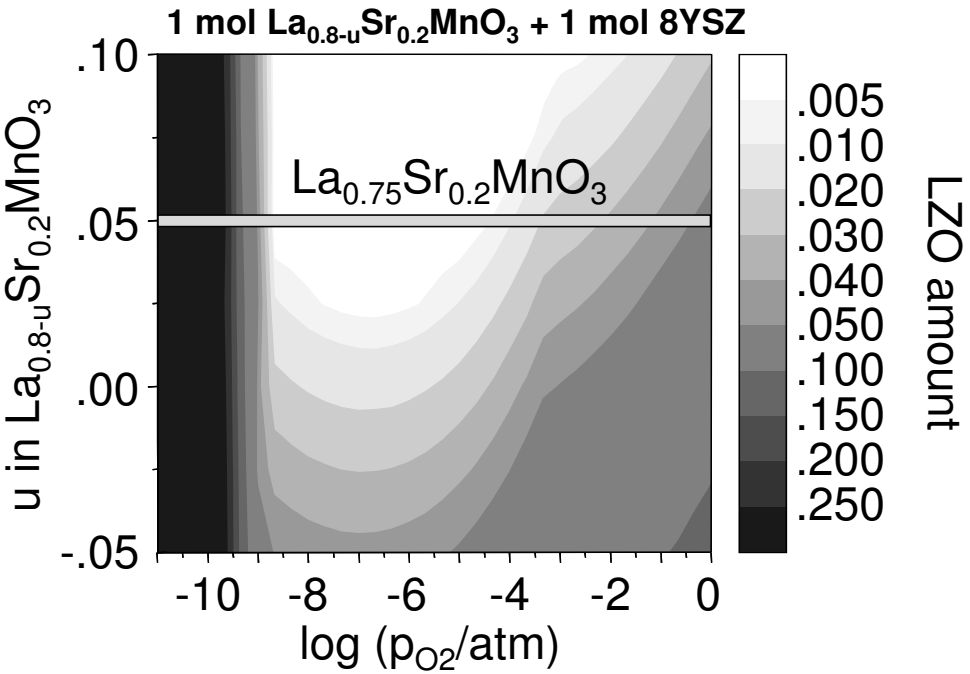

impact of cathode overvoltage η_{cat}

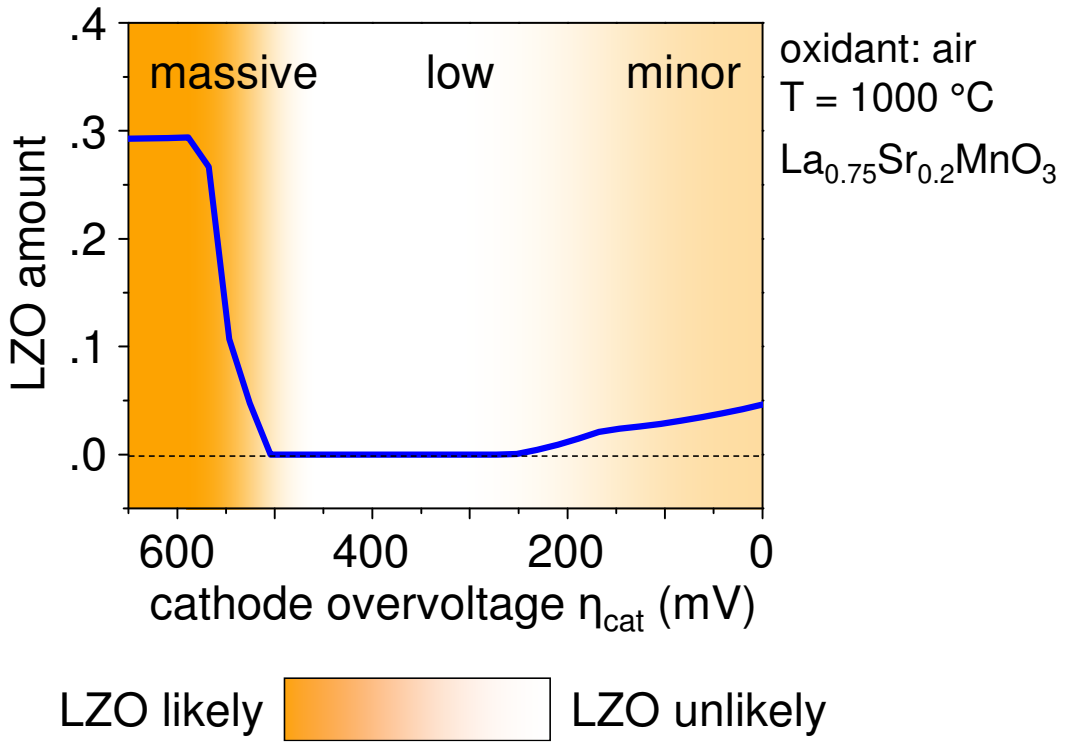

M. J. Heneka, E. Ivers-Tiffée: Degradation of SOFC Single Cells Under Severe Current Cycles. In: S. C. Singhal, J. Mizusaki (Hrsg.), Proc. 9th Int. Symp. on SOFC, PV 2005-07, The Electrochemical Society, 534-543 (2005)

Cathode Degradation
Growth of Secondary Phases at the Cathode/Electrolyte-Interface

Interface LSM/YSZ
(LSM: $La_{0.8}Sr_{0.2}MnO_{3+\delta}$)

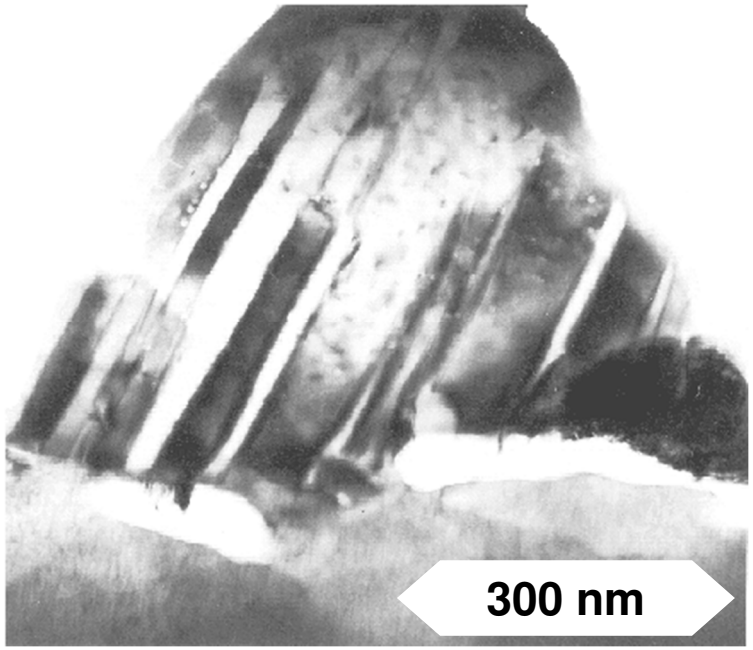

LSM cathode

YSZ electrolyte

Interface LSCM/YSZ
(LSMC: $La_{0.8}Sr_{0.2}Co_{0.5}Mn_{0.5}O_{3+\delta}$)

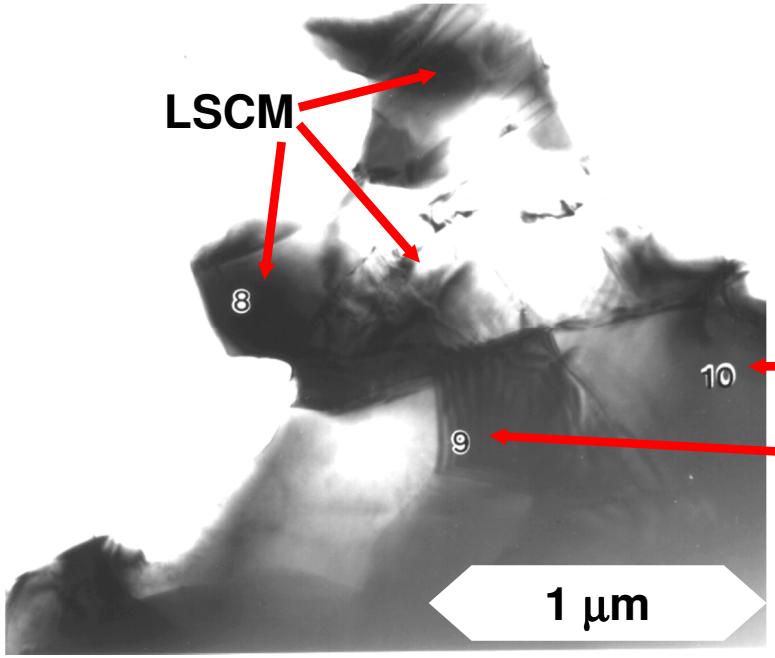

LSCM cathode

$La_2Zr_2O_7$

$SrZrO_3$

YSZ electrolyte

Low Cathode Resistance
after Formation

High Cathode Resistance
Growth of Secondary Phases

Startup Behavior of SOFC Single Cells and Stacks
Formation and Degradation

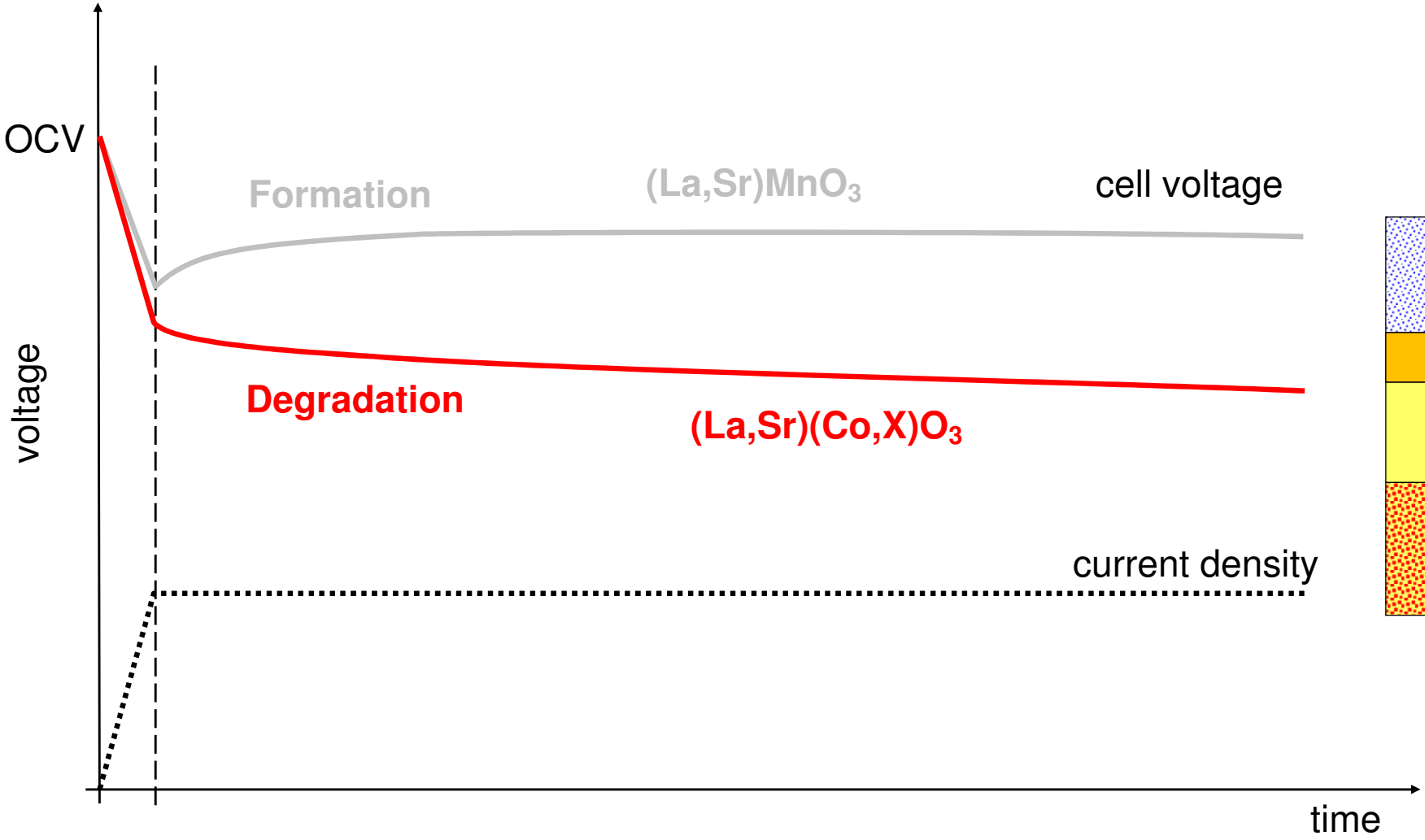

Cathode/Electrolyte Interface

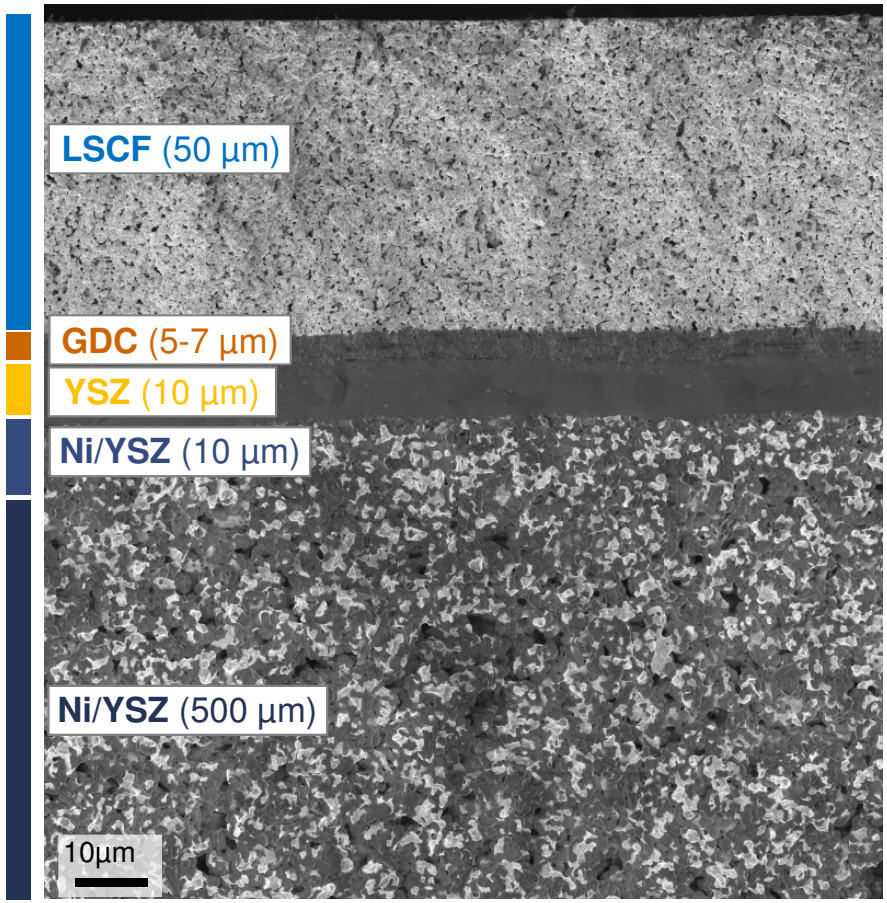

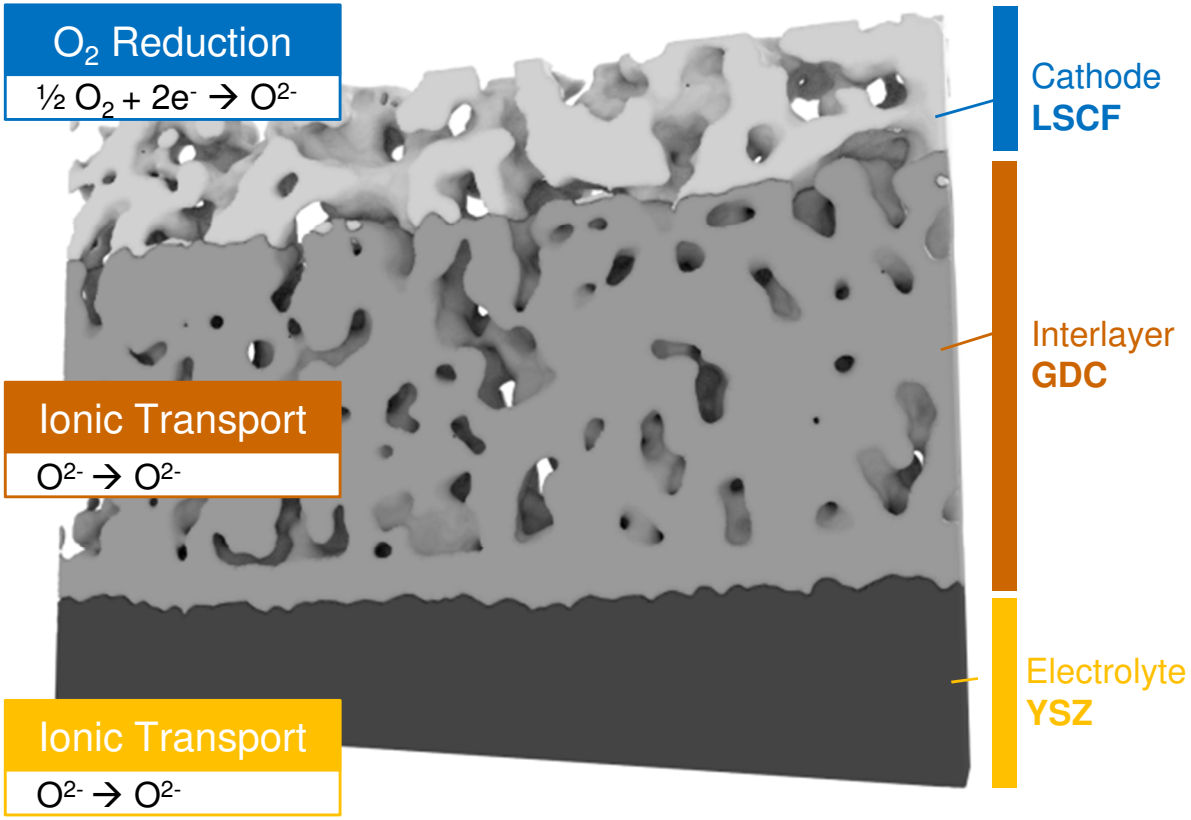

LSCF $La_{0.58}Sr_{0.4}Co_{0.2}Fe_{0.8}O_{3-\delta}$
GDC $Ce_{0.8}Gd_{0.2}O_{2-\delta}$
YSZ $Y_{0.16}Zr_{0.84}O_{2-\delta}$

Cathode/Electrolyte Interface
Distribution of Secondary Phases

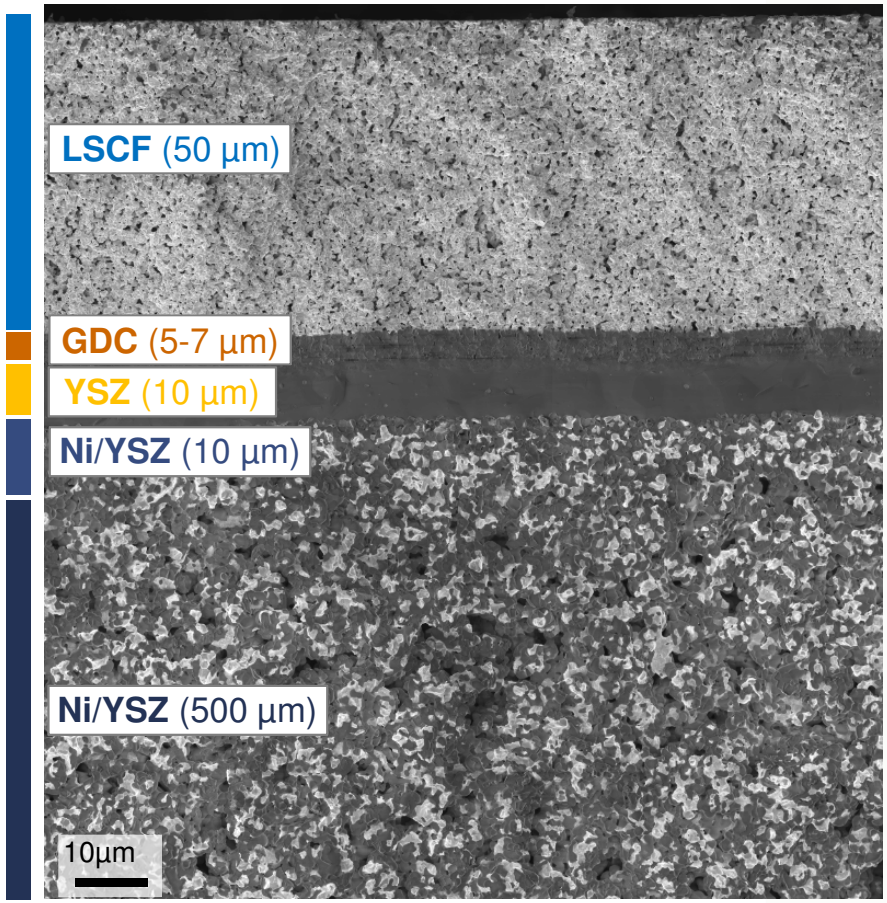

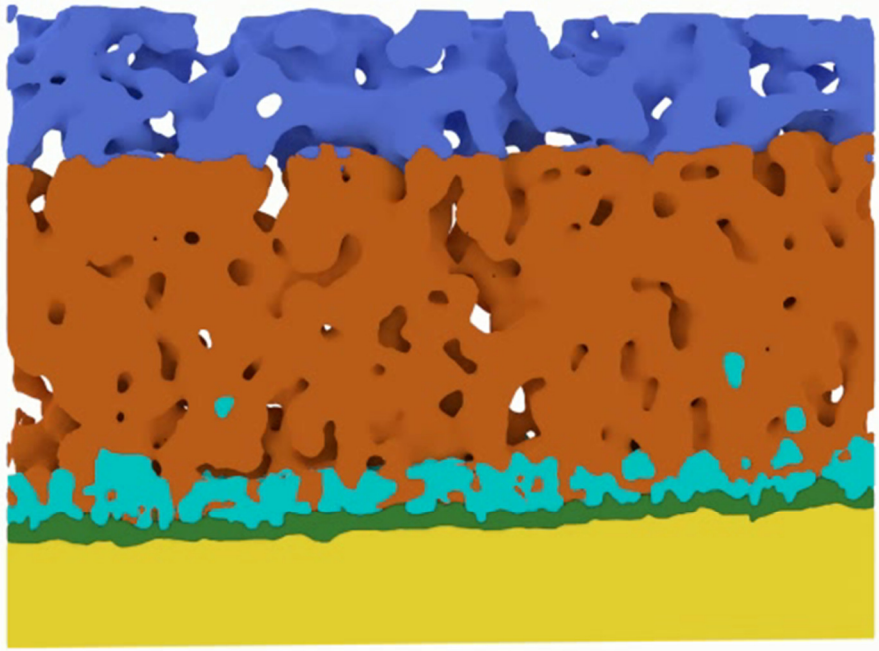

FIB/SEM focused ion beam / scanning electron microscopy **EHT** extra-high tension voltage
STEM/EDXS scanning transmission electron microscopy / energy dispersive x-ray spectroscopy

[1] J. Szász, F. Wankmüller, V. Wilde, H. Störmer, D. Gerthsen, and E. Ivers-Tiffée, *ECS Trans.*, vol. 66, no. 2, pp. 79–87, 2015.
[2] J. Szász, F. Wankmüller, V. Wilde, H. Störmer, D. Gerthsen, and E. Ivers-Tiffée, *ECS Trans.*, vol. 68, no. 1, pp. 763–771, 2015.
[3] F. Wankmüller, J. Szász, V. Wilde, H. Störmer, D. Gerthsen, and E. Ivers-Tiffée, *12th EFCF Proceedings*, 2016.

Quelle: IAM-ET

Cathode/Electrolyte Interface
Impact of Processing Conditions

GDC sintering temperature

1100°C 1200°C 1300°C 1400°C

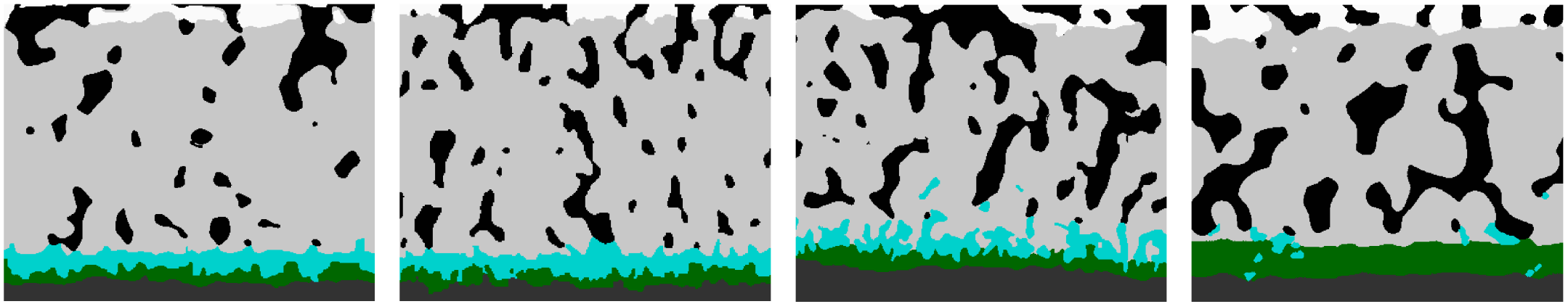

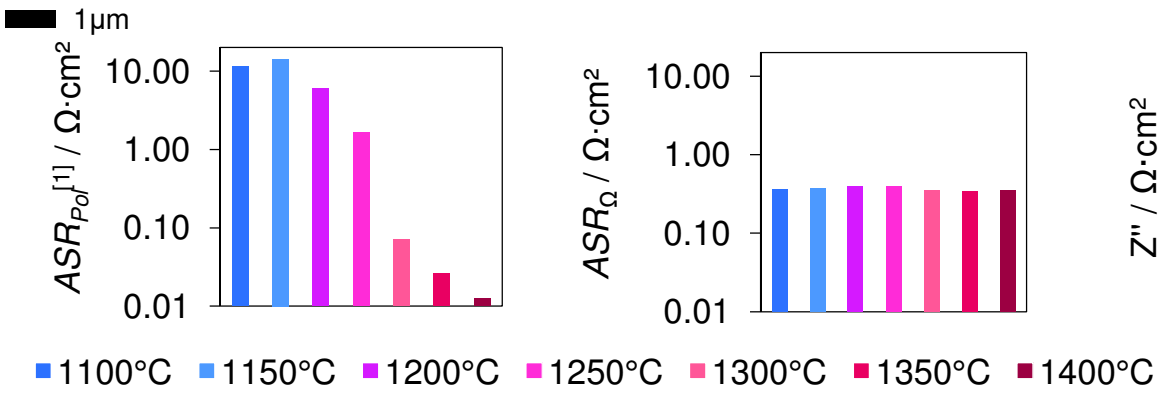

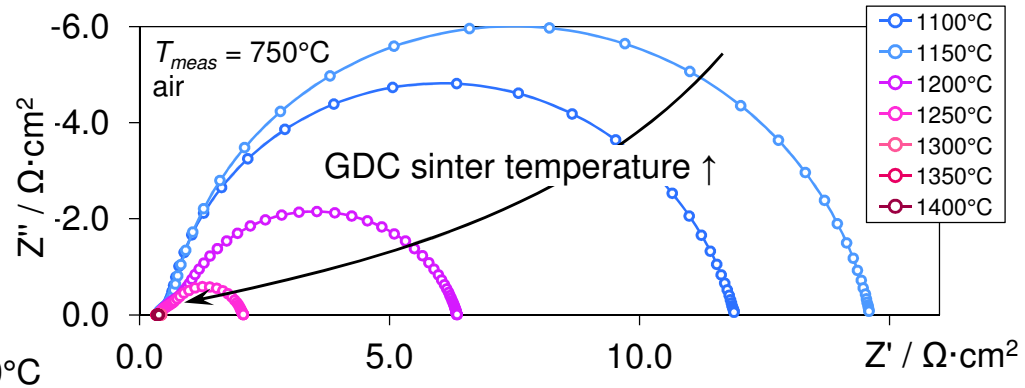

Cathode/Electrolyte Interface
Cathode Overpotential and Current Pathways

Continuous $SrZrO_3$
■ 1200°C

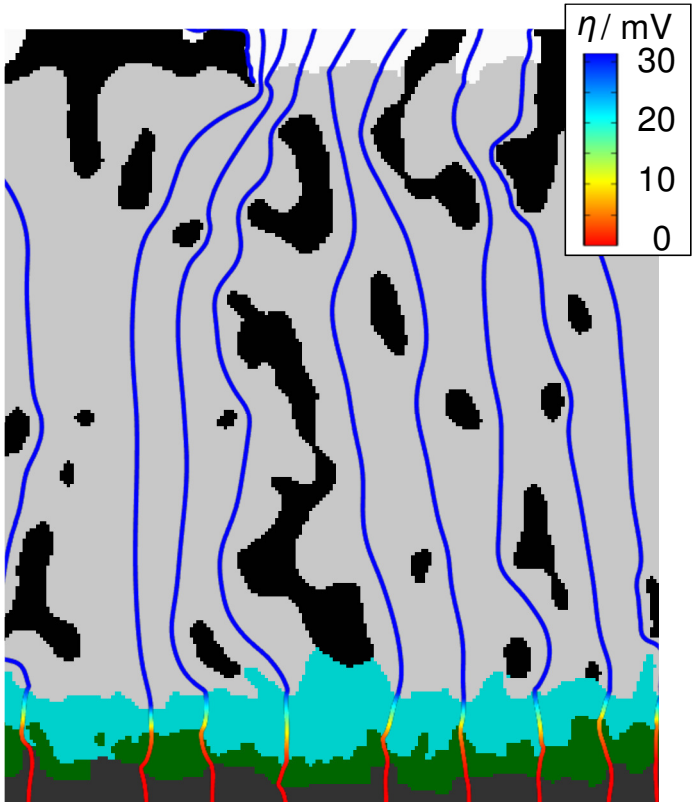

Intermittent $SrZrO_3$
■ 1300°C

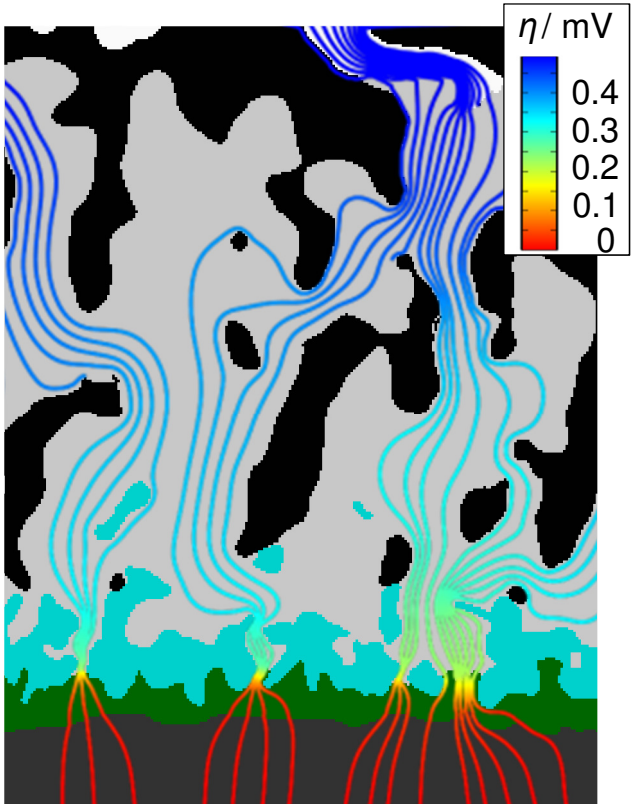

Continuous Interdiffusion
■ 1400°C

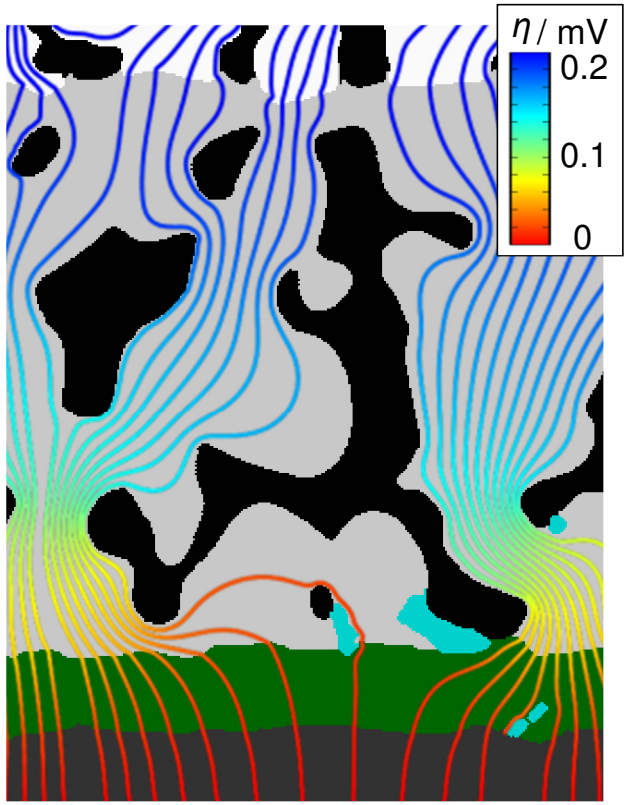

@f = 0.01 Hz j =10mA/cm² T_{meas} = 800°C

Degradation Processes in Solid Oxide Fuel Cells

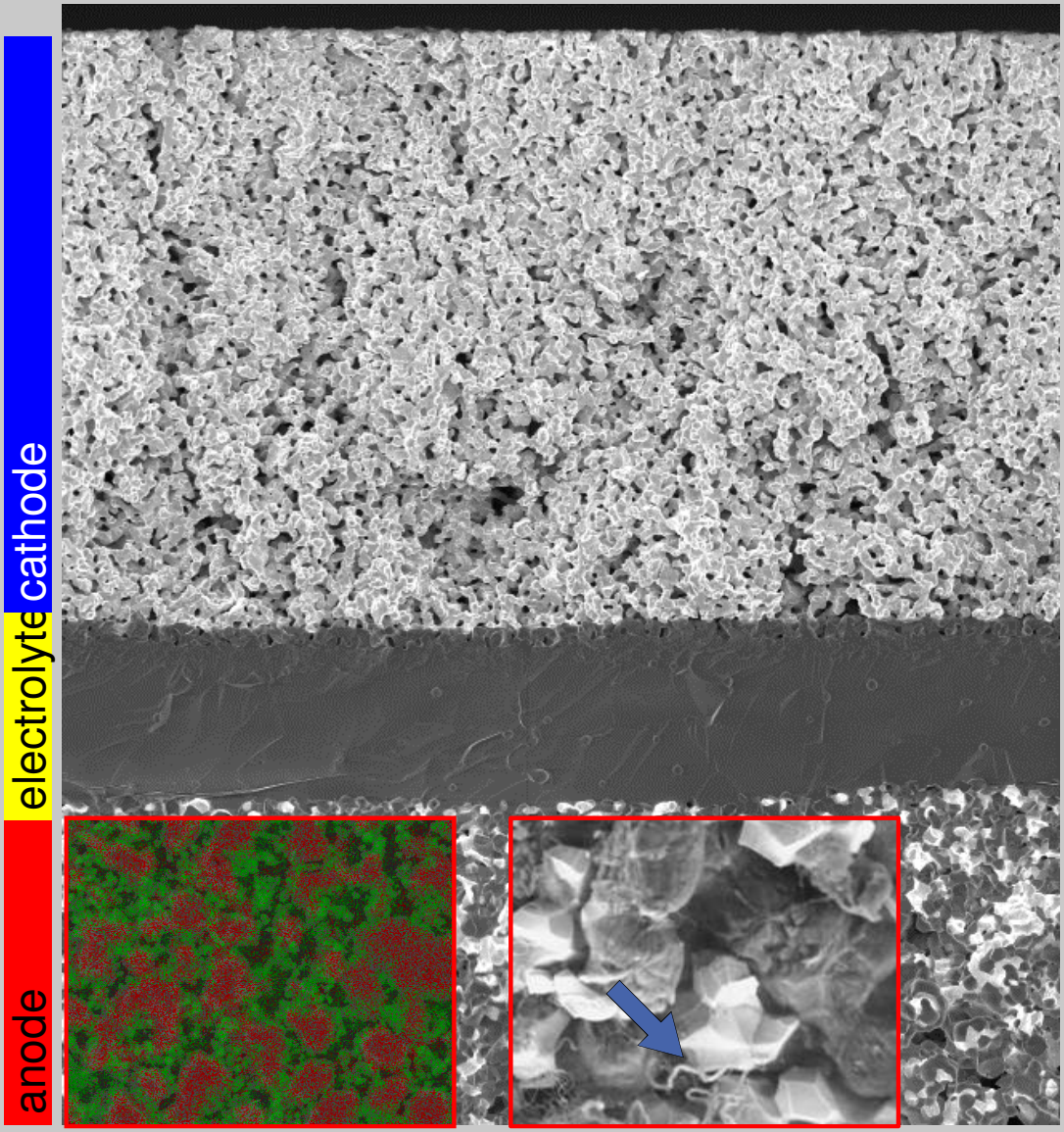

in SOFC many potentially competing degradation mechanisms are known:

- Ni-agglomeration
  A. C. Müller et. al., *Proc. 3rd European SOFC Forum*, pp. 353-362 (1998).
- carbon deposition
  E. Ivers-Tiffée et. al., *Handbook of Fuel Cells – Fundamentals, Technology and Applications*, pp. 933-956 (2009).

Extrinsic Degradation
Cracking of an Anode Supported Electrolyte after Redox-Cycling

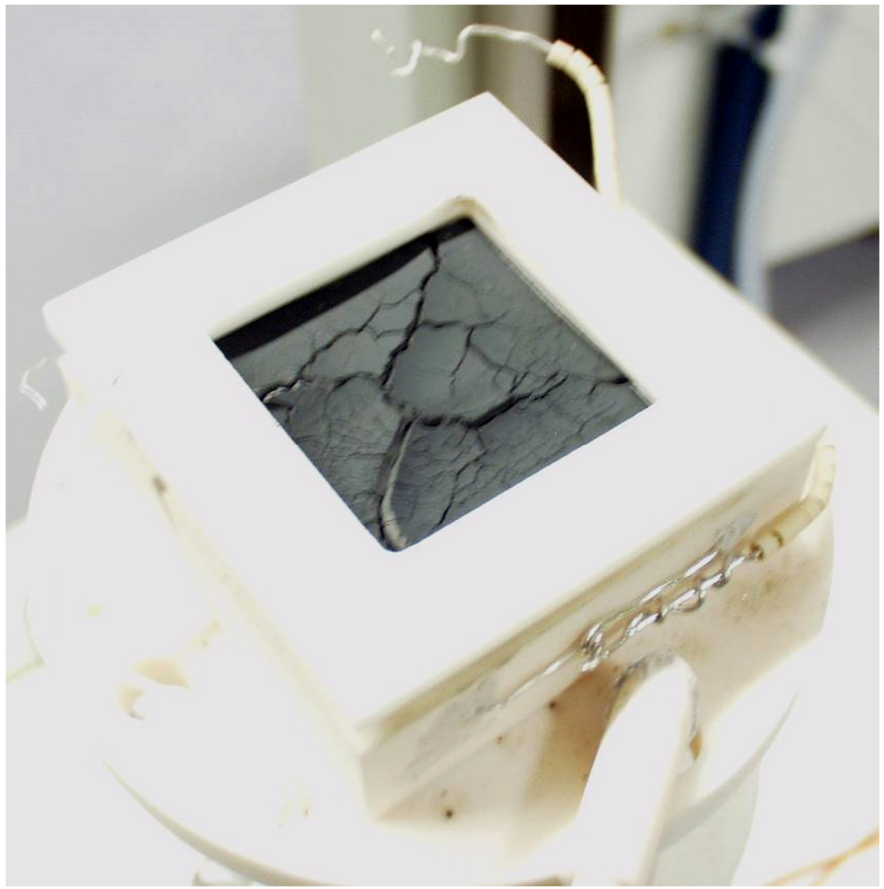

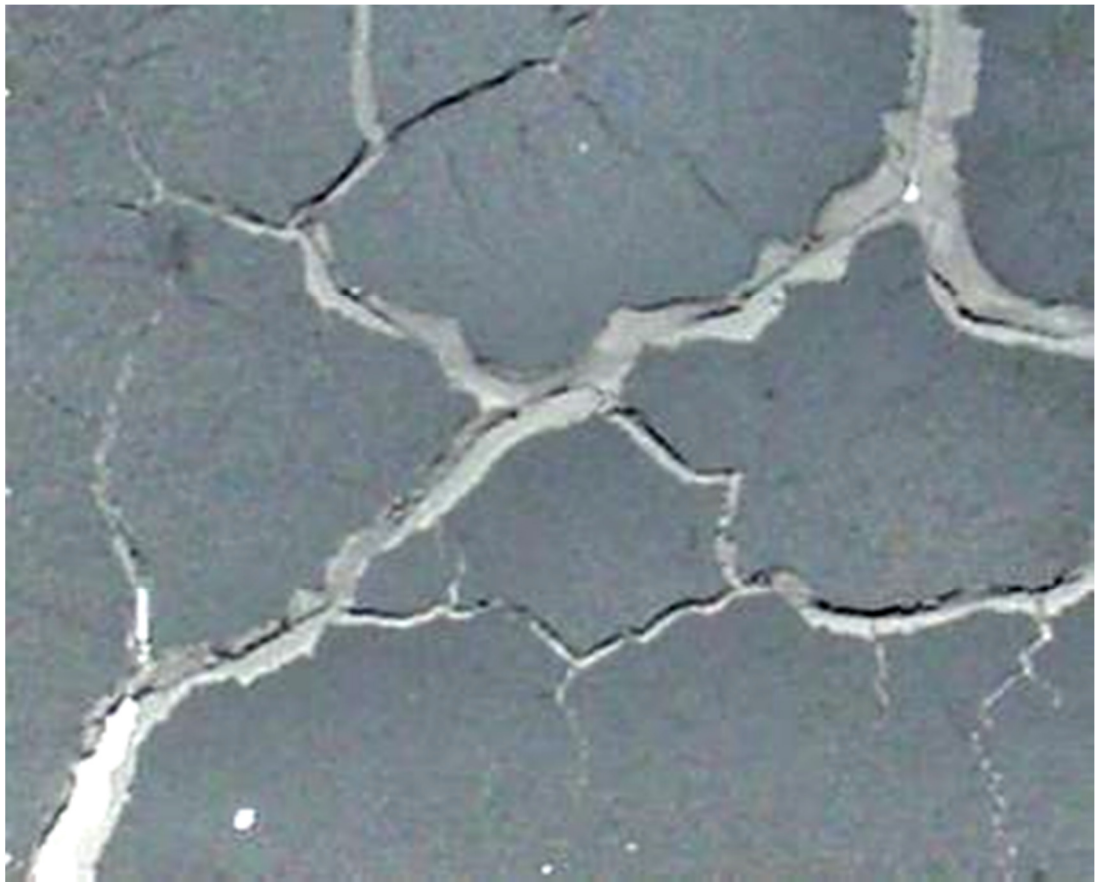

Impact of Redox Cycle on Length Change of Ni/YSZ Bulks: Different Sintering Temperatures

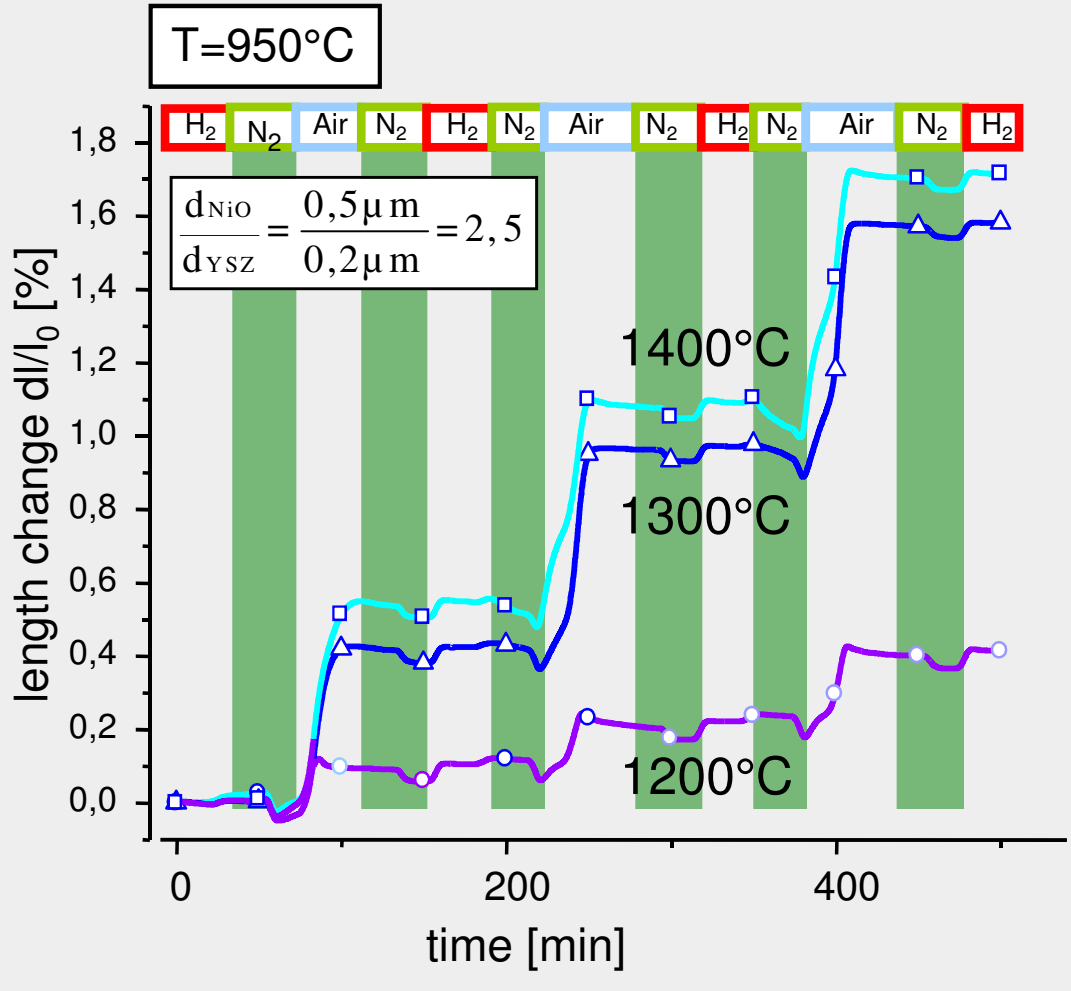

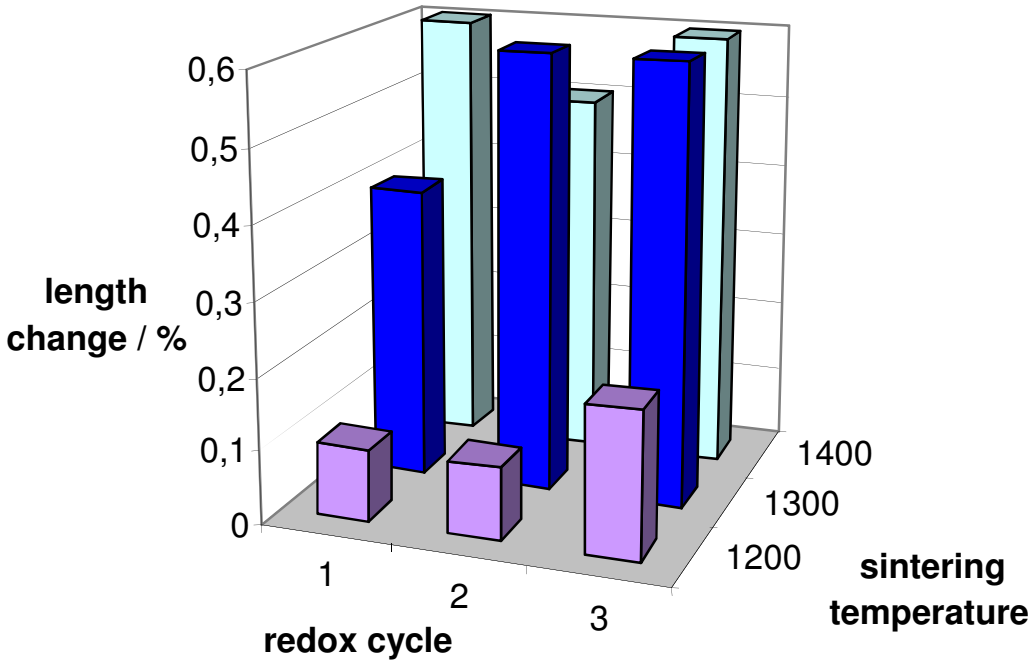

➢ minimum length change at lowest sintering temperature of 1200 °C

Impact of Redox Cycles on Microstructure of Ni/YSZ Bulks Different Sintering Temperatures

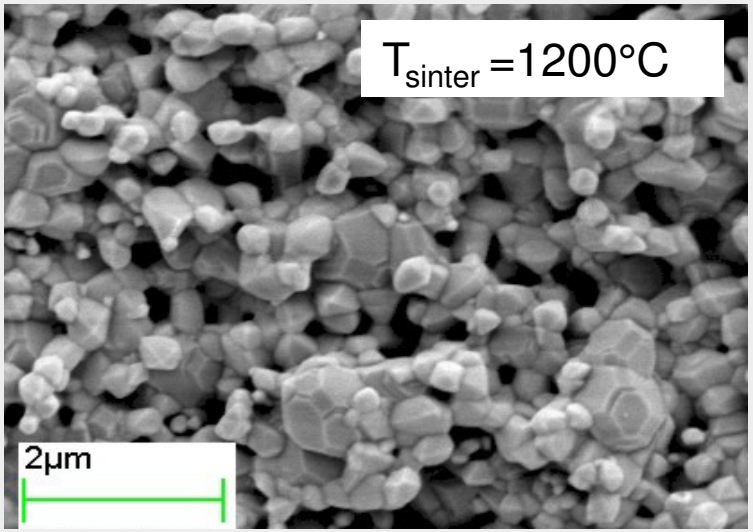

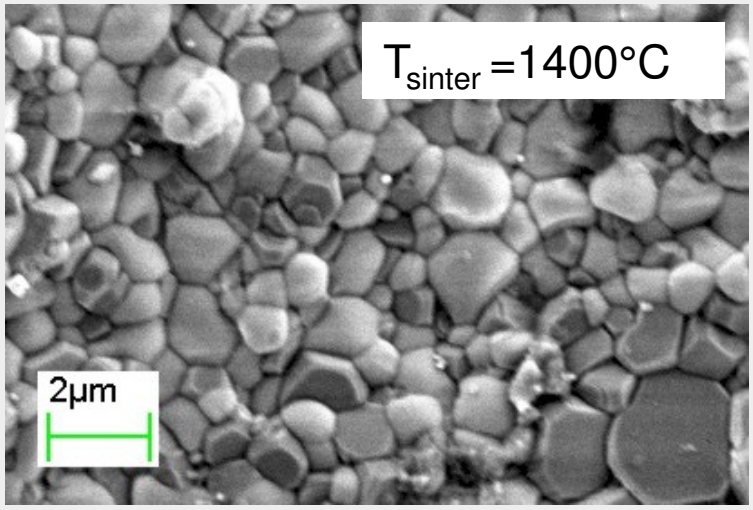

d_{50}: NiO=0,5µm
d_{50}: YSZ=0,2µm

length change
dl/l_0 = 0,4%

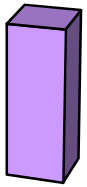

3 redox cycles

length change
dl/l_0 = 1,7%

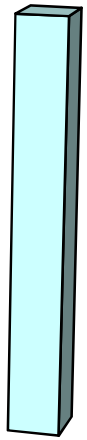

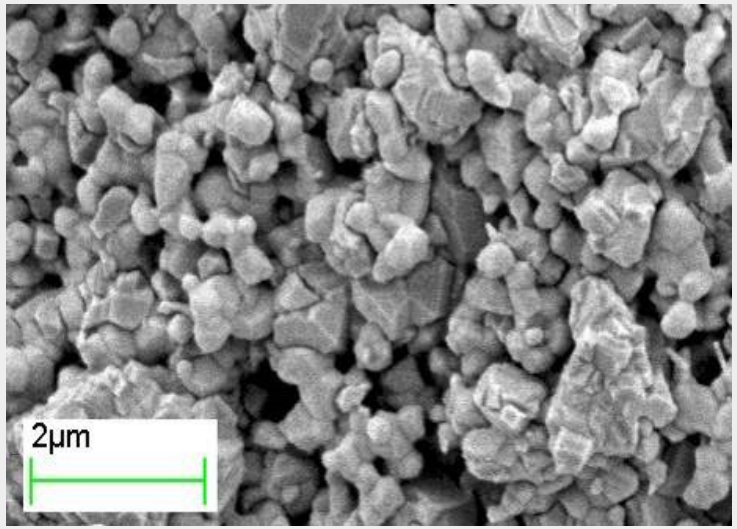

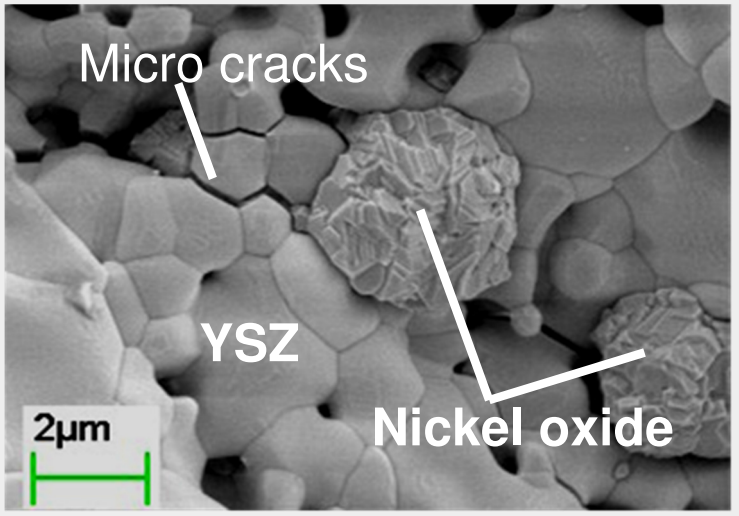

Degradation Tests for SOFC
Redox Stability (100 Redox-Cycles in 35 h)

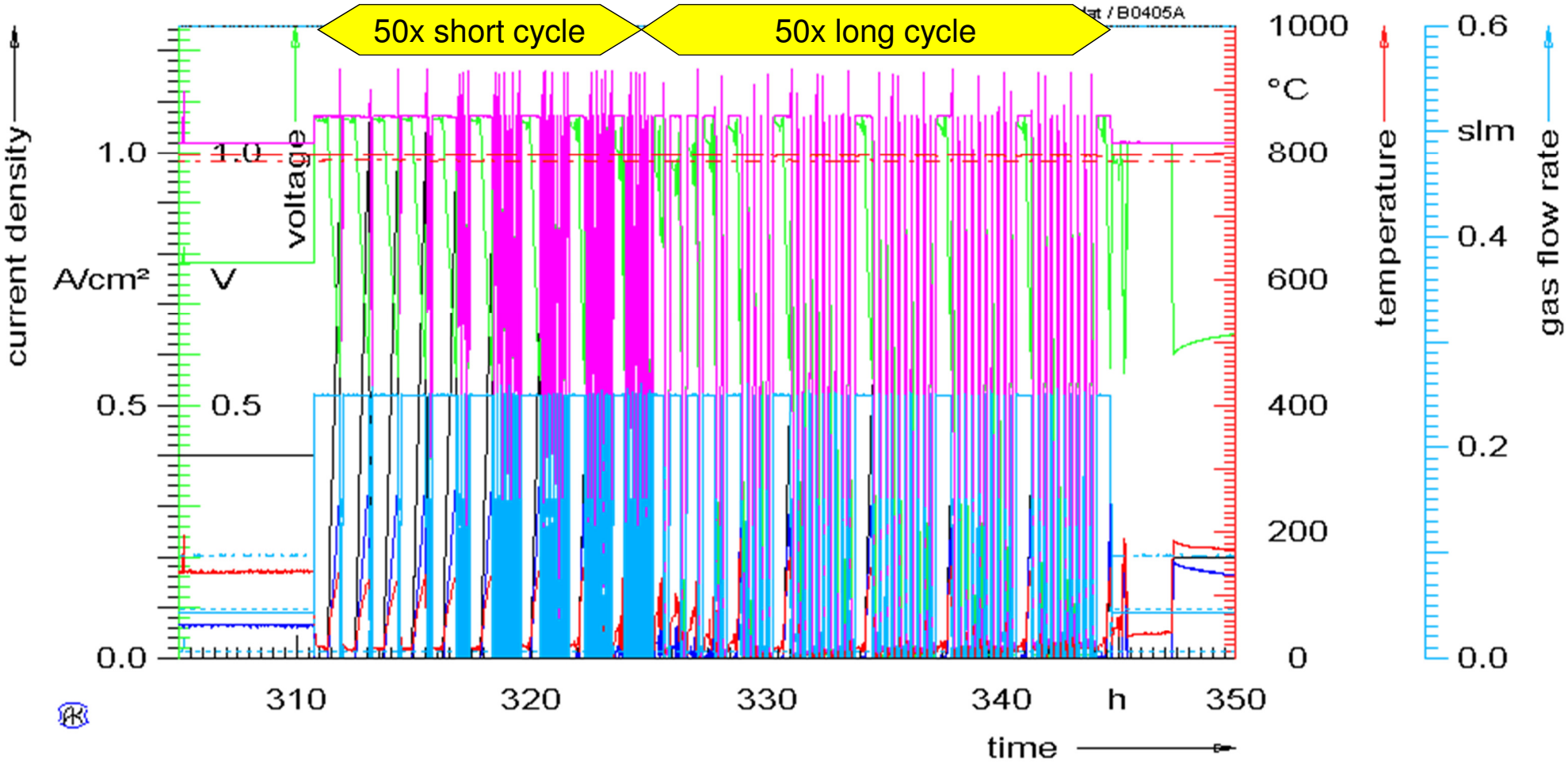

Redox Stability of Electrolyte Supported SOFC

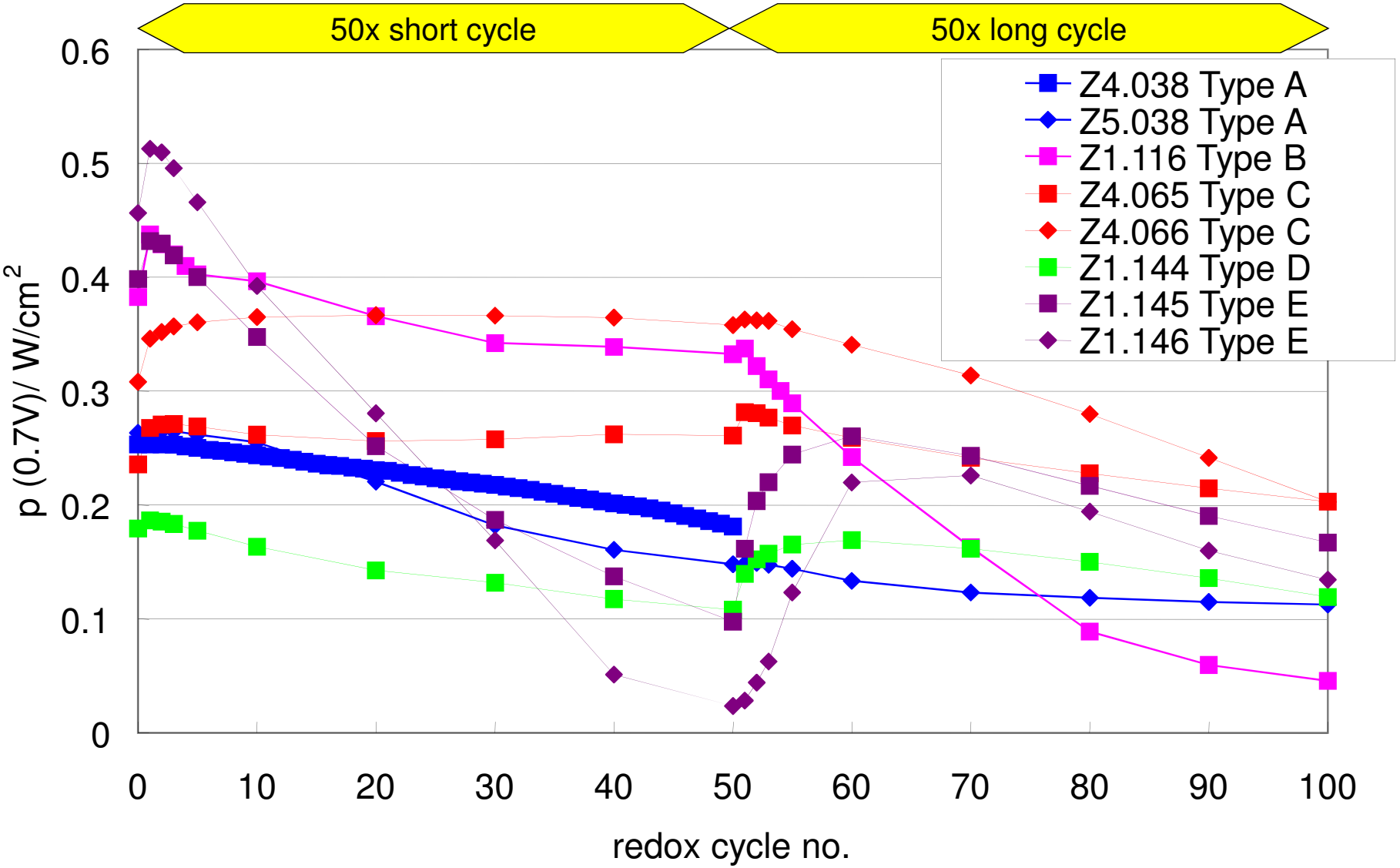

Operation on Hydrocarbons
Severe Degradation with higher Hydrocarbons CnHm

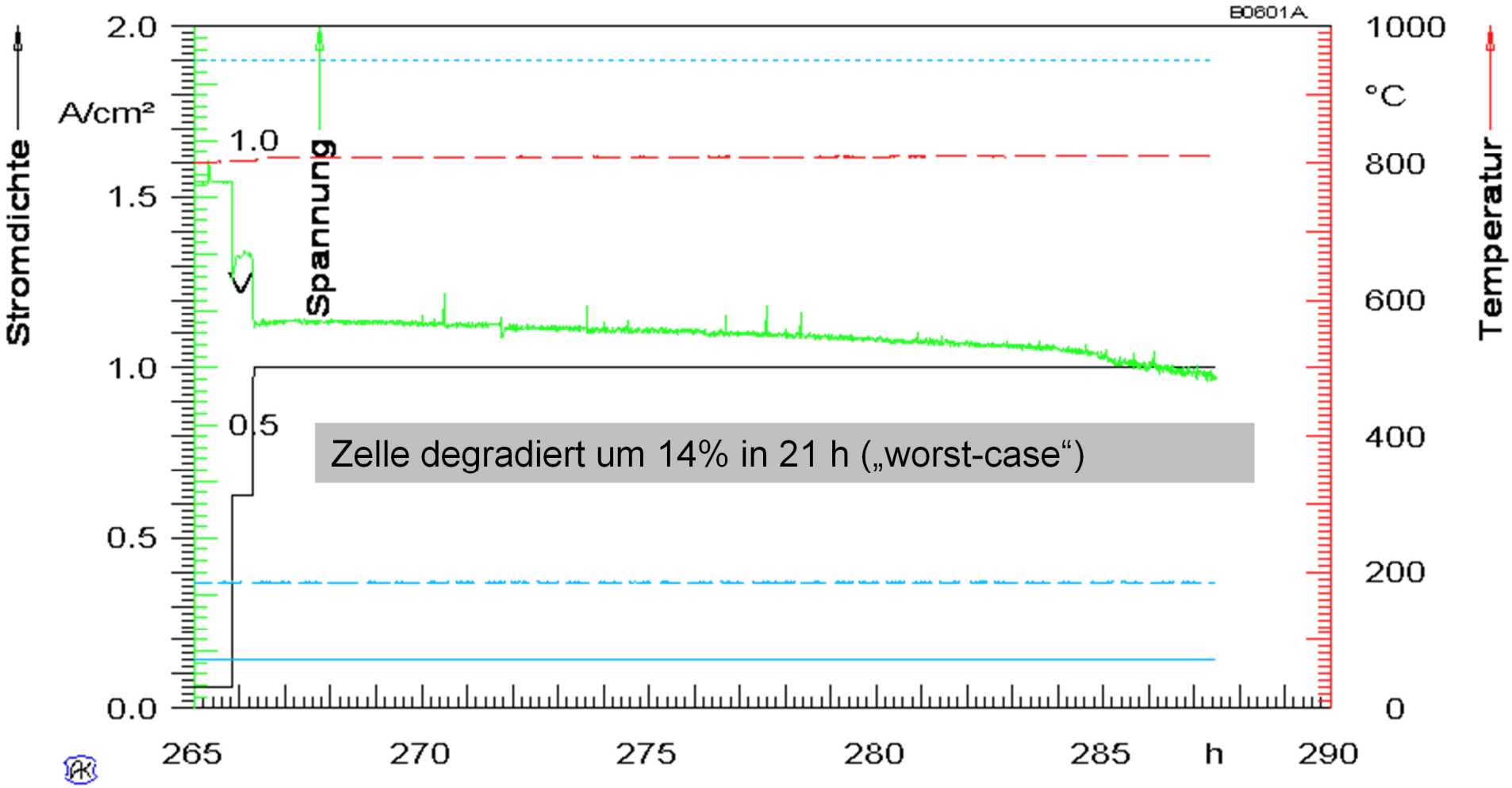

Gasgemisch: H_2, CO, H_2O, CO_2, N_2, C_2H_2 (Ethin), C_7H_8 (Toluol), Methylnaphtalin ($C_{11}H_{10}$)

Operation on Hydrocarbons
Severe Degradation with higher Hydrocarbons CnHm

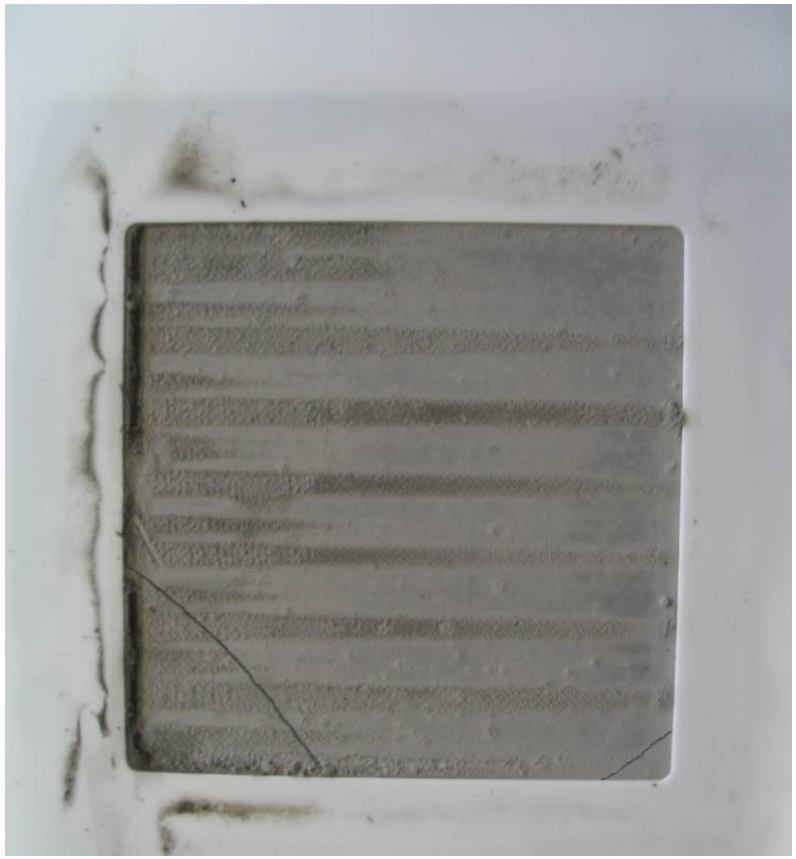

Flussrichtung

Aufgekohlte Zelle nach Betrieb mit einem Gasgemisch bestehend aus aus H_2, CO, H_2O, CO_2, N_2, C_2H_2 (Ethin), C_7H_8 (Toluol) und Methylnaphtalin ($C_{11}H_{10}$)

Durability Testing of Solid Oxide Cells
Research Center Jülich ASC-Stacks (2007 ff)

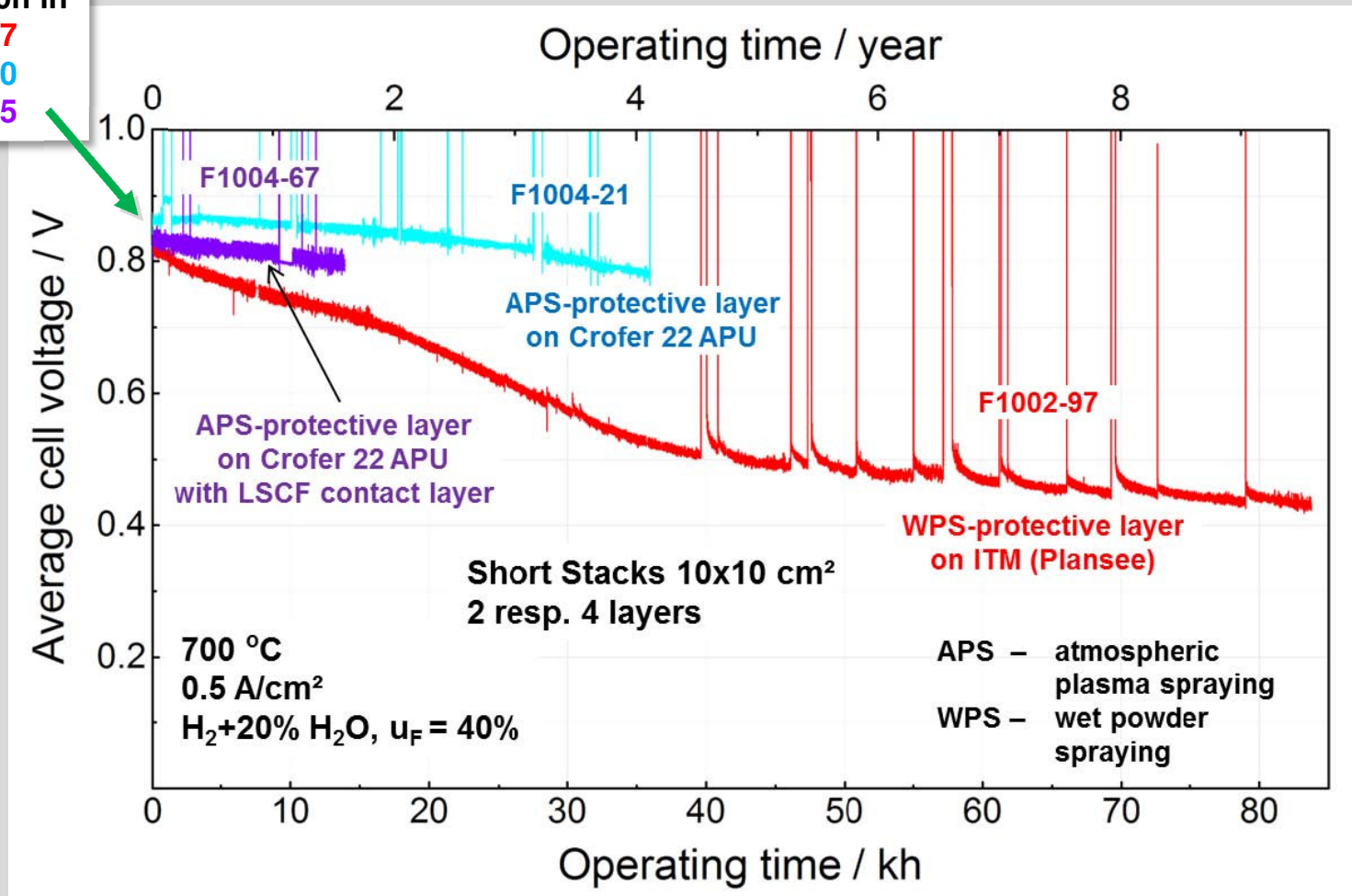

L. Blum et al., *ECS Trans.*, **78** (1), p. 1791 (2017)

duration
> 80 000 h
~ 10 years
2007 – today

degradation
0.3 ... 0.6 % / 1 000 h

results
available after 5...10 years

accelerate testing !

Accelerated Testing

"conventional" life testing

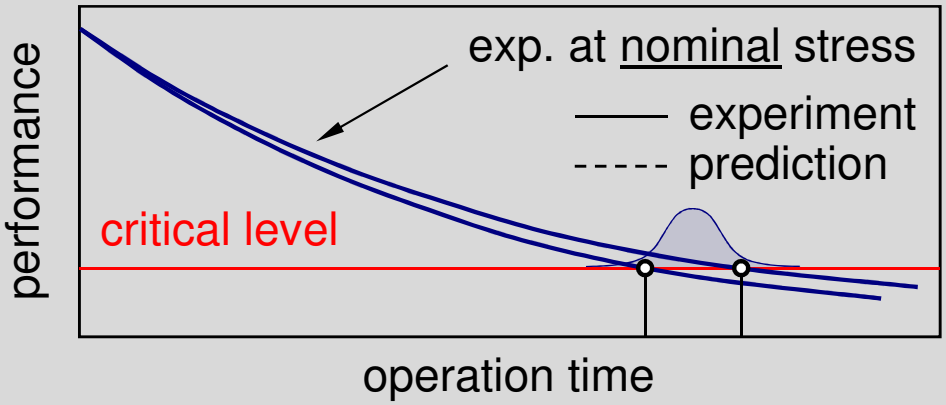

accelerated life testing

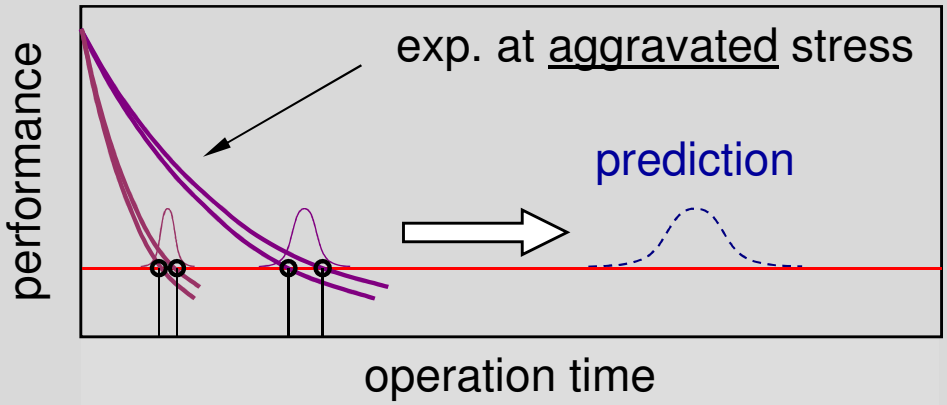

degradation testing

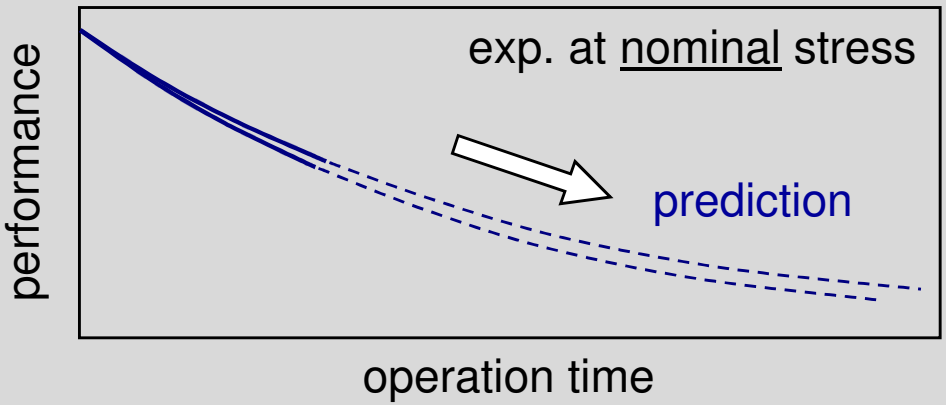

accelerated degradation testing

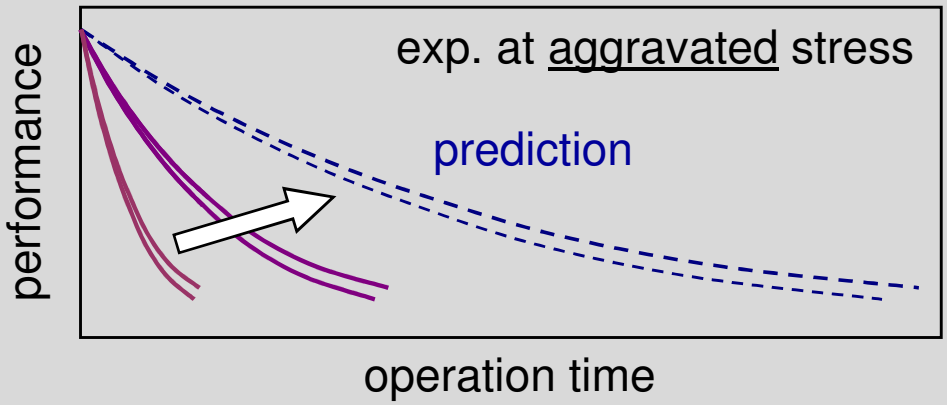

Accelerated Testing
Approach and Advantages

approach

- degradation is accelerated by means of aggravated stress (current load, temperature, etc.).
- life-stress relationship is modelled by the use of failure data.
- extrapolation of life-stress model gives a prediction for service life at nominal stress.

advantages of ALT

- physical consequences of degradation appear more clearly, mechanisms are identified more easily.
- precious measurement time is saved, lifetime is evaluated rapidly.

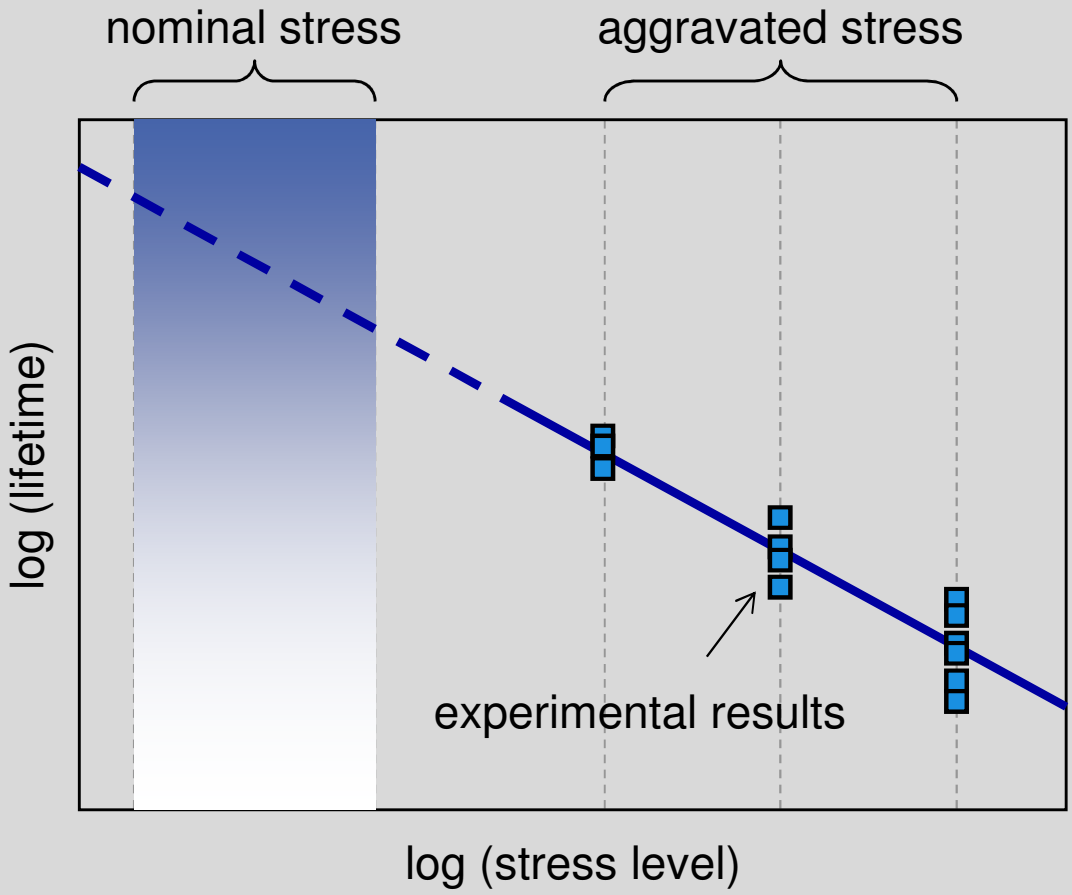

W. Nelson, Accelerated Life Testing, John Wiley & Sons (1990).

Accelerated Life Testing
Competing Degradation Processes in Solid Oxide Cells

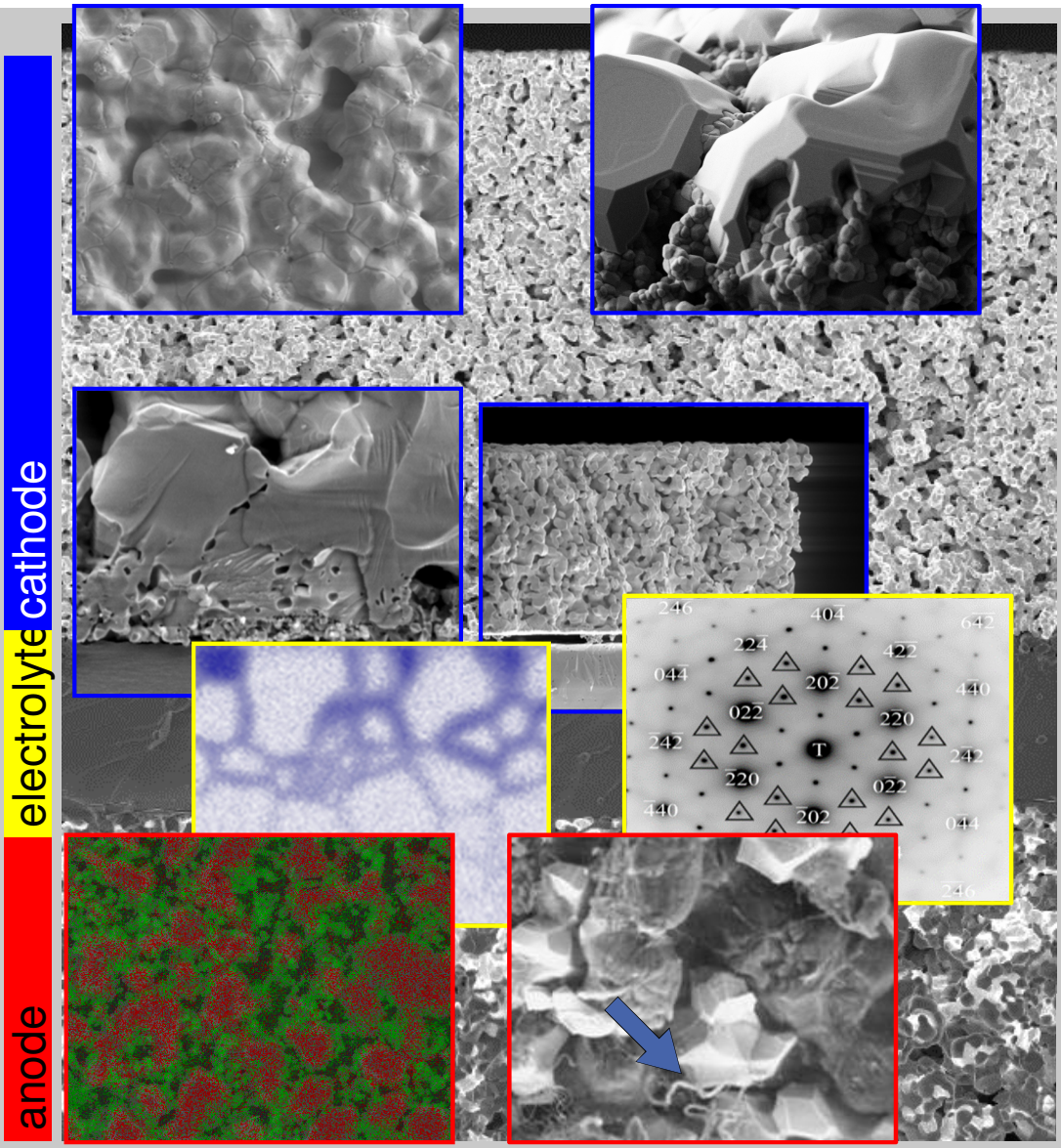

in SOC many potentially competing degradation mechanisms are known:

- densification of electrodes
- formation of micropores
  A. Weber et. al., *Denki Kagaku* **64**, pp. 582-589 (1996).
- formation of chromium compounds on the cathode
- delamination of the cathode
  M. J. Heneka et. al., Proc. 9th Int. Symp. on SOFC, pp. 534-543 (2005).
- Mn-interdiffusion
  A. Weber, in J. Garche (Ed.), Encyclopedia of Electrochemical Power Sources, Amsterdam: Elsevier, pp. 120-134 (2009).
- intrinsic electrolyte degradation
  B. Butz et. al., *Solid State Ionics* **177**, pp. 3275-3284 (2006).
- Ni-agglomeration
  A. C. Müller et. al., *Proc. 3rd European SOFC Forum*, pp. 353-362 (1998).
- carbon deposition
  E. Ivers-Tiffée et. al., *Handbook of Fuel Cells – Fundamentals, Technology and Applications*, pp. 933-956 (2009).

⇨ in addition, activation processes that improve the performance take place
A. Weber et. al., *Denki Kagaku* **64**, pp. 582-589 (1996).

Accelerated Life Testing
Competing Degradation Processes

aging mechanism A
- experimental results
- life-stress model
- extrapolation

aging mechanism B
- different life-stress dependency

aging mechanism B
- different dependency on stress level
- minor impact at aggravated stress
- lifetime limiting at nominal stress

ALT approach will fail

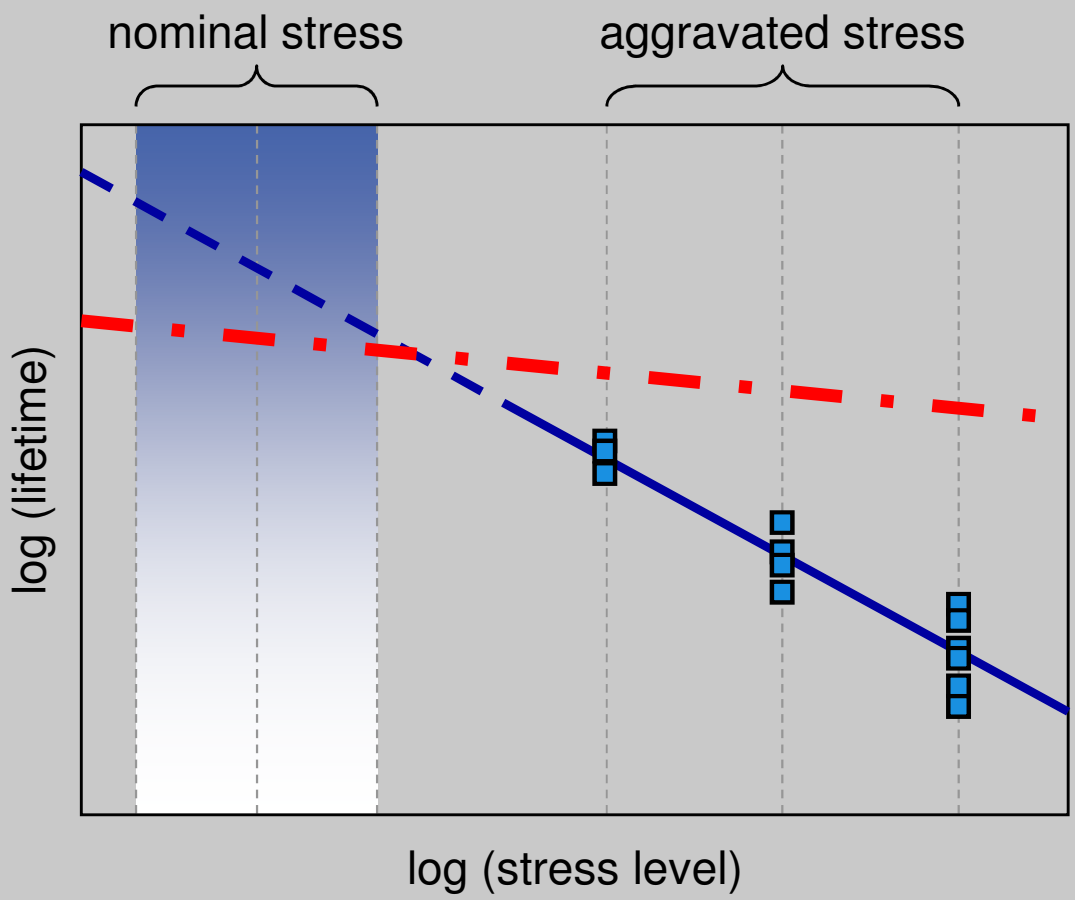

A. Weber.et al., *ECS Trans.*, **68** (1), p. 1953 (2015)

Degradation Testing
Deconvolution of Competing Degradation Processes

aging mechanism A
- experimental results
- life-stress model
- extrapolation

aging mechanism B
- different life-stress dependency

→ **deconvolute aging mechanisms**

- ~~overall performance, lifetime (summarized / averaged quantities)~~
- physicochemical processes acquired via their electrochemical impedance (additive quantities)

EIS: electrochemical impedance spectroscopy

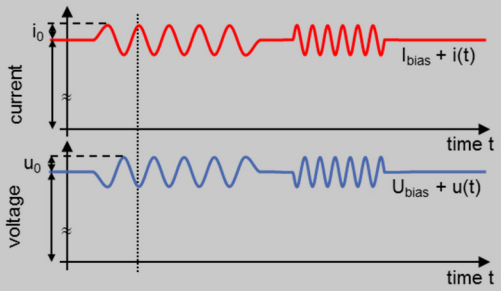

- sinusoidal electrical stimulation (current)
- linear regime → small amplitude
- sinusoidal electrical response (voltage)

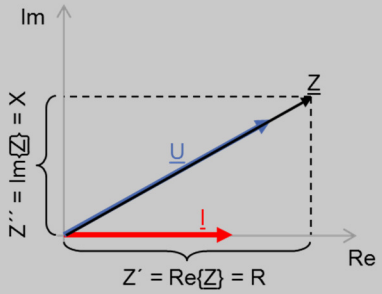

- variation of the stimulation frequency → processes in the cell with a lower relaxation frequency are not stimulated

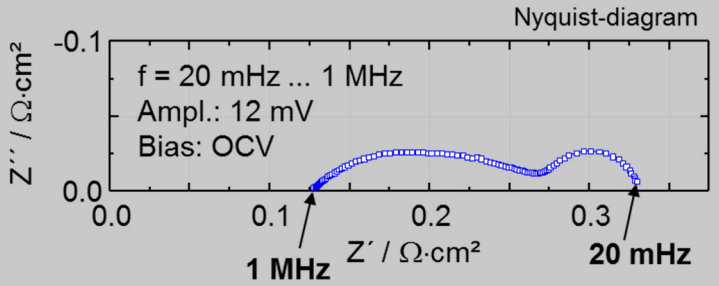

electrochemical impedance spectrum

Loss mechanisms in SOFCs
Processes contributing to the Area Specific Resistance (ASR)

Transport in the gas phase: gas flow and diffusion

Transport in the solid phase: electronic and ionic current

Reactions: charge transfer, surface exchange, electrooxidation, surface catalysis

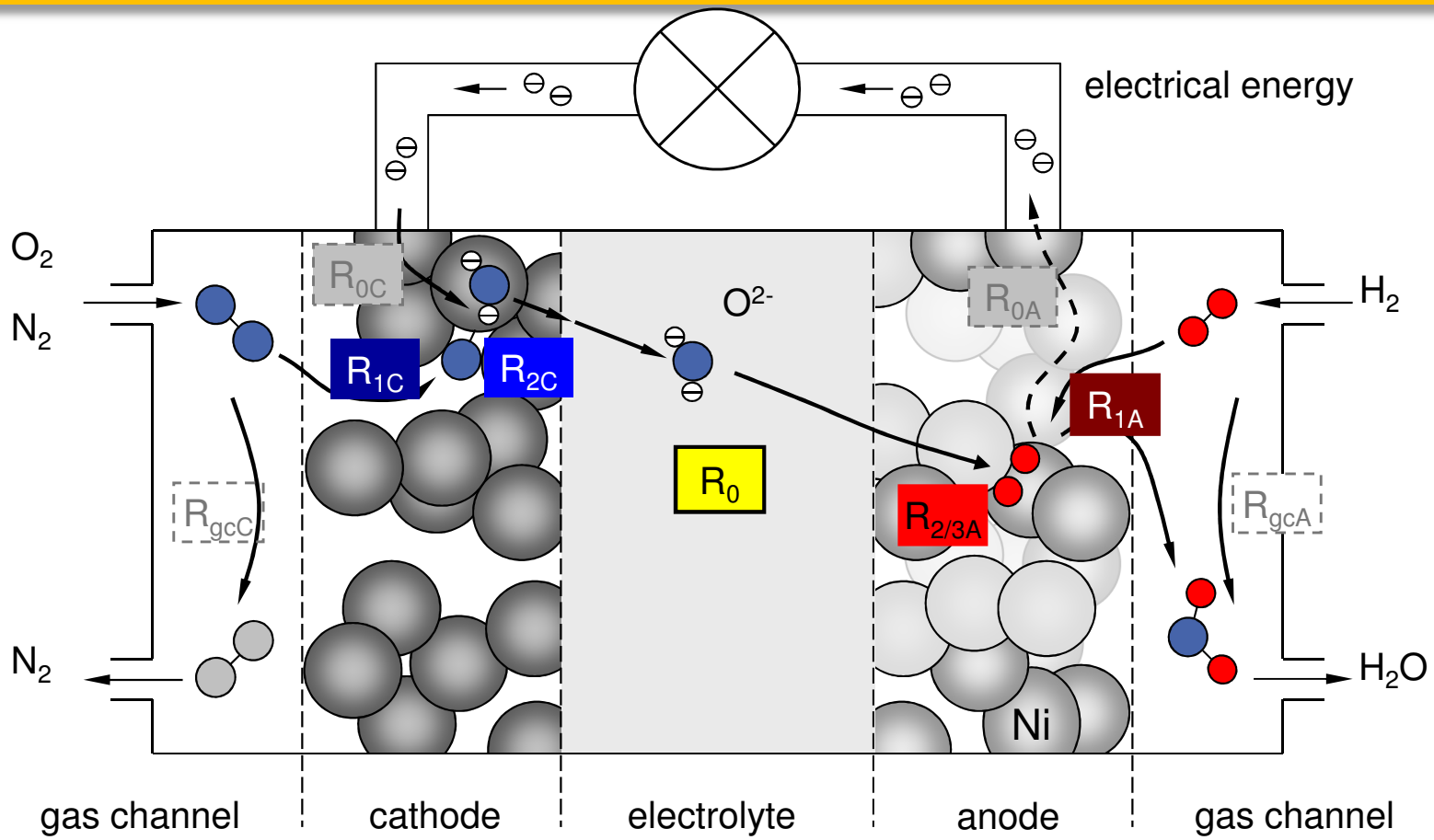

related resistances

R_{gcC}	gas conversion
R_{1C}	gas diffusion (cathode)
R_{0C}	electronic current (cathode)
R_{2C}	surface exchange and O^{2-} bulk diffusion
R_0	ionic current (electrolyte)
$R_{2/3A}$	electrooxidation and ionic transport in the anode
R_{0A}	electronic current (anode)
R_{1A}	gas diffusion (anode)
R_{gcA}	gas conversion

Impedance based Cell Model I
Deconvolution of electrochemical Processes

Electrochemical Impedance Spectroscopy EIS

ASC: Anode-Supported Cell
OCV: Open Circuit Voltage

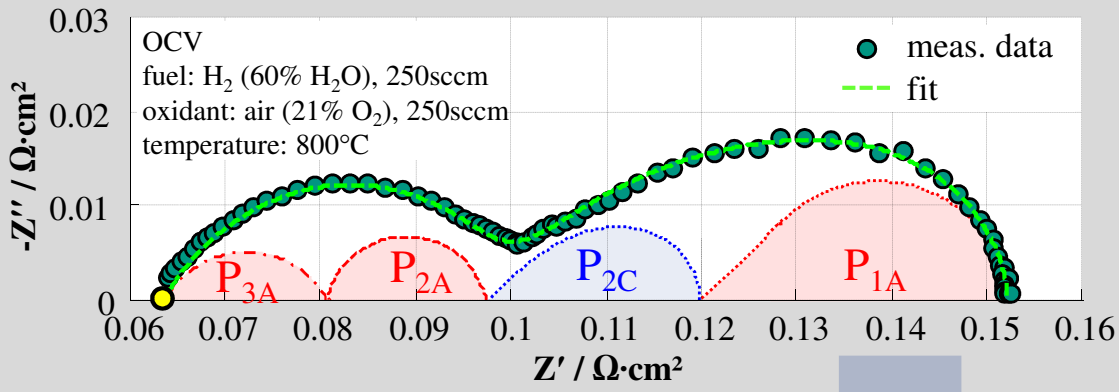

Distribution of Relaxation Times DRT $\underline{Z}(\omega) = R_{Pol} \int_0^\infty \frac{\gamma(\tau)}{1+j\omega\tau} d\tau$

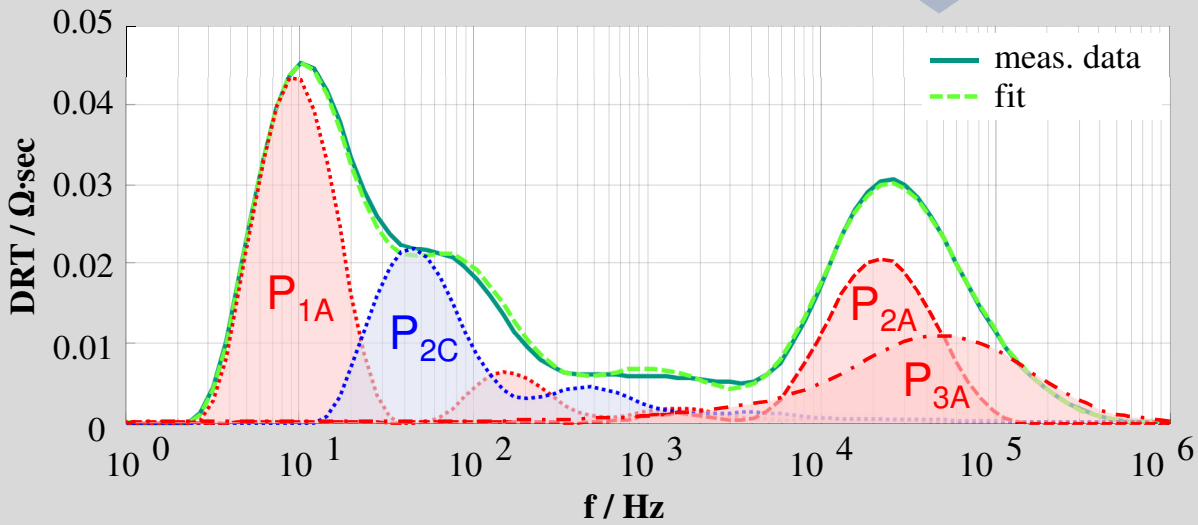

equivalent circuit model

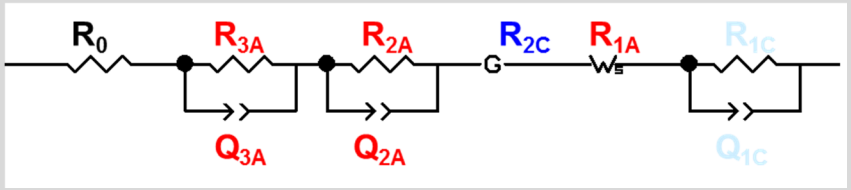

process	physicochemical origin
P_{1C}	gas diffusion (cathode)
P_{2C}	oxygen reduction reaction (cathode)
R_0	ionic (and electronic) conduction
P_{2A} / P_{3A}	hydrogen electrooxidation coupled with gas diffusion and ionic transport
P_{1A}	gas diffusion (porous substrate)

Institut für Angewandte Materialien
Elektrochemische Technologien

H. Schichlein, et. al., *J. Appl. Electrochem.* **32**(8), pp. 875–882 (2002)
A. Leonide, et. al., *J. Electrochem. Soc.* **155** (1), B36 (2008)

Model Application
ASRs of the Cell Components

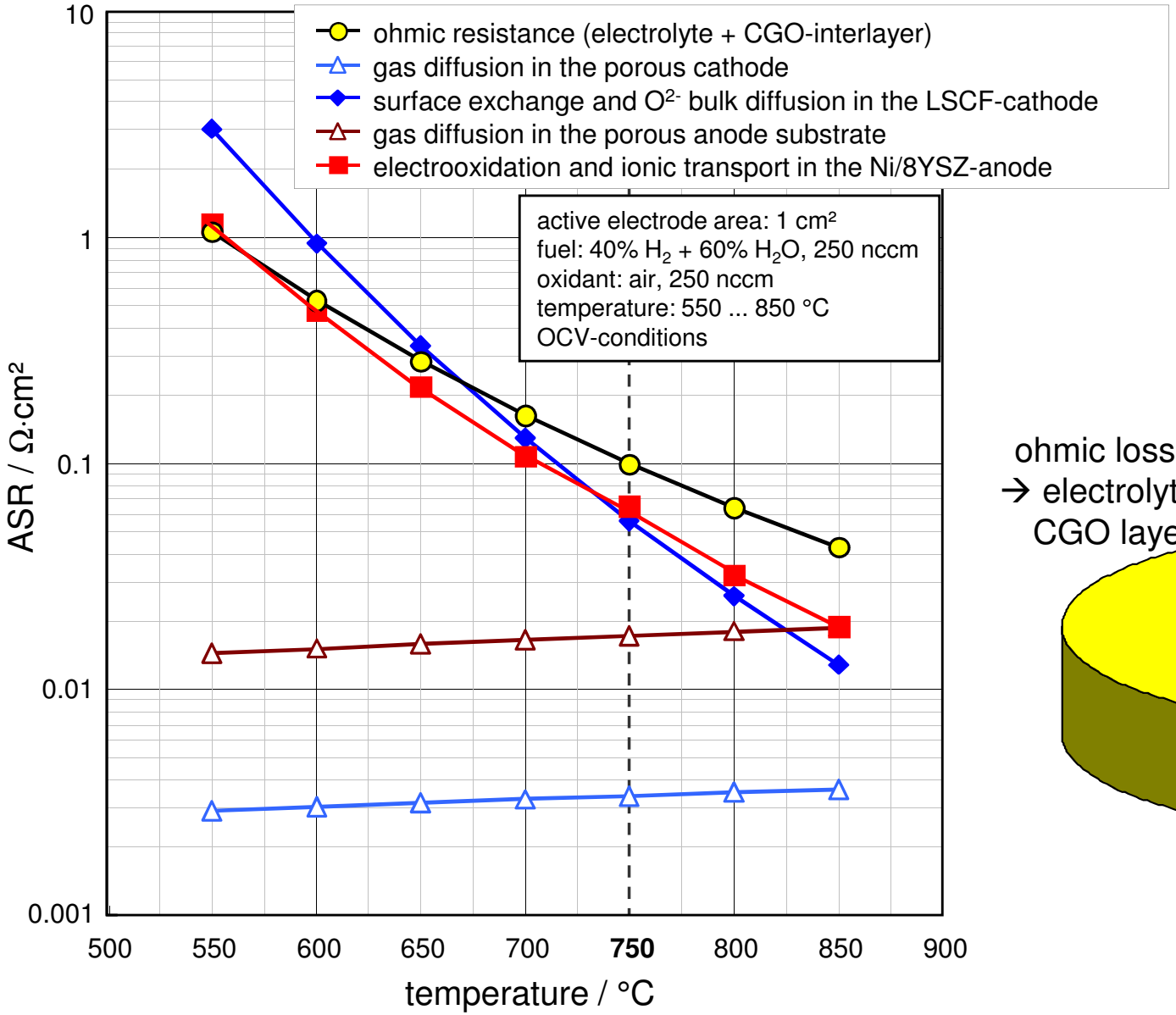

FZ Jülich ASC

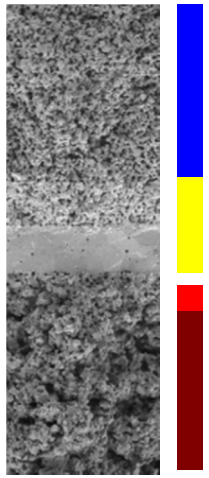

at 750 °C:

gas diffusion polarization
→ anode substrate

ohmic losses
→ electrolyte +
CGO layer

charge transfer reaction
and ionic transport
in the AFL

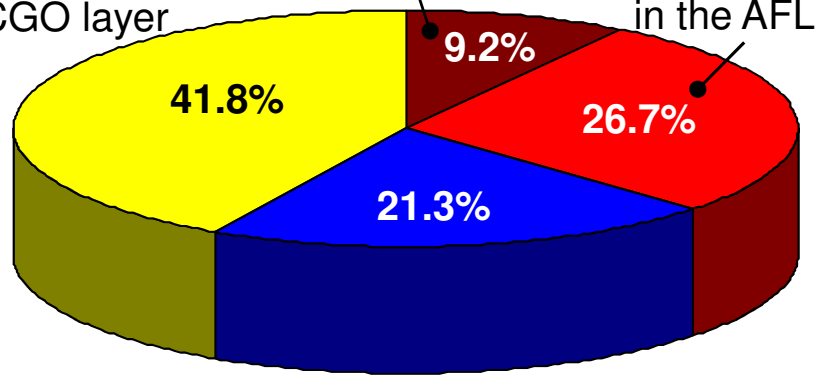

oxygen reduction reaction
→ cathode layer

Applicability of the Model to different Cell Types
Cell Types analyzed in National and European Projects

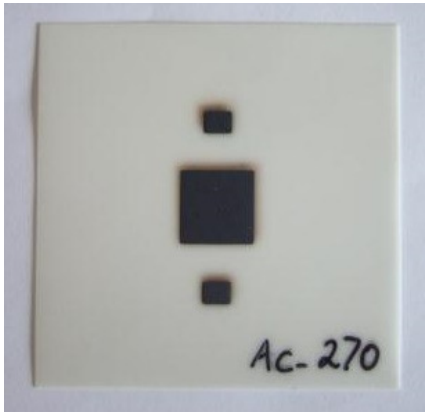

ESC

H.C.Starck

$SrTiO_3$-based ASC

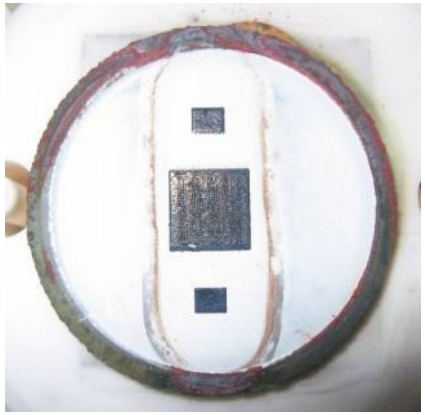

VPS-MSC

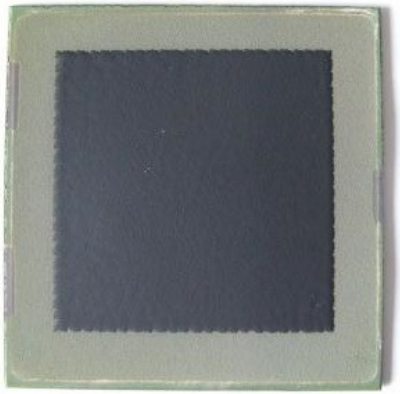

APS-MSC

UNIVERSITY WEST

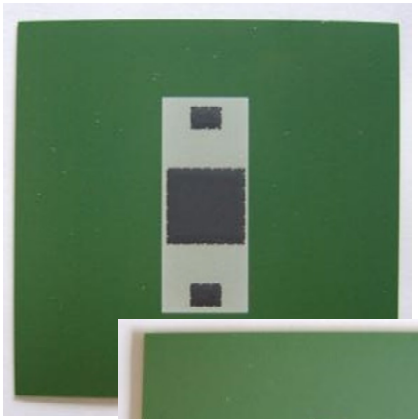

CeramTec
THE CERAMIC EXPERTS

SOLID POWER

ASC´s (before reduction)

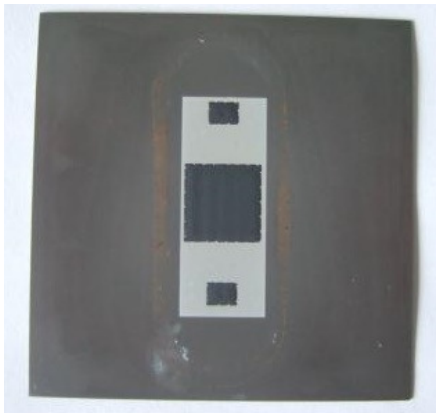

ASC (reduced)

TOPSOE FUEL CELL
clean, efficient and reliable

cofired MSC

DTU

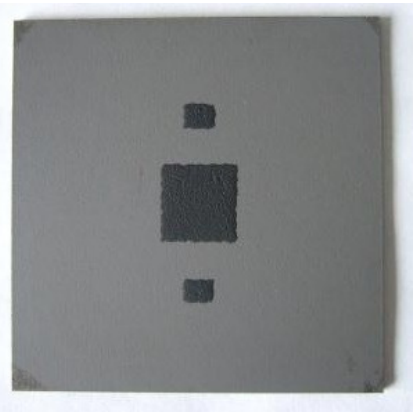

PVD MSC

PLANSEE

C. Endler-Schuck et al., *J. FC Science and Technology* **8**, p. 41001 (2011)
Q. Ma et al., *J. Power Sources* **196**, p. 7308 (2011)
P. Blennow et al., *J. Power Sources* **196**, p. 7117 (2011)
F. Han et al., *J. Power Sources* **218**, p. 157 (2012)
T. Franco et al., *Proc. 10th Eur. SOFC Forum*, p. A0906 (2012)
A. Kromp et al., *Fuel Cells* **13**, p. 598 (2013)

Applicability of the Model to different Cell Types

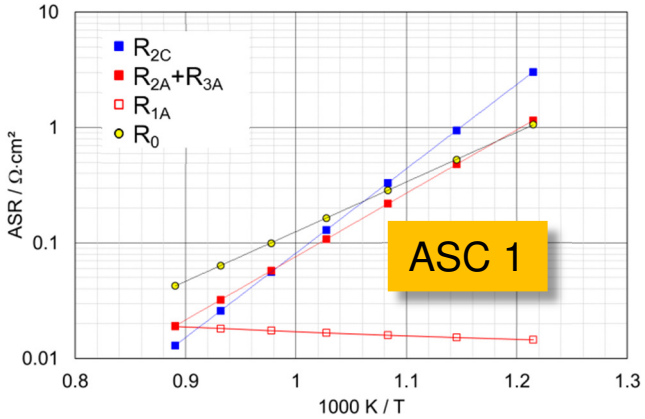

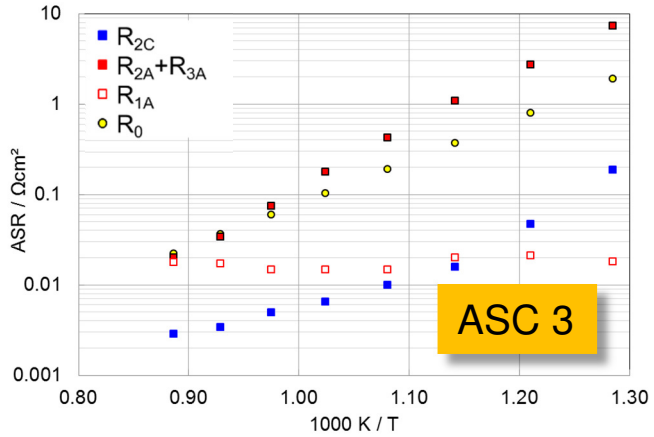

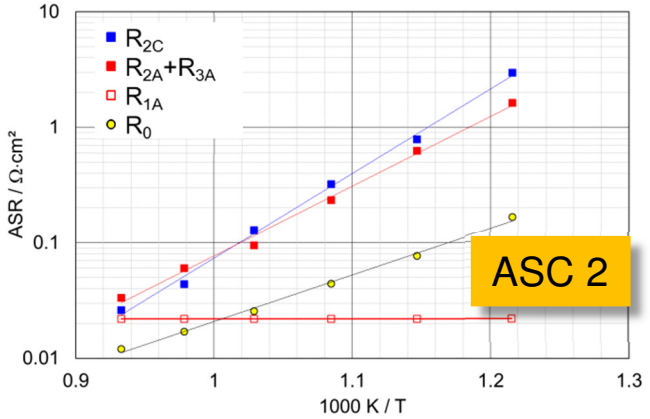

quite similar processes in all cells

- gas diffusion in the pores
- electronic / ionic currents in solids
- a MIEC-cathode
- a cermet anode

+ polarization at insulating interlayers

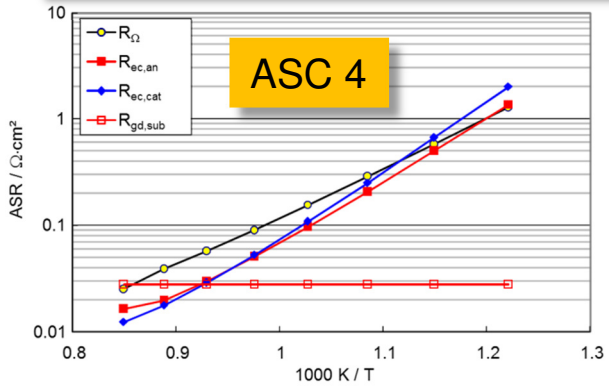

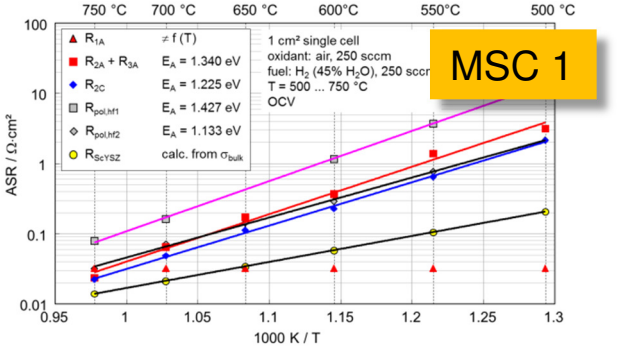

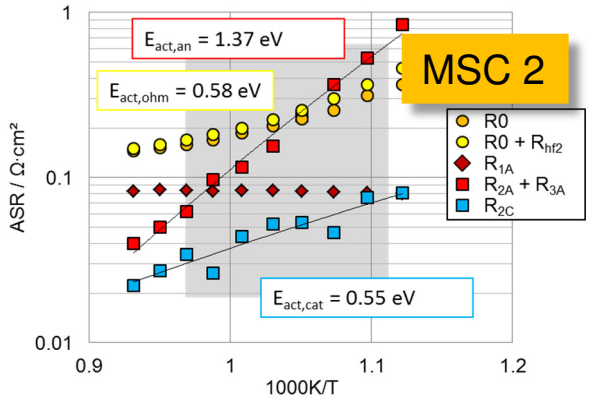

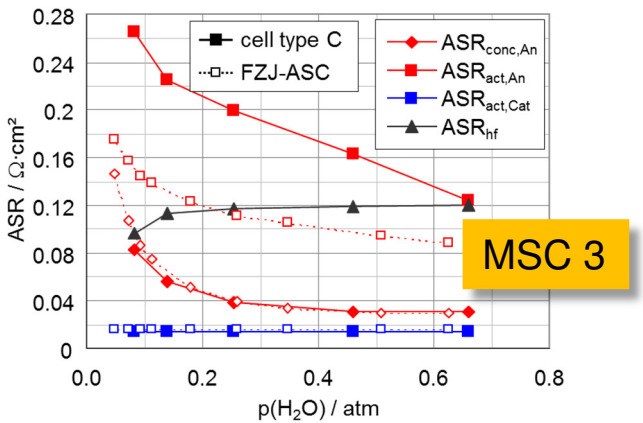

P. Blennow et al., *J. Power Sources* **196**, p. 7117 (2011)
F. Han et al., *J. Power Sources* **218**, p. 157 (2012)
T. Franco et al., *Proc. 10th Eur. SOFC Forum*, p. A0906 (2012)
A. Kromp et al., *Fuel Cells* **13**, p. 598 (2013)

Impedance based Cell Model II
Physicochemical Performance Model → Power Density

model equations with 13 parameters from EIS

Nernst equation U_{OCV}

ohmic loss $R_{ohm} = \frac{T}{B_{ohm}} \cdot \exp\left(\frac{E_{act,ohm}}{R \cdot T}\right)$

Butler-Volmer equation

$$j = j_{0,El}\left[exp\left(\alpha_{El}\frac{n_e F \eta_{act,El}}{RT}\right) - exp\left(-(1-\alpha_{El})\frac{n_e F \eta_{act,El}}{RT}\right)\right]$$

$$j_{0,an} = \gamma_{an}(pH_{2,an})^{a}(pH_2O_{an})^{b}\exp\left(-\frac{E_{act,an}}{RT}\right)$$

$$j_{0,cat} = \gamma_{cat}(pO_{2,cat})^{m}\exp\left(-\frac{E_{act,cat}}{RT}\right)$$

Fick's law inserted + Nernst equation with $D_i^{eff} = \psi_{el} \cdot D_i$

Cell voltage $U_{cell}(j) = U_{OCV} - (\eta_{ohm}(j) + \eta_{conc,an}(j) + \eta_{conc,cat}(j) + \eta_{act,an}(j) + \eta_{act,cat}(j))$

durability model ?

model parameters p_i = f(time, operating conditions)

model validation

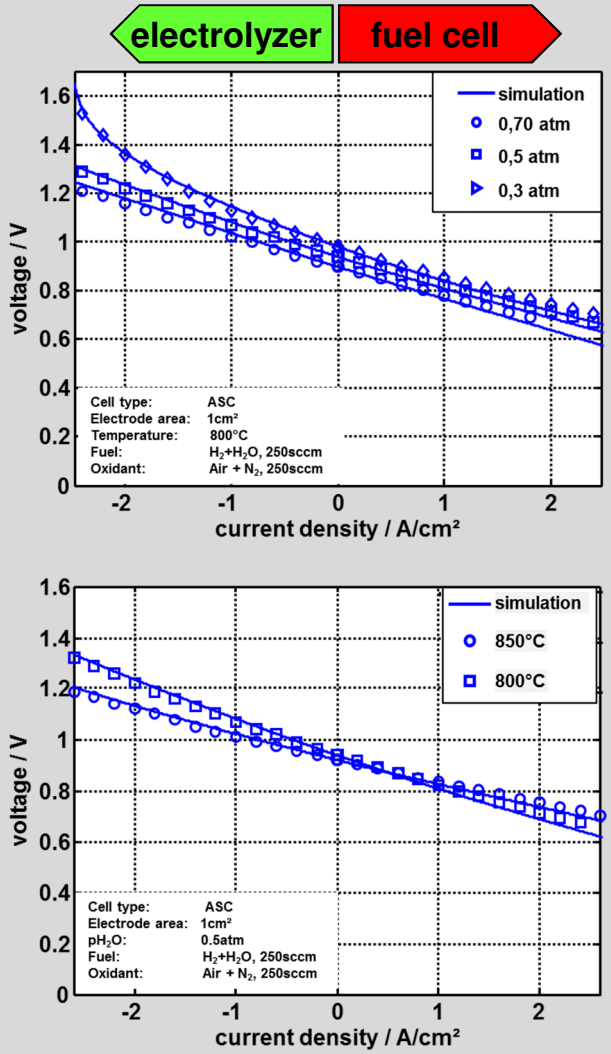

excellent agreement

- different temperatures
- different gases
- fuel cell and electrolyzer mode

A. Leonide et al, ECS Trans. **28** (11), 341 (2010)
J.-C. Njodzefon.et al., *J. Electrochem. Soc.*, **160** (4), p. F313 (2013)

Modelling III
Single Cell Durability Model

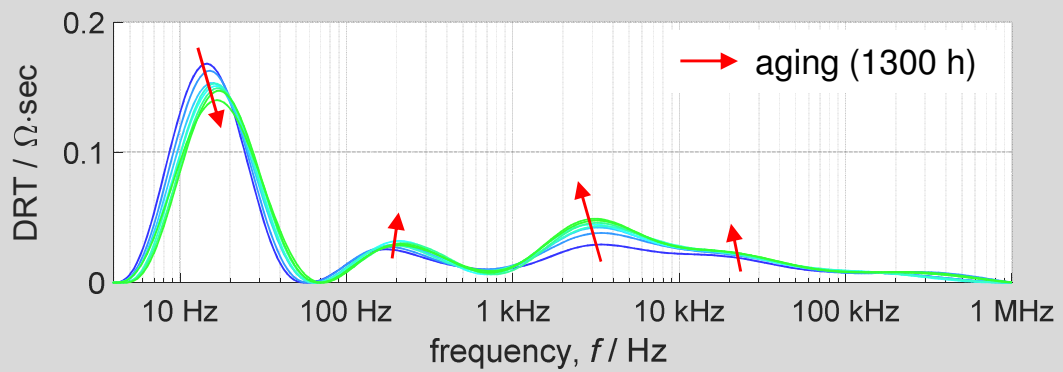

test matrix (varied parameters)

- temperature
- current density
- fuel composition
- oxidant composition
- ... to be extended

test duration: 1300 h (> 4000 h)

time dependency of model parameters → $\sqrt{t}$

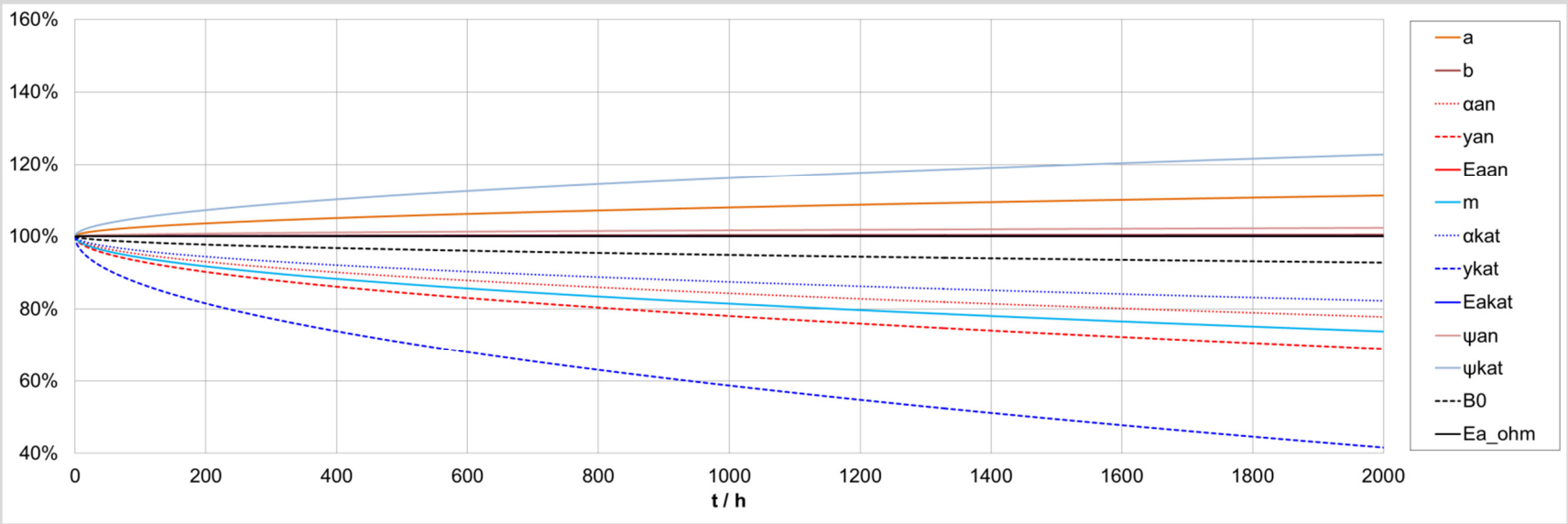

operating point
T = 900 °C
10% H_2 / 90% H_2O
0 A/cm²

Single Cell Durability Model Validation

measured and simulated cell degradation

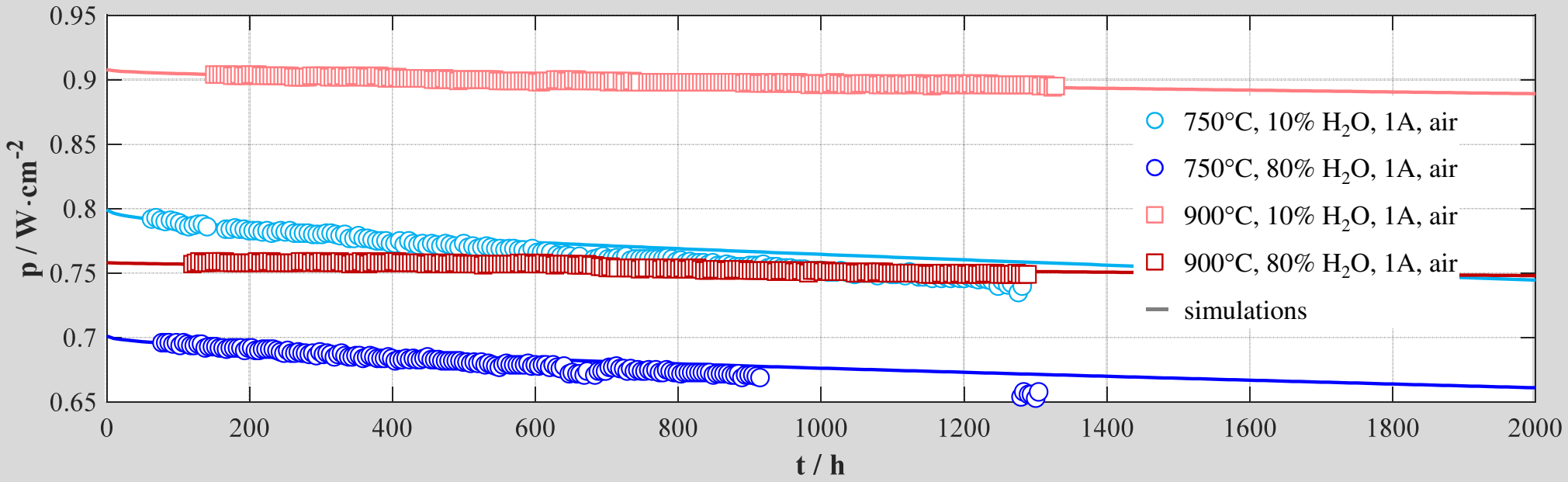

- simulations in good agreement with the measurements
- error < 2.5 mW·cm²

SOFC Stacks
Spatial Gradients → Localized Degradation

planar SOC stack

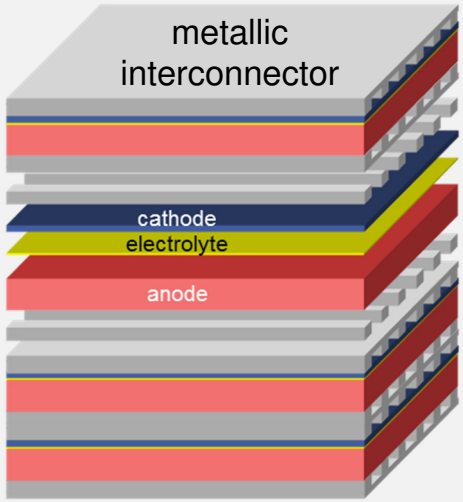

- in plane conduction
- gas conversion
- heat generation
- heat dissipation

spatial gradients

spatial gradients

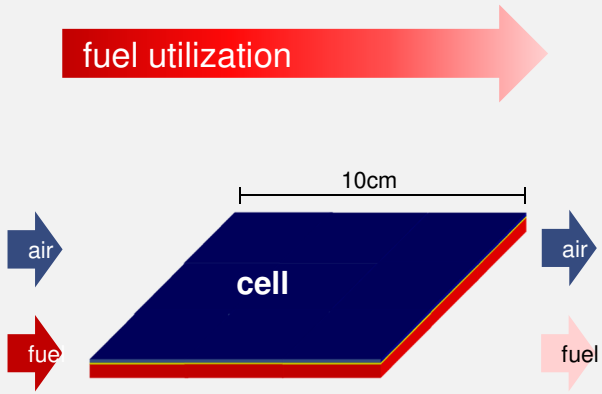

fuel utilization

temperature

electromotive force

current density

degradation model

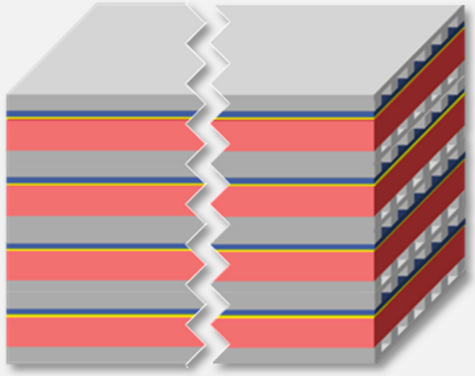

local operating conditions

local degradation

temporal change of
local cell parameters

temporal change of
local operating conditions

Modelling IV
FEM Repeat Unit Model → space-resolved Performance

parametrization

0D stationary performance model[1]

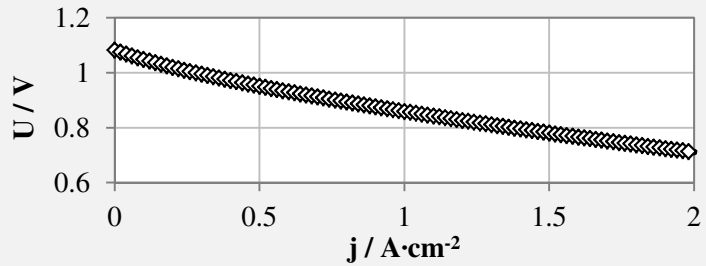

13 parameters

3D reconstruction[2,3]

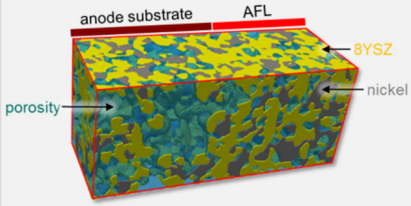

microstructure properties

Conductivity measurements[4]

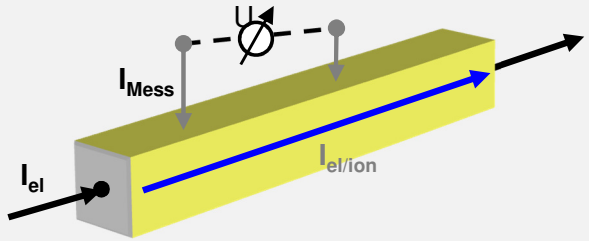

conductivities

RPU of a stack layer

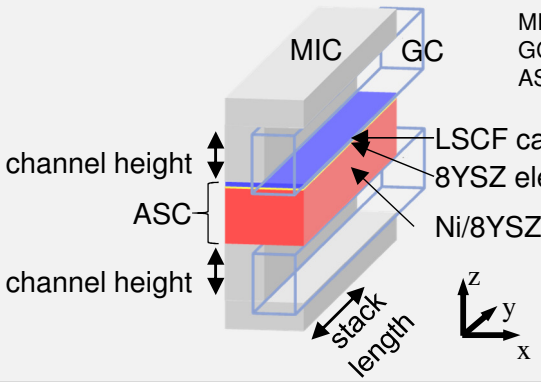

MIC: metallic interconnector
GC: gas channel
ASC: anode supported cell

LSCF cathode
8YSZ electrolyte + CGO
Ni/8YSZ anode

2D model geometry

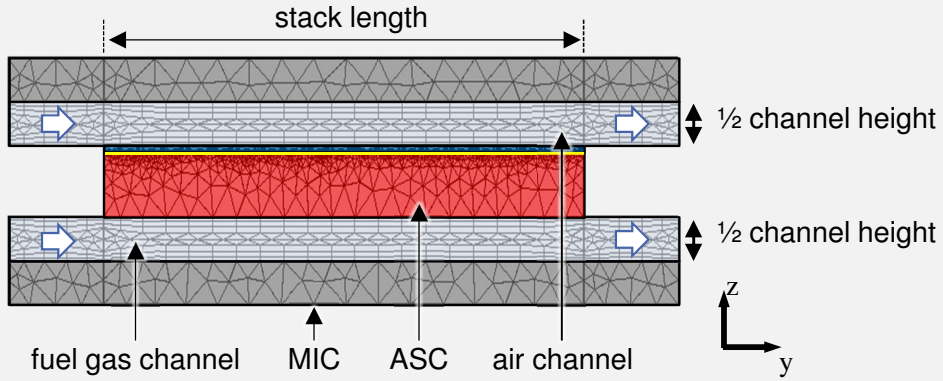

model equation[5,6,7]

impulse balance – Navier Stokes

$$\rho(\vec{U}\cdot\nabla)\vec{U} = -\nabla p + \nabla\left(\eta\left(\nabla\vec{U} + (\nabla\vec{U})^T\right)\right)$$

mass balance – dusty gas

$$\frac{N_i}{D_{i,Kn}} + \sum_{i\neq j}\frac{x_j N_i - x_i N_j}{D_{i,j}^{eff}} = -\frac{1}{RT}\left[\nabla x_i p + x_i \nabla p \frac{\kappa p}{\mu D_{i,Kn}}\right]$$

energy balance

$$\nabla\cdot\left(\rho\vec{u}\, c_p T\right) = -\nabla\cdot\vec{q} + \dot{S}_Q$$

electrochemistry – Butler-Volmer

$$j_{ct,el} = j_{0,el}\left[exp\left(\alpha_{el}\frac{n_e F\cdot\eta_{act,el}}{RT}\right) - exp\left(-(1-\alpha_{el})\frac{n_e F\cdot\eta_{act,el}}{RT}\right)\right]$$

charge transport – ohmic law

$$\nabla j = -\nabla\cdot(\sigma_{ec/ion}(T)\cdot\nabla\Phi)$$

COMSOL MULTIPHYSICS

[1] A. Leonide, et. al., *J. Power Sources*, **196**, p. 7343, (2011).
[2] J. Joos, et. al. , *J. Power Sources* **196**, pp. 7302-7307 (2011).
[3] J. Joos, et. al., *J. Power Sources* **246,** pp. 819-830 (2014).
[4] M. Kornely, et. al., *J. Power Sources* **196**, pp. 7209-7216 (2011).
[5] H. Geisler, et. al., *J. Electrochem. Soc.*, **161** (6), p. F778–F788 (2014).
[6] H. Geisler, et. al., *ECS Transaction*, **68** (1), p. 2151-2158 (2015).
[7] N. Russner, et. al, *ECS Transaction*, **78** (1), p. 2673-2682 (2017).

Modelling V
Stack Durability Model

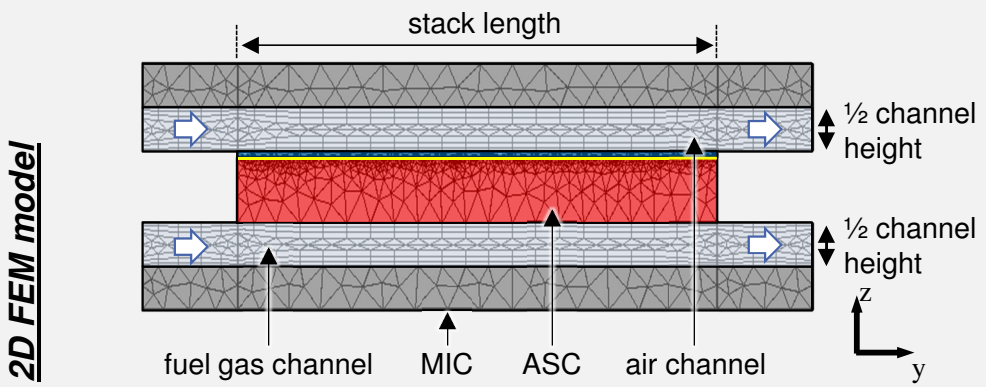

geometry

- stack width: 129mm
- stack length: 65mm
- channel height: 0.34mm

operation conditions (co-flow)

- 0.3 A/cm² (f.u. 36%)
- fuel: H_2/N_2 (50/50) + 3% H_2O, 1l/m
- oxidant: air (21% O_2), 2l/min
- temperature: 750°C

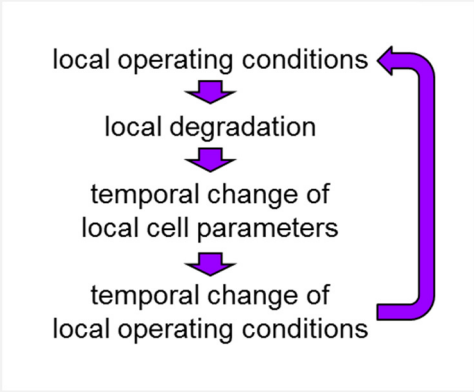

spatial distribution of the operating conditions

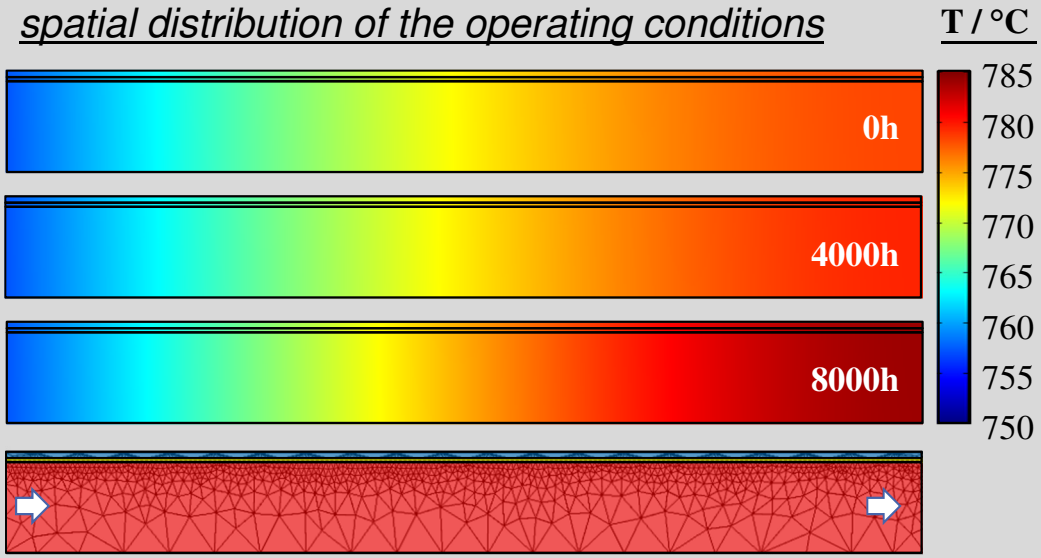

➢ **T_{max} and T-gradient increases**

S. Dierickx et al., Proc. 13th Europ. SOFC & SOE Forum, A1401 (2018)

Modelling V
Stack Durability Model

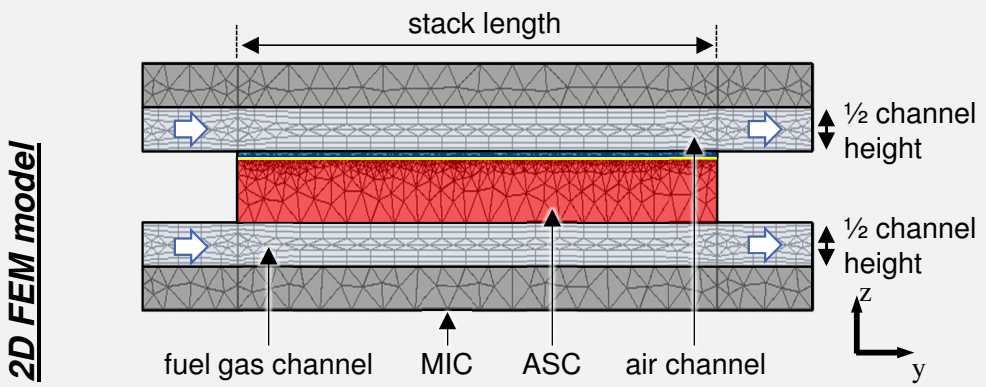

geometry

- stack width: 129mm
- stack length: 65mm
- channel height: 0.34mm

operation conditions (co-flow)

- 0.3 A/cm² (f.u. 36%)
- fuel: H_2/N_2 (50/50) + 3% H_2O, 1l/m
- oxidant: air (21% O_2), 2l/min
- temperature: 750°C

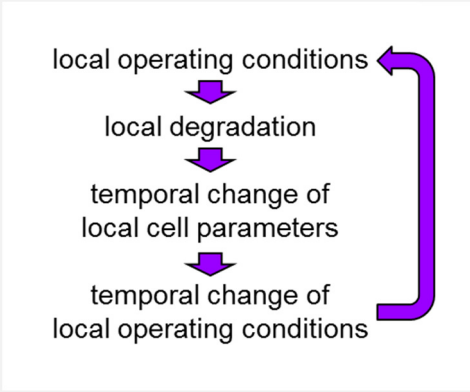

spatial distribution of the operating conditions

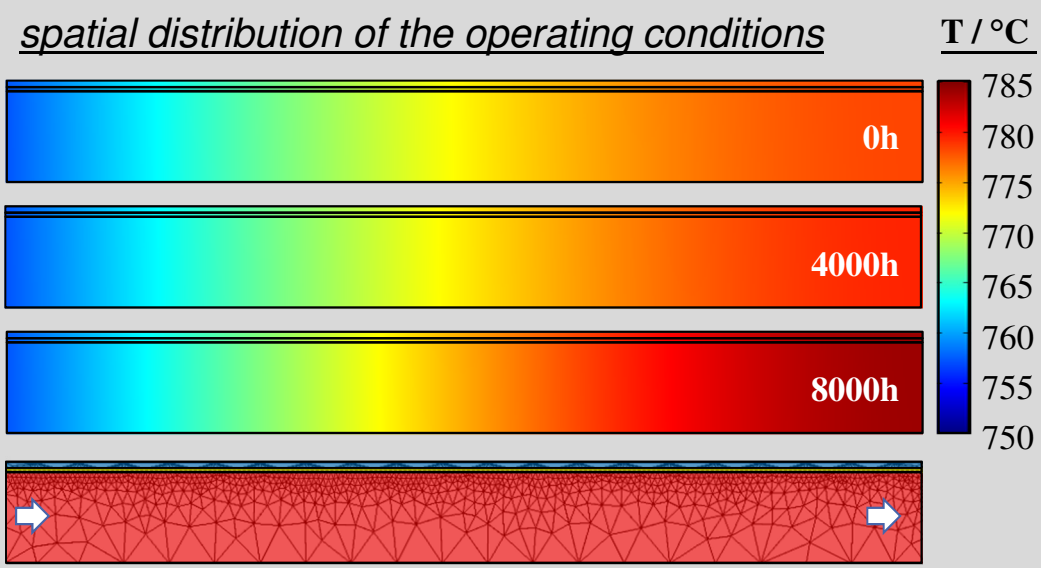

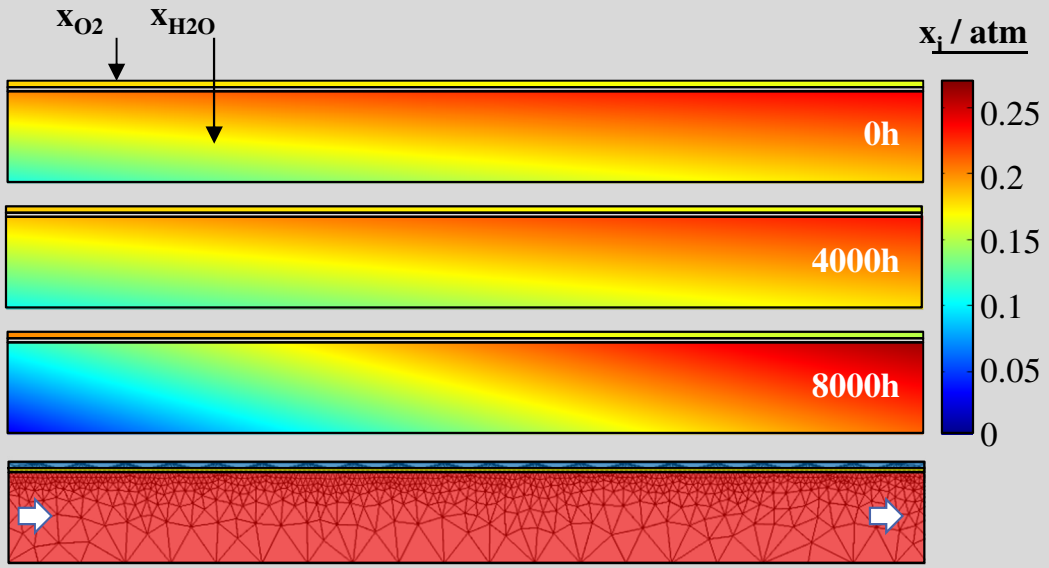

➢ **T_{max} and T-gradient increases**

➢ **local changes of O_2- and H_2O-concentration**